1976

Stability and spectra of the bumpy theta pinch

Thomas E. Cayton
College of William & Mary - Arts & Sciences

STABILITY AND SPECTRA OF THE BUMPY THETA PINCH

A Thesis

Presented to

The Faculty of the Department of Physics

The College of William and Mary in Virginia

In Partial Fulfillment

Of the Requirements for the Degree of

Doctor of Philosophy

---

by

Thomas E. Cayton

June 1976

APPROVAL SHEET

This dissertation is submitted in partial fulfillment of

the requirements for the degree of

Doctor of Philosophy

Thomas E. Cayton
Author

Approved, March 1976

G. Vahala
George M. Vahala

Carl E. Carlson
Carl E. Carlson

Frederic R. Crownfield, Jr.
Frederic R. Crownfield, Jr.

S. Peter Gary
S. Peter Gary

Frank Hohl
Frank Hohl
NASA

TABLE OF CONTENTS

ACKNOWLEDGMENTS

I wish to express my gratitude to the following persons:

Marilyn, my wife, for her love, understanding, patience, and support during the many years of graduate school and for her typing of the first draft of this dissertation;

George Vahala for coming to the College of William and Mary, for directing this research problem, for his expertise and his clarity of exposition, for his persistence and his flexibility;

Fred Crownfield for meaningful discussions and for his scrupulous reading of this dissertation and his many helpful and clarifying comments;

S. Peter Gary for his inquiring comments and his reading of this dissertation;

Mike Schmidt for his friendship and his assistance during the initial phases of this study and for his interest in and discussions about this research problem;

Jeff Lindemuth for his friendship and interest in this undertaking and his kindly aid in numerical analysis and in the operation of the William and Mary computers;

Walter Schoellmann for his friendship and hospitality which brought my wife and me to Williamsburg and the College of William and Mary, and for many hours spent philosophizing about physics in general and plasma physics in particular;

J. Freidberg and H. Weitzner for their helpful comments;

Sylvia Stout for her expert typing of the final version of this dissertation;

Hans von Baeyer and the Department of Physics for their support and encouragement;

Many unnames professors and students for the impressions and motivations they gave me.

LIST OF FIGURES

ABSTRACT

The bumpy theta pinch magnetic confinement configuration results when the magnetic surfaces of a theta pinch equilibrium, right circular cylinders, are modified slightly by the addition of a weak $\ell = 0$ helical field.

In this dissertation ideal magnetohydrostatic equilibria of the bumpy theta pinch configuration are found via perturbation theory; the equilibrium magnetic field consists of the basic theta pinch field plus a subsidiary field which is determined from the numerical solution of a linear boundary-value problem.

The stability properties of these equilibria are investigated using the equations of ideal magnetohydrodynamics which have been linearized about the static equilibrium. An expansion is performed on the linearized equations and yields a system of ordinary differential equations; the small deviation of the equilibrium magnetic surfaces from right circular cylinders is the small parameter of this expansion. The system of equations with appropriate boundary conditions constitutes an eigenvalue problem for the growth rates or oscillation frequencies of the normal modes. This eigenvalue problem is solved numerically. A portion of the spectrum of eigenvalues is obtained for a variety of parameter values. These include: a) the wavelength of the bumpy equilibrium magnetic field; b) the plasma beta; c) the position of a conducting wall

relative to the plasma; d) the azimuthal wavenumber; e) the axial wavenumber of the perturbed quantities. The unstable point spectrum is found to be non-Sturmian although Sturmian behavior sometimes occurs.

This work is a generalization of the previous treatments based on a long wavelength assumption. These long wavelength theories involve two separate asymptotic expansions in terms of two small parameters; the wavenumber of the bumpy subsidiary field, k, is the parameter of the primary expansion while the amplitude of the subsidiary field, δ, is the small parameter of the secondary expansion. The long wavelength assumption is not made in this work, but it can be employed at any stage of the calculation. This finite wavelength theory may be applicable to existing experimental configurations whereas the long wavelength theory may not be applicable because the explicit assumptions about the scaling of the two expansion parameters are almost always violated by the actual configurations. For instance, typical parameter values from the helical field experiments on a three meter theta pinch at Los Alamos Scientific Laboratory are:

$$k \sim .19, \qquad \delta \sim .06,$$
$$\beta \sim .8, \qquad t_0 \sim 20\text{-}30 \text{ n sec.},$$

here t_0 is the transit time of an Alfven wave across the plasma column. The long wavelength theory explicitly assumes that $0 < k << \delta << 1$; this condition is violated by the above parameter values. The finite wavelength theory assumes $0 < \delta << 1$, while k is arbitrary. If one utilizes the long wavelength theory, nevertheless, one finds the growth rate for

the very long wavelength, m = 1 perturbations to be

$$\gamma = 3.0 \times 10^{5} \text{ sec}^{-1} ,$$

while the finite wavelength theory gives

$$\gamma = 3.1 \times 10^{5} \text{ sec}^{-1} .$$

Thus, the results of the long wavelength theory are close to the predictions of the finite wavelength theory when the wavenumber, k, is not too large even though the ordering is violated. When the wavenumber is not small, there are major differences between the long wavelength and finite wavelength theories in both the equilibrium field and the normal mode equations governing the linear perturbations.

STABILITY AND SPECTRA OF THE BUMPY THETA PINCH

I. INTRODUCTION

Confinement of dense, hot plasmas is a major goal of the international programs to achieve controlled thermonuclear fusion for the production of useful power, consequently, the physics of plasma-magnetic field systems is of considerable interest and importance. The theoretical problem of magnetic confinement of plasmas involves studies of systems; it is not sufficient to investigate the properties of magnetized, infinite homogeneous plasmas, or plasma with small linear gradients since fusion reactor design entails practical geometries. The dilemma is to choose a sufficiently accurate model of the plasma from which solutions can be constructed in a nontrivial geometry. To describe these "systems" one usually resorts to a continuum approximation of the plasma rather than a detailed kinetic picture; one must sacrifice a substantial portion of the physics in order to solve the mathematical problems in the actual geometry of the fusion reactor. It is hoped that the physics relevant to the description of the basic features of the plasma is not excluded by the continuum approximation; indications are that it is not. These approximate descriptions of plasmas which interacts with magnetic fields of a given geometry are the "studies of systems" mentioned above.

One example of a plasma-magnetic field system is the theta pinch equilibrium which confines a plasma by an axially symmetric magnetic field; the magnetic field lines are straight and parallel (the natural coordinates to describe this configuration are the standard cylindrical

polar coordinates). The theta pinch equilibrium is an ideal configuration because of its simplicity and its stability under perturbation, but, unfortunately, it is not a confining configuration and experimental devices utilizing this configuration are plagued by severe end losses. The compressed plasma does not diffuse rapidly across the magnetic field or physically transgress the magnetic field, it simply flows out the ends of the device.[1] A conceptual high beta (the plasma beta is the ratio of the kinetic pressure of plasma to the total pressure, kinetic plus magnetic; for confinement, beta must be less than unity; high beta means values close to but less than unity) fusion reactor retains, as much as possible, the simplicity and stability properties of the theta pinch equilibrium, while minimizing the end loss problem. Among several schemes conceived to realize this specification are: a) a large aspect ratio toroidal theta pinch,[1] which eliminates the ends altogether (and, hence, the end losses; however, the toroidal configuration is unstable); b) very long ($\sim$ kilometers) linear theta pinches[2] which essentially eliminate the end effects; c) combination theta pinch-magnetic mirror devices[3] in which the magnetic-mirror fields act to impede the axial flow of the plasma. All of these configurations result from slight modifications of the theta pinch equilibrium due to the introduction of small axial inhomogeneities in the magnetic field. In the case of the toroidal theta pinch and the mirrored theta pinch these inhomogeneities are intentional and are produced by external windings or shaping of the main compression coil. The inhomogeneities in the long theta pinch are unavoidable because of the use of discrete compression coils.

The bumpy theta pinch equilibrium and its stability properties are of interest because of the relevance to experimental devices like those mentioned above and also because it involves only a slightly more complicated geometry than the ordinary theta pinch equilibrium. In this dissertation the bumpy theta pinch equilibrium and its linear stability properties are examined using the equations of ideal magnetohydrodynamics (MHD). While, if the plasma parameters are in a certain limited regime, the actual behavior of the real plasma may be described by equations which resemble those of MHD,[4,5] it should be realized that ideal MHD does not describe any real plasma. For instance, the operation of many devices which are modeled by MHD rely on a finite resistivity of the plasma for Ohmic heating, while ideal MHD has zero resistivity. Ideal MHD is a mathematical model of an idealized system, analogous to potential theory in fluid mechanics.[6] Grad's philosophy is that by studying such mathematical models one is able to build up an institution about a basically nonexistent fluid by the use of profound and powerful mathematical techniques; in practice, one visualizes the behavior of the real fluid in terms of deviations from this firmly established and quantitative ideal. This may or may not be a fruitful exercise depending on the validity of the model. There is a vast literature of applications of ideal MHD to thermonuclear containment problems and little doubt about the validity of the approximations involved. Recently, experimental data from the SCYLLAC toroidal sector experiments[1] confirmed the behavior predicted by ideal MHD analysis.

A. The Bumpy Theta Pinch

The bumpy theta pinch configuration was first considered by Haas and Wesson;[7] their sharp boundary[5] MHD calculation predicted that the plasma was unstable but that if the plasma beta were sufficiently high wall stabilization occurred (see Fig. 1a). They assumed that the axial dependence of all quantities was much weaker than the radial dependence, thus, the wavelength of the inhomogeneities in the equilibrium magnetic field is very much larger than the radius of the plasma column. Calculations which make this assumption are termed "long wavelength". Weitzner[8] and, simultaneously, Freidberg and Marder[9] examined the case of long wavelength bumpy fields but allowed for diffuse equilibrium profiles (Gaussian-like profiles only); Weitzner assumed that the magnetic field was basically that of a theta pinch plus a very small amplitude, long wavelength, $\ell = 0$ helical (bumpy) field (helical fields have dependence on θ and z in the form $\cos(\ell\theta - kz)$; Freidberg and Marder allowed a finite amplitude, long wavelength $\ell = 0$ helical field. Weitzner calculated eigenvalues through the numerical solution of differential equations, whereas Freidberg and Marder utilized the Rayleigh-Ritz variational method. A small difference in the computed growth rates of the unstable modes resulted from the inclusion of finite amplitude $\ell = 0$ helical fields as opposed to very small $\ell = 0$ fields; both calculations predicted growth rates for unstable modes (see Fig. 1b) comparable to those given by Haas and Wesson only if the plasma beta was not large. Neither diffuse profile calculation showed any high beta wall stabilization as predicted by the sharp boundary calculation. Since a sharp boundary plasma is a

limiting case of a diffuse profile plasma, the two theories seemed to contradict one another.

This paradox was resolved by Freidberg, Marder, and Weitzner[10] who calculated the growth rates of unstable perturbations of the equilibrium of theta pinch field plus very small, long wavelength, $\ell = 0$ helical field with relatively sharp, diffuse profile equilibrium quantities. They found a conventional spectrum of unstable eigenvalues (see Fig. 1c) when the plasma beta was not too large; the most unstable mode had no nodes in the radial direction, the second most unstable had one radial node, etc.; the growth rates of the most unstable mode agreed, to within 15%, with those predicted by the sharp boundary theory. However, for high beta values the spectrum was drastically altered and unconventional; the unstable mode with no radial nodes was stabilized while a stable mode with no radial nodes attained a finite oscillation frequency. This rather complicated transition agrees qualitatively and quantitatively with the predictions of sharp boundary theory. Diffuse profile theory predicts the existence of unstable modes for high beta values; this is the case, but the most unstable mode exhibits one radial node rather than no nodes. Sharp boundary theory simply cannot account for modes other than the gross $n = 0$ mode. Since diffuse profile theory can display the modes with more complicated nodal structure while the sharp boundary theory cannot, the paradox was resolved. This is one indication that stability criteria based on sharp boundary ideal MHD may not be reliable.

In a similar diffuse profile calculation Vahala[11] investigated the influence of weak shear on the stability of the long wavelength equilibrium of the bumpy theta pinch.

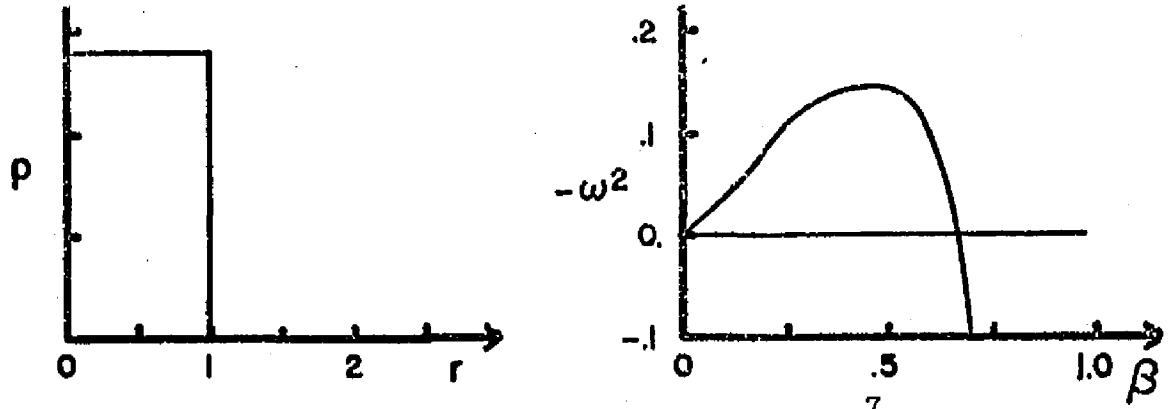

Fig. 1a. Results of sharp boundary ideal MHD analysis[7] of perturbations with time dependence $e^{-i\omega t}$ showing stabilization for $\beta > .7$ ($m = 1$, $\ell = 0$; m and ℓ are the azimuthal and axial wavenumbers).

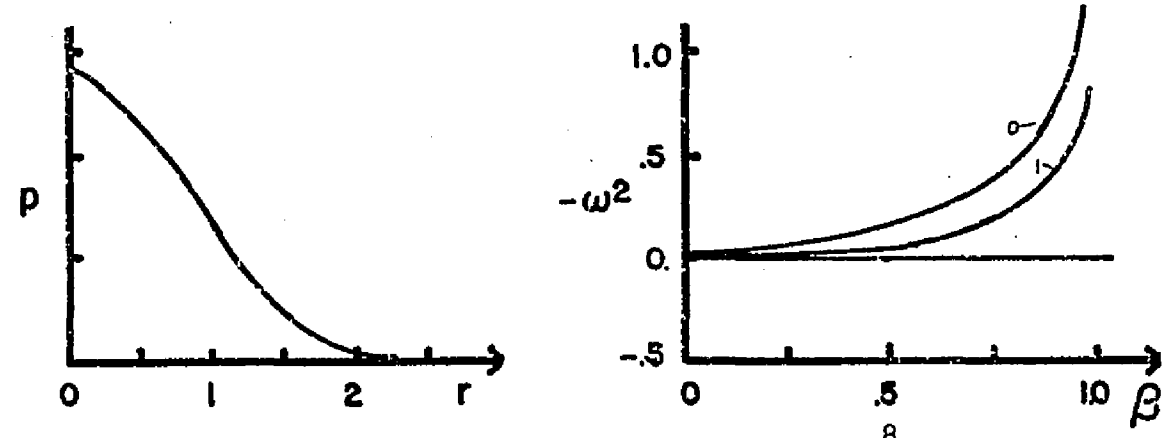

Fig. 1b. Results of diffuse profile ideal MHD analysis[8] of perturbations with time dependence $e^{-i\omega t}$ showing no high β stabilization ($m = 1$, $\ell = 0$). The small numbers denote the numbers of radial nodes of the eigenfunctions.

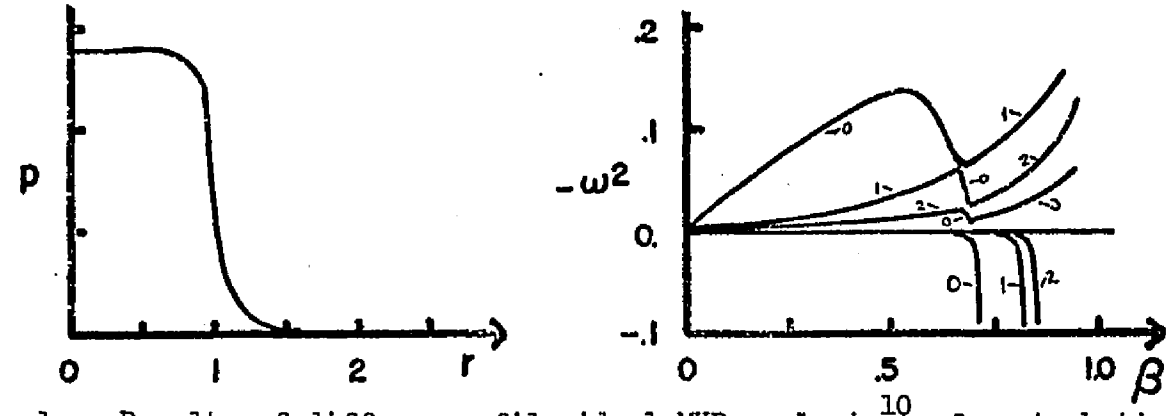

Fig. 1c. Results of diffuse profile ideal MHD analysis[10] of perturbations with time dependence $e^{-i\omega t}$ showing a complicated transition at high β for sharp profiles, but agreement with sharp boundary (Fig. 1a) predictions ($m = 1$, $\ell = 0$). The small numbers count the eigenfunction radial nodes.

In this dissertation the ideal MHD stability of an equilibrium which consists of a theta pinch field plus a very small, finite wavelength, $\ell = 0$ helical field is considered. ("Finite wavelength" means that the wavelength of axial inhomogeneities in the equilibrium magnetic field is of the same order as the plasma column radius.) The first objective is to ascertain the influence of the finite wavelength on the equilibrium quantities and on the growth rates or oscillation frequencies of the normal modes. The second objective is to see how the finite wavelength affects the spectral properties of the normal mode equations. In actual experimental devices[1,12,13] the wavelength of the bumpy field ranges from large values to small values (λ_E = 40 plasma radii in SCYLLAC, λ_E = 2 plasma radii in ELMO bumpy torus); hence a finite wavelength theory is needed.

In Chapter II, the equilibrium of an ideal MHD fluid will be examined in general and then the specific finite wavelength bumpy theta pinch equilibrium will be computed. In Chapter III, the normal mode equations describing the behavior of small perturbations of the equilibrium quantities will be derived from the linearized equations of ideal MHD. An eigenvalue problem will be developed and solved numerically for the very long wavelength kink modes (very long wavelength perturbations of the finite wavelength equilibrium) which are the only experimentally observed modes.[1,10] In Chapter IV, the nature of the spectrum of eigenvalues will be inspected. In Chapter V, the treatment is extended to the case where the bumpy field lines will be allowed to become very loosely wound helices. The pitch of the helix will be large enough so that the equilibrium quantities satisfy the same conditions derived in Chapter II,

but a new term will arise in the normal mode equations which depends on the pitch of the equilibrium magnetic field lines. Another eigenvalue problem will be developed and solved numerically and the behavior of the eigenfunctions described. The remainder of the present chapter will be devoted to general properties of ideal magnetohydrodynamics. These are extremely important to this study. It will be shown that although the approximations severely limit the range of applicability of the model, it is based on a firm and elegant mathematical foundation. Because of this, one may be certain of the resulting solutions. It will also be shown that in a bounded domain MHD yields continuous sets of eigenvalues and singular eigenfunctions in addition to the point eigenvalues and well behaved eigenfunctions usually associated with the classical theory of oscillations. The continua of ideal MHD result from very singular features of wave propagation that will be elucidated in what follows. First, the system of equation which constitute the MHD model will be described; then the method of characteristics will be employed to determine the mathematical classification of the system and to illuminate the nature of wave propagation in the MHD fluid. Finally, the equations of MHD will be linearized about a time independent, spatially dependent state. The equations which govern the equilibrium and linear ones which govern the perturbations will be employed in later chapters to study the equilibrium and stability properties of the bumpy theta pinch.

B. Ideal Magnetohydrodynamics

In the calculations described in this work the hot plasma is considered to be a perfect fluid which is also a perfect electrical

conductor but which has the magnetic permeability of the vacuum. The time and length scales of all quantities are assumed to be such that the displacement current in Maxwell's equations may be ignored with negligible error; the electrostatic part of the Lorentz force is also neglected.[4,5,6] These assumptions, together with a thermodynamic equation of state for the fluid, lead to a closed system of partial differential equations which describes the evolution of the idealized plasma-magnetic field system. It will be shown that, mathematically, this system of equations is a conventional symmetric hyperbolic type. Because of this property one is able to refer to theorems on the existence and uniqueness of initial-value and boundary-value problems and thus to know the particular circumstances in which the problem is well-posed.[14] If the mathematical structure were unconventional, one could not be assured of a well-posed problem and the attractiveness of the system would be considerably diminished. The omission of $\dot{\underset{\sim}{D}}$ and $q\underset{\sim}{E}$ thus yields a mathematically recognizable system, in particular one which is Galilei-invariant, as distinguished from the naively "more accurate" system with Maxwell's equations and Lorentz force intact, but with no invariance principle and no simple theory.[6]

Ideal magnetohydrodynamics (MHD) consists of the following set of partial differential equations involving the fluid velocity field, $\underset{\sim}{u}$; the mass density, ρ; the scalar pressure, p; the magnetic induction, $\underset{\sim}{B}$; the current density, $\underset{\sim}{J}$; the electric field, $\underset{\sim}{E}$; the entropy density, s; and the electric charge density, ρ_e.

Conservation of mass: $$\frac{\partial \rho}{\partial t} + \nabla \cdot (\rho \underset{\sim}{u}) = 0 \qquad (1)$$

Equation of motion: $$\rho\left(\frac{\partial}{\partial t} + \underset{\sim}{u}\cdot\nabla\right)\underset{\sim}{u} = -\nabla p + \frac{1}{c}\underset{\sim}{J}\times\underset{\sim}{B} + \rho_e\underset{\sim}{E} \qquad (2)$$

Ampere's Law: $$\nabla \times \underset{\sim}{B} = \frac{4\pi}{c}\underset{\sim}{J} + \frac{1}{c}\frac{\partial \underset{\sim}{E}}{\partial t} \quad (3)$$

Faraday's Law: $$\nabla \times \underset{\sim}{E} = -\frac{1}{c}\frac{\partial \underset{\sim}{B}}{\partial t} \quad (4)$$

Poisson's Equation: $$\nabla \cdot \underset{\sim}{E} = 4\pi \rho_e \quad (5)$$

Nonexistence of monopole: $$\nabla \cdot \underset{\sim}{B} = 0 \quad (6)$$

Ohm's Law (Perfect Conductor): $$\underset{\sim}{E} + \frac{1}{c}\underset{\sim}{u} \times \underset{\sim}{B} = 0 \quad (7)$$

Conservation of Entropy: $$\left(\frac{\partial}{\partial t} + \underset{\sim}{u}\cdot\nabla\right) s = 0 \quad (8)$$

Equation of state: $$p = p(\rho, s) \quad \text{or} \quad s = s(p, \rho) \quad (9)$$

It is convenient to change the units of the electrical quantities from cgs units to a system where the constants are unity, thus

$$\underset{\sim}{B} = \sqrt{4\pi}\,\underset{\sim}{B}' \quad , \quad \underset{\sim}{J} = \frac{c}{\sqrt{4\pi}}\,\underset{\sim}{J}'$$

Dropping the primes and eliminating the algebraic relations, one finds the following equations for ideal MHD flow

$$\frac{\partial \rho}{\partial t} + (\underset{\sim}{u}\cdot\nabla)\rho + \rho(\nabla\cdot\underset{\sim}{u}) = 0 \quad (10)$$

$$\rho\left(\frac{\partial}{\partial t} + \underset{\sim}{u}\cdot\nabla\right)\underset{\sim}{u} = -\nabla p + (\nabla \times \underset{\sim}{B}) \times \underset{\sim}{B} \quad (11)$$

$$\frac{\partial \underset{\sim}{B}}{\partial t} = \nabla \times (\underset{\sim}{u} \times \underset{\sim}{B}) \quad (12)$$

$$\frac{\partial s}{\partial t} + (\underset{\sim}{u}\cdot\nabla)s = 0 \quad (13)$$

$$\nabla \cdot \underset{\sim}{B} = 0 \tag{14}$$

$$p = p(\rho, s) \tag{15}$$

On taking the divergence of Eq. (12), one finds

$$\nabla \cdot \frac{\partial \underset{\sim}{B}}{\partial t} = \frac{\partial}{\partial t}(\nabla \cdot \underset{\sim}{B}) = 0$$

Thus, Eq. (14) must be interpreted as a constraint on the values of the components of B, unless one is dealing with time independent or steady phenomena. Equation (14) will be used to describe the equilibrium state but will not be used to determine the time evolution of small perturbations but only as an initial condition. Using Eq. (15) one may rewrite Eq. (10) and close the system of partial differential equations; the closed system is

$$\frac{1}{\rho c_s^2}\left(\frac{\partial}{\partial t} + \underset{\sim}{u} \cdot \nabla\right) p + \nabla \cdot \underset{\sim}{u} = 0 \tag{16}$$

$$\rho\left(\frac{\partial}{\partial t} + \underset{\sim}{u} \cdot \nabla\right)\underset{\sim}{u} = -\nabla p + (\underset{\sim}{B} \cdot \nabla)\underset{\sim}{B} - \nabla\left(\frac{1}{2}B^2\right) \tag{17}$$

$$\left(\frac{\partial}{\partial t} + \underset{\sim}{u} \cdot \nabla\right)\underset{\sim}{B} = (\underset{\sim}{B} \cdot \nabla)\underset{\sim}{u} - \underset{\sim}{B}(\nabla \cdot \underset{\sim}{u}) \tag{18}$$

$$\left(\frac{\partial}{\partial t} + \underset{\sim}{u} \cdot \nabla\right) s = 0 \tag{19}$$

where c_s is the acoustic speed in the fluid $c_s^2 = \left(\frac{\partial p}{\partial \rho}\right)_s$. These equations may be written in matrix form as

$$A\frac{\partial V}{\partial t} + B\frac{\partial V}{\partial x} + C\frac{\partial V}{\partial y} + D\frac{\partial V}{\partial z} = 0 \tag{20}$$

where V is an eight component vector and A - D are 8 x 8 matrices. The explicit matrices are real and symmetric. Thus, the system is termed "symmetric". Care must be exercised in classifying the system, Eqs. (16)-(19) since only seven arbitrary functions may be specified initially, p, s, three components of $\underset{\sim}{u}$, and two components of $\underset{\sim}{B}$, the eighth, the third component of $\underset{\sim}{B}$, being determined from the constraint, $\nabla \cdot \underset{\sim}{B} = 0$; the system of equations with the constraint is a seventh order system of partial differential equations.

Systems of partial differential equations are categorized according to their characteristic surfaces. Following Jeffrey and Taniuti[15] one considers certain generalized surfaces or manifolds in four dimensional space-time across which the normal derivatives of V cannot be computed, such a manifold is defined to be a characteristic surface. If all the characteristic surfaces are real surfaces, then the system of partial differential equations is hyperbolic; if all the characteristic surfaces are complex, the system is elliptic; if some characteristic surfaces are real and some are complex, the system is of mixed type.

Consider a surface defined by the equation

$$\phi(\underset{\sim}{x}, t) = 0 \tag{21}$$

The differential equation for this surface is

$$\nabla\phi \cdot d\underset{\sim}{x} + \frac{\partial \phi}{\partial t} dt = 0 = |\nabla\phi| dx_n + \frac{\partial \phi}{\partial t} dt \tag{22}$$

where (dx_n, dt) is a displacement in the direction normal to the surface. If this surface is characteristic, then the normal speed associated with it is

$$\frac{dx_n}{dt} = -\frac{\partial\phi}{\partial t}\Big/|\nabla\phi| \tag{23}$$

In a surface like that defined by Eq. (21), one may define a new coordinate system and rewrite the system of partial differential equations, like Eq. (20), casting it in the form

$$M^0\frac{\partial V}{\partial\phi} + M^i\frac{\partial V}{\partial\xi_i} = 0 \tag{24}$$

where the M^j are the coefficient matrices and the ξ_k are the new coordinates in the surface $\phi = 0$. That part of Eq. (24) (as applied to Eq. (20)), involving the normal derivative at the surface is found to be

$$\left[A\frac{\partial\phi}{\partial t} + B\frac{\partial\phi}{\partial x} + C\frac{\partial\phi}{\partial y} + D\frac{\partial\phi}{\partial z}\right]\frac{\partial V}{\partial\phi}. \tag{25}$$

The normal derivatives cannot be computed from specified values in the surface whenever the determinant of the coefficient matrix vanishes; thus, when this condition is satisfied the surface $\phi = 0$ is a characteristic surface.

The characteristic surfaces are found from the vanishing of the determinant of the coefficient matrix of $\frac{\partial V}{\partial\phi}$; this yields an algebraic relation among the various partial derivatives of ϕ; when these are known the normal speeds of the discontinuities can be computed by Eq. (23). To find these discontinuities one moves off the characteristic surface ($\phi = 0$) an arbitrarily small distance, ε, both parallel (call this the + side) and antiparallel (call this the - side) to the unit normal. Then, if one subtracts the one form of Eq. (24) valid on the - side from the one valid on the + side and takes the limit as the small distance, ε,

vanishes, one finds that only those terms involving the normal derivative survive since all the other derivatives are continuous across the characteristic surface. The characteristic equation is then

$$\left(A\frac{\partial\phi}{\partial t} + \underset{\sim}{A}\cdot\nabla\phi\right)\left[\frac{\partial V}{\partial\phi}\right]^{+}_{-} = 0$$

If V changes continuously from a value V on the - side to a value V + δV on the + side then the jump in the normal derivative across the characteristic surface, $\left[\frac{\partial V}{\partial\phi}\right]^{+}_{-}$, is proportional to the change δV across the surface, and the characteristic equation may be written in terms of these δV.

$$\left[A\frac{\partial\phi}{\partial t} + B\frac{\partial\phi}{\partial x} + C\frac{\partial\phi}{\partial y} + D\frac{\partial\phi}{\partial z}\right]\delta V = 0 \qquad (26)$$

Thus for a system of partial differential equations, like Eq. (20), one may write down the characteristic equation by simply replacing $\frac{\partial V}{\partial t}$ by $\frac{\partial\phi}{\partial t}\,\delta V$ and $\frac{\partial}{\partial \underset{\sim}{x}} V$ by $\nabla\phi\cdot\delta V$. The δV are the "discontinuities" that have been mentioned.

Upon applying the above prescription to the system of MHD equations (16)-(19) and the constraint, Eq. (14), one finds

$$\frac{1}{\rho c_s^2}\left(\frac{\partial\phi}{\partial t} + \underset{\sim}{u}\cdot\nabla\phi\right)\delta p + \nabla\phi\cdot\delta\underset{\sim}{u} = 0 \qquad (27)$$

$$\rho\left(\frac{\partial\phi}{\partial t} + \underset{\sim}{u}\cdot\nabla\phi\right)\delta\underset{\sim}{u} + \nabla\phi\,\delta p - (\underset{\sim}{B}\cdot\nabla\phi)\delta\underset{\sim}{B} + \nabla\phi(\underset{\sim}{B}\cdot\delta\underset{\sim}{B}) = 0 \qquad (28)$$

$$\left(\frac{\partial\phi}{\partial t} + \underset{\sim}{u}\cdot\nabla\phi\right)\delta\underset{\sim}{B} - (\underset{\sim}{B}\cdot\nabla\phi)\,\delta\underset{\sim}{u} + \underset{\sim}{B}(\nabla\phi\cdot\delta\underset{\sim}{u}) = 0 \qquad (29)$$

$$\left(\frac{\partial\phi}{\partial t} + \underset{\sim}{u}\cdot\nabla\phi\right)\delta s = 0 \qquad (30)$$

supplemented by the constraint

$$\nabla\phi \cdot \delta\underset{\sim}{B} = 0 \tag{31}$$

One of the characteristic equations is identified to be Eq. (23), namely

$$\left(\frac{\partial\phi}{\partial t} + \underset{\sim}{u}\cdot\nabla\phi\right)\delta s = 0 \tag{32}$$

If $\frac{\partial\phi}{\partial t} + \underset{\sim}{u}\cdot\nabla\phi = 0$, then an arbitrary discontinuity in the entropy density propagates with the speed of the fluid element. This describes the motion of a shock, but since this work will only address wave propagation with the entropy conserved ($\delta s = 0$) the normal speed, u_n (the flow velocity), does not occur as a root of the characteristic equation.

One finds upon scalar multiplication of Eq. (28) by $\nabla\phi$, and scalar multiplication of Eq. (28) and (29) by $\underset{\sim}{B}$ that the resulting equations, together with Eq. (27) form a closed system

$$\frac{1}{\rho c_s^2}\left(\frac{\partial\phi}{\partial t} + \underset{\sim}{u}\cdot\nabla\phi\right)\delta p + \left(\nabla\phi\cdot\delta\underset{\sim}{u}\right) = 0 \tag{33}$$

$$\rho\left(\frac{\partial\phi}{\partial t} + \underset{\sim}{u}\cdot\nabla\phi\right)\left(\nabla\phi\cdot\delta\underset{\sim}{u}\right) + |\nabla\phi|^2\delta p + |\nabla\phi|^2\left(\underset{\sim}{B}\cdot\delta\underset{\sim}{B}\right) = 0 \tag{34}$$

$$\rho\left(\frac{\partial\phi}{\partial t} + \underset{\sim}{u}\cdot\nabla\phi\right)\left(\underset{\sim}{B}\cdot\delta\underset{\sim}{u}\right) + \left(\underset{\sim}{B}\cdot\nabla\phi\right)\delta p = 0 \tag{35}$$

$$\left(\frac{\partial\phi}{\partial t} + \underset{\sim}{u}\cdot\nabla\phi\right)\left(\underset{\sim}{B}\cdot\delta\underset{\sim}{B}\right) - \left(B\cdot\nabla\phi\right)\left(\underset{\sim}{B}\cdot\delta\underset{\sim}{u}\right) + B^2\left(\nabla\phi\cdot\delta\underset{\sim}{u}\right) = 0 \tag{36}$$

In matrix form, these become

$$\begin{pmatrix} \frac{1}{\rho c_s^2}\frac{d\phi}{dt} & 1 & 0 & 0 \\ |\nabla\phi|^2 & \rho\frac{d\phi}{dt} & 0 & |\nabla\phi|^2 \\ \underset{\sim}{B}\cdot\nabla\phi & 0 & \rho\frac{d\phi}{dt} & 0 \\ 0 & B^2 & -\underset{\sim}{B}\cdot\nabla\phi & \frac{d\phi}{dt} \end{pmatrix} \begin{pmatrix} \delta p \\ \nabla\phi\cdot\delta\underset{\sim}{u} \\ \underset{\sim}{B}\cdot\delta\underset{\sim}{u} \\ \underset{\sim}{B}\cdot\delta\underset{\sim}{B} \end{pmatrix} = 0 \qquad (37)$$

The determinant of the coefficient matrix is

$$\frac{1}{\rho c_s^2}\left[\rho^2\left(\frac{\partial\phi}{\partial t}+\underset{\sim}{u}\cdot\nabla\phi\right)^4-\rho\left(\frac{\partial\phi}{\partial t}+\underset{\sim}{u}\cdot\nabla\phi\right)^2\left(\rho c_s^2+B^2\right)|\nabla\phi|^2+\rho c_s^2\left(\underset{\sim}{B}\cdot\nabla\phi\right)^2|\nabla\phi|^2\right]$$

if this determinant vanishes the discontinuities of Eq. (37) move with the normal speeds determined from Eq. (23). These are the fast magnetosonic wave and the slow magnetosonic wave. If one regards the discontinuity in the normal component of velocity, $(\nabla\phi\cdot\delta\underset{\sim}{u})$, as the arbitrary quantity, then all the other discontinuities associated with the fast and slow magnetosonic wave, δp, $(\underset{\sim}{B}\cdot\delta\underset{\sim}{u})$ and $(\underset{\sim}{B}\cdot\delta\underset{\sim}{B})$ are computed from it by elimination in Eqs. (33)-(36). Since the normal velocity component is discontinuous at the characteristic surface, one infers from the divergence theorem that the velocity field is not divergence free and hence that the fast and slow magnetosonic waves involve compression of the plasma.

Since $(\nabla\phi\cdot\delta\underset{\sim}{u})$ is regarded as the fundamental quantity, the other discontinuities being determined from it, and since Eq. (37) yields the fast and slow magnetosonic waves which involve only the normal

component of $\delta\underset{\sim}{u}$, one may find the waves associated with the components of $\delta\underset{\sim}{u}$ which are tangent to the characteristic surface by assuming $\nabla\phi\cdot\delta\underset{\sim}{u} = 0$. By the divergence theorem these are waves which do not compress the plasma. Upon vector multiplication of Eqs. (28) and (29) by $\nabla\phi$ one finds

$$\rho\left(\frac{\partial\phi}{\partial t} + \underset{\sim}{u}\cdot\nabla\phi\right)(\nabla\phi\times\delta\underset{\sim}{u}) - (\underset{\sim}{B}\cdot\nabla\phi)(\nabla\phi\times\delta\underset{\sim}{B}) = 0$$

$$\left(\frac{\partial\phi}{\partial t} + \underset{\sim}{u}\cdot\nabla\phi\right)(\nabla\phi\times\delta\underset{\sim}{B}) - (\underset{\sim}{B}\cdot\nabla\phi)(\nabla\phi\times\delta\underset{\sim}{u}) = 0$$

these are written in matrix form as

$$\begin{pmatrix} \rho\frac{d\phi}{dt} & -\underset{\sim}{B}\cdot\nabla\phi \\ -\underset{\sim}{B}\cdot\nabla\phi & \frac{d\phi}{dt} \end{pmatrix}\begin{pmatrix} \nabla\phi\times\delta\underset{\sim}{u} \\ \nabla\phi\times\delta\underset{\sim}{B} \end{pmatrix} = 0 \qquad (38)$$

The determinant of the coefficient matrix is

$$\rho\left(\frac{\partial\phi}{\partial t} + \underset{\sim}{u}\cdot\nabla\phi\right)^2 - (\underset{\sim}{B}\cdot\nabla\phi)^2 = 0$$

If this determinant vanishes, the discontinuities in the tangential component of velocity and magnetic induction move with the normal speeds determined by Eq. (23). The propagation of magnetic shear is one property of an Alfven wave.

Thus, the hydromagnetic waves result from the six roots of the characteristic equation; this is a sixth order polynomial in $\frac{\partial\phi}{\partial t}$ and $\nabla\phi$. Denoting the normal speed by $c = \frac{\partial\phi}{\partial t} / |\nabla\phi|$, and the normal component of velocity by $u_n = (\underset{\sim}{u}\cdot\nabla\phi)/|\nabla\phi|$ one obtains the following roots

$$(c - u_n)^2 = c_A^2\cos^2\theta \qquad (39)$$

$$(c-u_n)^2 = \frac{1}{2}\left[(c_s^2+c_A^2) + \sqrt{(c_s^2+c_A^2)^2 - 4c_s^2c_A^2\cos^2\theta}\right] \quad (40)$$

$$(c-u_n)^2 = \frac{1}{2}\left[(c_s^2+c_A^2) - \sqrt{(c_s^2+c_A^2)^2 - 4c_s^2c_A^2\cos^2\theta}\right] \quad (41)$$

where c_A is the Alfven speed, $c_A^2 = B^2/\rho$, and θ is the angle between the unit normal to the surface and the direction of the magnetic induction, $\underset{\sim}{B}$, i.e.

$$\underset{\sim}{B}\cdot\nabla\phi = |\underset{\sim}{B}||\nabla\phi|\cos\theta$$

These roots can be found by direct evaluation of the characteristic determinant, but then the additional information contained in the characteristic equation (such as the facts that compressibility effects propagate with the fast and slow waves and that Alfven waves do not compress the plasma but do propagate magnetic shear) is not available. The most important point is that all the normal speeds are real so that the system of equations is hyperbolic. This guarangees that the initial-value problem is well-posed mathematically and hence that normal mode analysis is legitimate. For visualization, one plots these roots on a normal speed diagram, Fig. (2), which is a polar plot of speed versus orientation with the magnetic induction. Equation (39) describes the Alfven wave and is represented by two circles in the normal speed diagram; Eq. (41) describes the slow magnetosonic wave and is represented by two oval curves within the circles corresponding to the Alfven wave; Eq. (40) describes the fast magnetosonic wave and is represented by a single closed curve which contains all the other curves. Figure (2) shows the normal speeds for the case where $c_A^2 = \sqrt{2}c_s^2$.

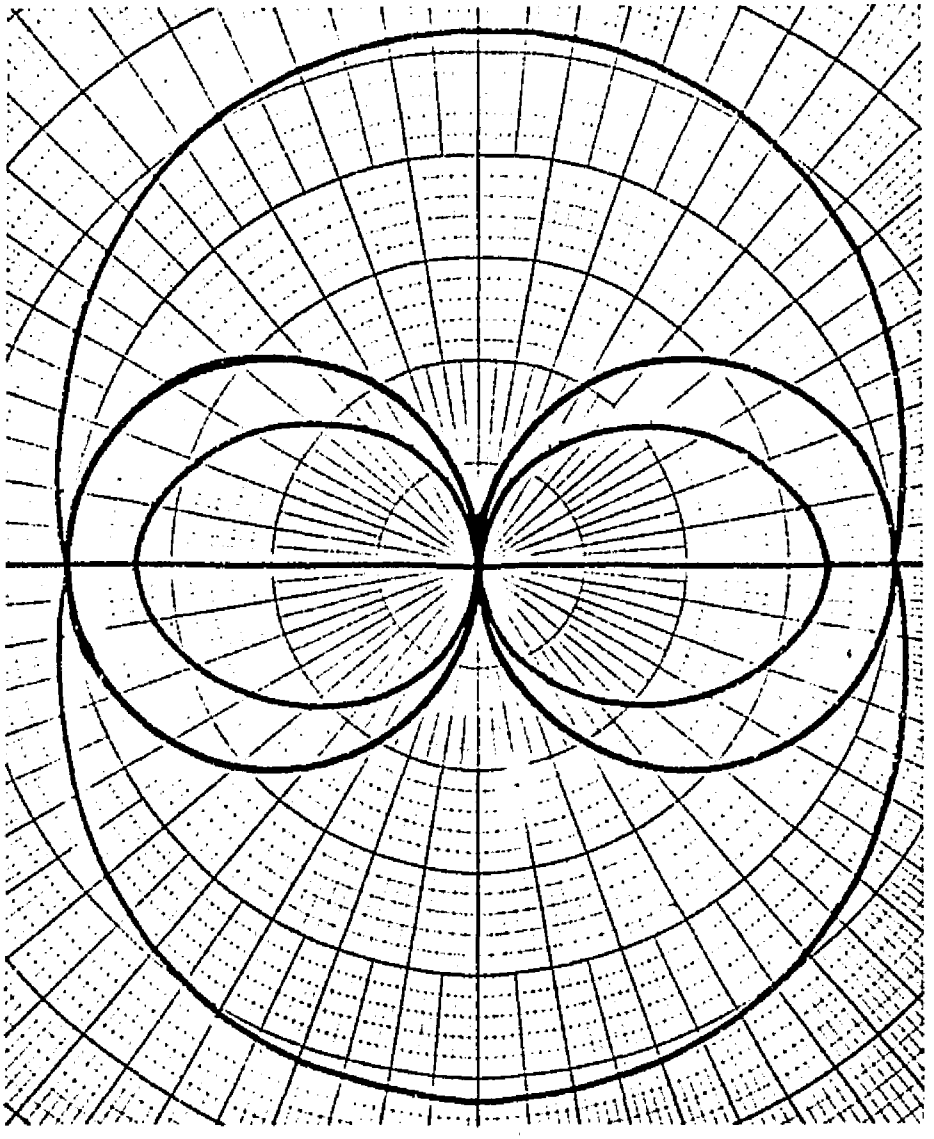

Fig. 2. Normal speed loci for hydromagnetic waves; two circles which touch the origin represent the Alfven wave; two ovals which touch the origin represent the slow magnetosonic wave; the large oval which encircles the origin represent the fast magnetosonic wave.

If one considers the equations of MHD which have been linearized about a constant, spatially homogeneous state, then the normal speed diagram gives the phase speed of plane waves propagating in any particular direction; note the singular behavior associated with propagation perpendicular to the magnetic field. The response of the fluid to a point disturbance at the origin may be ascertained from the diagram by superposing all the individual plane waves; after a time, t, the plane wave propagating in a particular direction moves the distance from the origin to a point on the normal speed locus; the envelope of these plane waves form the response to the initial point disturbance. The envelopes are called characteristic loci and their construction is illustrated in Figs. (3)-(5).

From elementary geometry one sees that the disturbance associated with the Alfven wave, Fig. (3), consists of two points of uncountable multiplicity which propagate strictly one-dimensionally along the magnetic field. The slow characteristic locus, Fig. (4), consists of two cusped, triangular shaped figures. Since the curvature of the slow normal speed locus can be approximated by a circle similar to the circle of the Alfven normal speed locus, there are two points of infinite multiplicity associated with the slow magnetosonic locus which propagate strictly one dimensionally along the magnetic field (see Appendix A), these points are the cusps located on the axis. The fast characteristic locus, Fig. (5), is the simplest curve geometrically and it resembles the fast normal speed locus. The fast characteristic locus becomes a circle, centered on the origin, if the magnetic field vanishes; it corresponds to an ordinary acoustic wave in the fluid. The Alfven and slow characteristic loci

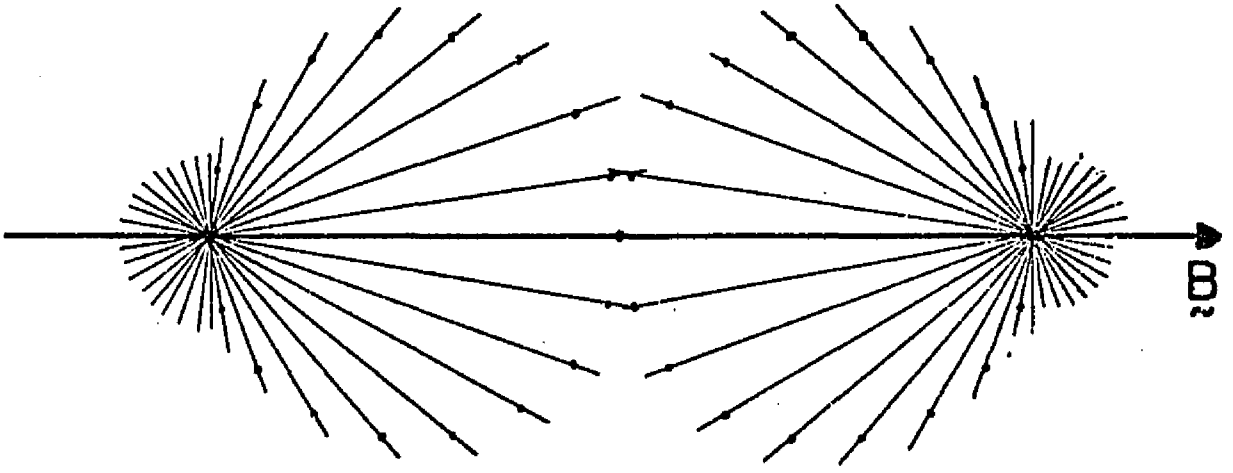

Fig. 3. Characteristic loci for the Alfven wave. The dots are points on the Alfven normal speed loci. The lines represent plane waves which intersect at two single points on the magnetic field lines; these two points propagate one dimensionally.

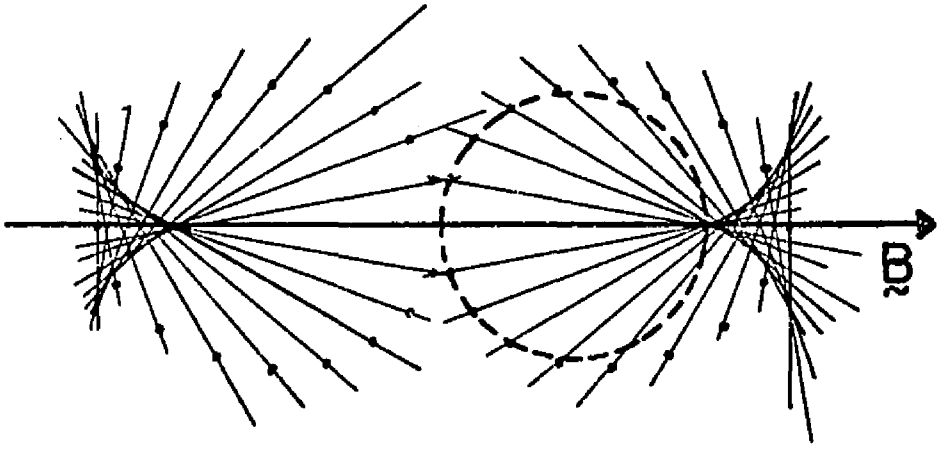

Fig. 4. Characteristic loci for the slow magnetosonic wave. The dots are points on the slow normal speed loci; the dashed circle illustrates that the cusp on the magnetic field line propagates one dimensionally as does the Alfven wave shown in Fig. 3.

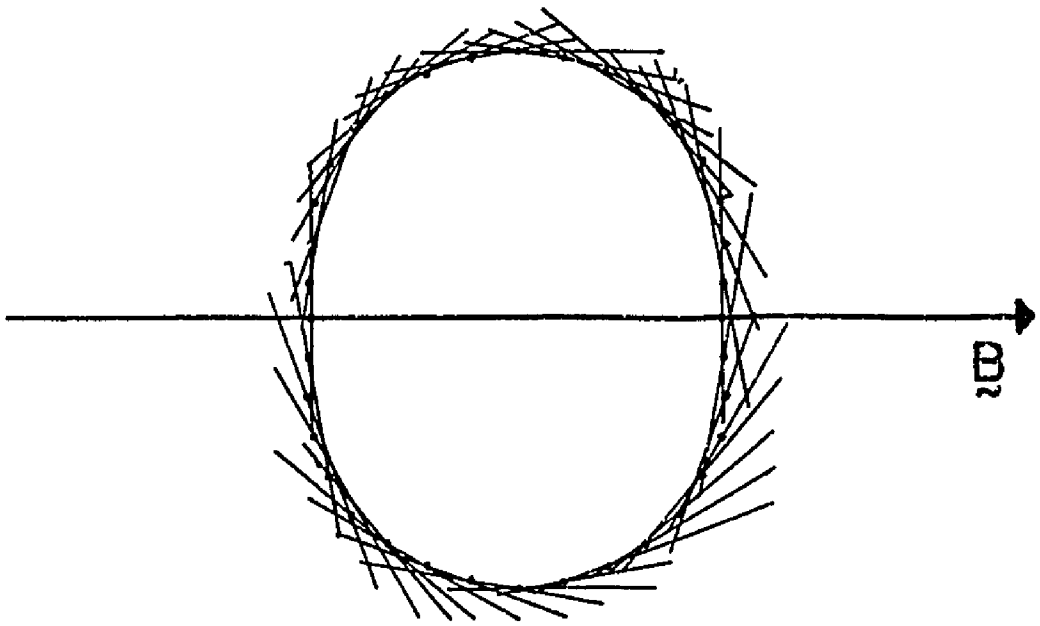

Fig. 5. Characteristic locus for the fast magnetosonic wave. As the magnetic field disappears the figure becomes less anisotropic eventually becoming a circle which represent an ordinary acoustic wave in the fluid. Note that the scale is twice that in Fig. 3 and 4.

degenerate into single, nonpropagating points if the magnetic field vanishes. With a nonzero magnetic field the diagram is anisotropic, the fast wave being flattened in the direction of the field, while the slow wave and Alfven wave move out preferentially along the direction of the magnetic field.

The most important aspect of these particular characteristic loci is the very singular behavior of the slow magnetosonic wave and Alfven wave: they are disturbances that propagate one-dimensionally in three dimensional space. One may consider, for instance, simple wave propagation in the x-y plane which is governed by the partial differential equation

$$\frac{1}{c^2}\frac{\partial^2\phi}{\partial t^2} - \left(\frac{\partial^2\phi}{\partial x^2} + \frac{\partial^2\phi}{\partial y^2}\right) = 0$$

Now consider the case where the disturbance propagates only in the x-direction, but where the velocity of propagation is a function of y. If the boundary conditions $\phi(0, y, t) = \phi(L, y, t) = 0$ are imposed and if the velocity of propagation is constant, then one finds discrete eigenvalues. If, however, the velocity of propagation is not constant, then the eigenvalues are continuous. The one dimensional propagation of the Alfven wave and the cusp of the slow magnetosonic wave can be expected to have a profound influence on eigenvalue problems which are derived from the linearized equations of ideal MHD. In fact, the exact normal mode equations for the ordinary theta pinch exhibit both the Alfven continuum and the cusp continuum explicitly.

C. Linearized MHD

The linearized equations describe the development of small deviations of the state variables from a time independent solution of Eqs. (10)-(15). Consider the state variables

$$\underset{\sim}{B} = B_0(\underset{\sim}{x}) + B_1(\underset{\sim}{x},t) \tag{42}$$

$$\underset{\sim}{u} = u_1(\underset{\sim}{x},t) \tag{43}$$

$$\rho = \rho_0(\underset{\sim}{x}) + \rho_1(\underset{\sim}{x},t) \tag{44}$$

$$p = p_0(\underset{\sim}{x}) + p_1(\underset{\sim}{x},t) \tag{45}$$

The general form of a state variable is $g = g_0(\underset{\sim}{x}) + g_1(\underset{\sim}{x}, t)$, where $|g_1| << |g_0|$. Substituting Eqs. (42)-(45) into Eqs. (10)-(15), one finds terms which involve only the equilibrium quantities as well as terms which are linear and of higher order in the small quantities. Equating the time independent terms and linear terms individually one finds the following equations

$$0 = -\nabla p_0 + (\nabla \times \underset{\sim}{B}_0) \times \underset{\sim}{B}_0 \tag{45}$$

$$\nabla \cdot \underset{\sim}{B} = 0 \tag{46}$$

$$p_0 = p_0(\rho_0, s_0) \tag{47}$$

$$\frac{\partial \rho}{\partial t} + (\underset{\sim}{u}_1 \cdot \nabla)\rho_0 + \rho_0(\nabla \cdot \underset{\sim}{u}_1) = 0 \tag{48}$$

$$\rho_0 \frac{\partial \underset{\sim}{u}_1}{\partial t} = -\nabla p_1 + (\nabla \times \underset{\sim}{B}_1) \times \underset{\sim}{B}_0 + (\nabla \times \underset{\sim}{B}_0) \times \underset{\sim}{B}_1 \tag{49}$$

$$\frac{\partial \underset{\sim}{B}_1}{\partial t} = \nabla \times (\underset{\sim}{u}_1 \times \underset{\sim}{B}_0) \tag{50}$$

$$\frac{\partial s_1}{\partial t} + (\underset{\sim}{u}_1 \cdot \nabla) s_0 = 0 \tag{51}$$

$$s_1 = s_1(p_1, \rho_1; s_0, p_0, \rho_0) \tag{52}$$

Equations (45)-(47) determine the time independent equilibrium quantities; Eqs. (48)-(52) determine the behavior of small deviations from these equilibrium values. This procedure is valid provided that the deviations remain small so that quadratic, and all higher degree, nonlinear terms are negligible compared to the linear terms.

Several important properties can be deduced from these linearized equations. First, one finds that there are two formulations in which the system, Eqs. (48)-(52), is self-adjoint; these formulations are the velocity formulation which results when Eq. (49) is differentiated once with respect to time, and the displacement formulation in which one considers the displacement, $\underset{\sim}{\xi}(\underset{\sim}{x}, t)$, of the plasma from its equilibrium position, where, $\underset{\sim}{\xi}(\underset{\sim}{x}, t)$ is such that $\underset{\sim}{u}_1(\underset{\sim}{x}, t) = \frac{\partial \underset{\sim}{\xi}}{\partial t}$. Either of these formulations produces the same differential operator, but the classes of functions on which the operator works are different. As a consequence, the definition of an instability is complicated; for instance, a displacement which increases linearly with time could be classified unstable in the displacement formulation, but would be classified stable in the velocity formulation. The general question of instability is not

addressed in this work as only exponential growth with time will be considered; in this case there is no difference between the two formulations. The calculation will be carried out using the velocity formulation of linearized ideal MHD.

The velocity formulation produces a self-adjoint differential equation and from this one can prove that an energy integral exists, that a variational method for computing eigenvalues and eigenfunctions exists, that the spectrum of eigenvalues consists solely of real values, and that any two eigenfunctions are orthogonal.[16] These general properties are very important for the specific calculation of the eigenmodes of the bumpy theta pinch that follows.

II. MAGNETOHYDROSTATIC EQUILIBRIA

A. General Theory

In static equilibrium the pressure, $p(\underset{\sim}{r})$, the magnetic induction, $\underset{\sim}{B}(\underset{\sim}{r})$, and the current density, $\underset{\sim}{J}(\underset{\sim}{r})$, of an ideal magnetohydrodynamic (MHD) plasma must satisfy the seven nontrivial ideal MHD equations

$$\nabla \cdot \underset{\sim}{B} = 0 \tag{1}$$

$$\nabla \times \underset{\sim}{B} = \underset{\sim}{J} \tag{2}$$

$$\nabla p = \underset{\sim}{J} \times \underset{\sim}{B} \tag{3}$$

Several properties of hydromagnetic equilibria can be deduced directly from these magnetohydrostatic equations. On taking the divergence of Eq. (2) one finds that the current density satisfies

$$\nabla \cdot \underset{\sim}{J} = 0 \tag{4}$$

Scalar multiplication of Eq. (3) by B and J gives, respectively

$$\underset{\sim}{B} \cdot \nabla p = 0 \tag{5}$$

$$\underset{\sim}{J} \cdot \nabla p = 0 \tag{6}$$

Equations (5) and (6) specify that the field and the current are everywhere tangent to surfaces of constant pressure; hence, J-lines and B-lines must cover constant pressure surfaces. The surfaces of constant pressure, therefore, are also magnetic surfaces.

Substituting Eq. (2) into Eq. (3) eliminates the auxiliary variable, J, and reduces the set (1)-(3) to four equations

$$\nabla \cdot \underset{\sim}{B} = 0 \tag{1}$$

$$\nabla p = (\nabla \times \underset{\sim}{B}) \times \underset{\sim}{B} \tag{3^1}$$

It is found from the method of characteristics (see Appendix C) that this fourth order system of partial differential equations is a mixed type, elliptic-hyperbolic, as opposed the three standard types of equations elliptic, parabolic, and hyperbolic. Furthermore, the characteristics for this system are doubly degenerate. Theorems regarding the existence of solutions of this complex system have not been established. Thus, in general, MHD equilibria may not exist.

In appendix C it is shown that the real characteristic surfaces which correspond to the hyperbolic part of the system (1) and (3^1) are determined by the equation

$$\underset{\sim}{B} \cdot \nabla \phi = 0$$

where $\phi(\underset{\sim}{r}) = 0$ defines the characteristic surface. This real surface is covered by B-lines and is, therefore, a magnetic surface which is also a constant pressure surface. Because the magnetic surfaces are characteristic, it is possible, when certain symmetries are present, to integrate away the hyperbolic part and thereby reduce the system (1) and (3^1) to a standard elliptic type.

In particular, on considering MHD equilibria in cylindrical polar coordinates which possess azimuthal symmetry - $f(\underset{\sim}{r}) = f(r, z)$, where f is any equilibrium quantity - the set of equations (1)-(3) is found to be explicitly

$$\frac{1}{r}\frac{\partial}{\partial r}\left(rB_r(r,z)\right) + \frac{\partial}{\partial z}B_z(r,z) = 0 \tag{7}$$

$$-\frac{\partial}{\partial z}B_\theta(r,z) = J_r(r,z) \tag{8}$$

$$\frac{\partial}{\partial z}B_r(r,z) - \frac{\partial}{\partial r}B_z(r,z) = J_\theta(r,z) \tag{9}$$

$$\frac{1}{r}\frac{\partial}{\partial r}\left(rB_\theta(r,z)\right) = J_z(r,z) \tag{10}$$

$$\frac{\partial}{\partial r}p(r,z) = J_\theta B_z - J_z B_\theta \tag{11}$$

$$0 = J_z B_r - J_r B_z \tag{12}$$

$$\frac{\partial}{\partial z}p(r,z) = J_r B_\theta - J_\theta B_r \tag{13}$$

Also, Eqs. (4) and (5) are

$$\frac{1}{r}\frac{\partial}{\partial r}\left(rJ_r(r,z)\right) + \frac{\partial}{\partial z}J_z(r,z) = 0 \tag{14}$$

$$B_r\frac{\partial}{\partial r}p(r,z) + B_z\frac{\partial}{\partial z}p(r,z) = 0 \tag{15}$$

By introducing two functions, $\psi(r, z)$ and $\chi(r, z)$, such that

$$B_r(r,z) = \frac{1}{r}\frac{\partial}{\partial z}\psi(r,z) \tag{16}$$

$$B_z(r,z) = -\frac{1}{r}\frac{\partial}{\partial r}\psi(r,z) \tag{17}$$

$$J_r(r,z) = -\frac{1}{r}\frac{\partial}{\partial z}\chi(r,z) \tag{18}$$

$$J_z(r,z) = \frac{1}{r}\frac{\partial}{\partial r}\chi(r,z) \tag{19}$$

Equations (7) and (14) are identically satisfied. It is also evident that Eqs. (16) and (17) imply

$$\underset{\sim}{B}\cdot\nabla\psi = 0 \tag{20}$$

Thus, B-lines lie on surfaces of constant ψ - the equation ψ = constant defines magnetic surfaces which are also constant pressure surfaces and which are characteristic. On using the definitions (16)-(19) Eq. (12) becomes

$$\left(\frac{1}{r}\frac{\partial\chi}{\partial r}\right)\left(\frac{1}{r}\frac{\partial\psi}{\partial z}\right)-\left(-\frac{1}{r}\frac{\partial\chi}{\partial z}\right)\left(-\frac{1}{r}\frac{\partial\psi}{\partial r}\right)=\frac{1}{r^2}\frac{\partial(\chi,\psi)}{\partial(r,z)}=0 \tag{21}$$

where $\frac{\partial(\chi,\psi)}{\partial(r,z)}$ is the Jacobian of the transformation. This implies that $\psi(r, z)$ and $\chi(r, z)$ are not independent functions but that

$$\chi = \chi(\psi) \tag{22}$$

Similarly, Eq. (15) becomes

$$\left(\frac{1}{r}\frac{\partial\psi}{\partial z}\right)\left(\frac{\partial p}{\partial r}\right)+\left(-\frac{1}{r}\frac{\partial\psi}{\partial r}\right)\left(\frac{\partial p}{\partial z}\right)=\frac{1}{r}\frac{\partial(p,\psi)}{\partial(r,z)}=0 \tag{23}$$

and yields

$$p = p(\psi) \tag{24}$$

This reiterates the facts provided by Eq. (20) - that the pressure is constant on surfaces of constant ψ. Equations (22) and (24) are important results; they provide two integrals of Eqs. (7)-(13).

Upon using the definitions (16)-(19) one finds that Eqs. (8)-(10) become

$$-\frac{\partial}{\partial z}B_\theta(r,z)=-\frac{1}{r}\frac{\partial}{\partial z}\chi(r,z) \tag{25}$$

$$\frac{1}{r}\frac{\partial^2}{\partial z^2}\psi(r,z)+\frac{\partial}{\partial r}\left(\frac{1}{r}\frac{\partial\psi}{\partial r}\right)=J_\theta(r,z) \tag{26}$$

$$\frac{1}{r}\frac{\partial}{\partial r}\left(r B_\theta(r,z)\right) = \frac{1}{r}\frac{\partial}{\partial r}\chi(r,z) \tag{27}$$

By inspection of Eqs. (25) and (27) one sees that

$$r B_\theta(r,z) = \chi(r,z) \tag{28}$$

Thus, all the components of $\underset{\sim}{J}$ and $\underset{\sim}{B}$ are given in terms of ψ and one functions of ψ, $\chi(\psi)$. Finally, substituting Eqs. (16)-(19), (26) and (28) into Eqs. (11) and (13), and using Eqs. (22) and (24) one finds (primes denote differentiation with respect to the argument)

$$p'(\psi)\frac{\partial\psi}{\partial r} = \left[\frac{\partial}{\partial r}\left(\frac{1}{r}\frac{\partial\psi}{\partial r}\right) + \frac{1}{r}\frac{\partial^2\psi}{\partial z^2}\right]\left(-\frac{1}{r}\frac{\partial\psi}{\partial r}\right) - \left(\frac{1}{r}\chi'(\psi)\frac{\partial\psi}{\partial r}\right)\left(\frac{\chi(\psi)}{r}\right)$$

$$p'(\psi)\frac{\partial\psi}{\partial z} = -\left[\frac{\partial}{\partial r}\left(\frac{1}{r}\frac{\partial\psi}{\partial r}\right) + \frac{1}{r}\frac{\partial^2\psi}{\partial z^2}\right]\left(\frac{1}{r}\frac{\partial\psi}{\partial z}\right) + \left(-\frac{1}{r}\chi'(\psi)\frac{\partial\psi}{\partial z}\right)\left(\frac{\chi(\psi)}{r}\right)$$

The equilibrium flux function, $\psi(r, z)$, must satisfy

$$\frac{\partial}{\partial r}\left(\frac{1}{r}\frac{\partial\psi}{\partial r}\right) + \frac{1}{r}\frac{\partial^2\psi}{\partial z^2} = -r p'(\psi) - \frac{1}{r}\chi(\psi)\chi'(\psi) \tag{29}$$

where $p(\psi)$ and $\chi(\psi)$ are arbitrary functions. Thus, the original fourth order system or partial differential equations has been reduced to a nonlinear, second order, elliptic partial differential equation, because the assumed symmetry of the equilibria permitted integration of the hyperbolic part. As a consequence of the two integrations, two arbitrary functions, $p(\psi)$ and $\chi(\psi)$, occur in the differential equation. Since Eq. (29) is nonlinear, nonunique solutions can exist.

B. Simple Equilibria

In the special case that equilibria exhibit translational symmetry in the axial direction in addition to azimuthal symmetry solutions

of Eq. (29) are easily determined. Since all the equilibrium quantities are functions of r alone, Eqs. (16) and (18) immediately give

$$B_r = 0$$

$$J_r = 0$$

and Eq. (29) is easily written

$$\left(\frac{1}{r}\psi'(r)\right)\left(\frac{1}{r}\psi'(r)\right)' = -r\left(\frac{1}{r}\psi'(r)\right)p'(\psi) - \frac{1}{r}\left(\frac{1}{r}\psi'(r)\right)\left(\frac{1}{2}\chi^2(\psi)\right)' \quad (30)$$

Upon using Eqs. (17) and (28), Eq. (30) becomes

$$\frac{d}{dr}\left[\frac{1}{2}B_z^2\right] = -\frac{d}{dr}[p] - \frac{1}{r^2}\frac{d}{dr}\left[\frac{1}{2}r^2B_\theta^2\right]$$

which is rewritten in the convenient form

$$\frac{d}{dr}\left[p + \frac{1}{2}(B_\theta^2 + B_z^2)\right] + \frac{B_\theta^2}{r} = 0 \quad (31)$$

Equation (31) is the well known pressure balance relation for the diffuse linear pinch[17] (screw pinch) configuration, the magnetic field of which is

$$\underset{\sim}{B} = B_\theta(r)\,\hat{\theta} + B_z(r)\,\hat{z} \quad (32)$$

One obtains the theta pinch configuration - the model system in this work-by choosing that B_θ vanish identically, i.e. specifying one of the arbitrary functions, $\chi(\psi) = 0$. Thus, for the theta pinch, the current density is

$$\underset{\sim}{J} = J_\theta(r)\,\hat{\theta} \quad (33)$$

the magnetic field is

$$\underset{\sim}{B} = B_z(r)\,\hat{z} \quad (34)$$

and the pressure balance relation is

$$\frac{d}{dr}\left[p+\frac{1}{2}B_z^2\right]=0 \tag{35}$$

Finally, it is noted that for both the theta pinch and screw pinch equilibria the equation

$$\psi(r) = \text{constant}$$

defines a family of magnetic surfaces which are right circular cylinders.

C. Bumpy Theta Pinch Equilibria

The properties of equilibria which are slight modifications of the theta pinch equilibrium will now be elucidated. The equilibria are to be axially symmetric and the magnetic surfaces which are defined by the equation

$$\psi(r,z) = \text{constant}$$

are assumed to deviate only slightly from right circular cylinders. It is also assumed that the equilibrium magnetic field has no θ-component (i.e., choose $\chi(\psi) \equiv 0$) so that the current density lies in the θ direction only

$$\underset{\sim}{J} = J_\theta(r,z)\,\hat{\theta}$$

Under these circumstances the differential equation (29) becomes

$$\frac{\partial}{\partial r}\left(\frac{1}{r}\frac{\partial\psi}{\partial r}\right)+\frac{1}{r}\frac{\partial^2\psi}{\partial z^2}=-r\,p'(\psi) \tag{36}$$

Approximate solutions of Eq. (36) will be constructed by standard perturbation analysis, but before proceeding, it is necessary to reduce (36) to dimensionless form.

From the physical quantities, r_0, the radius of the plasma column, ρ_0, the axial plasma density, and $\underset{\sim}{B}_0$, the magnetic induction at the surface of the plasma column, one finds a characteristic length,

$L = r_0$, a characteristic mass, $M = r_0^3 \rho_0$, and a characteristic time, $T = r_0/(B_0^2/\rho_0)$ (for uniform density, $\rho(r) = \rho_0$, this is the Alfven transit time across the plasma column), which are used to construct natural units for the problem. For convenience, the conversions between the dimensioned and dimensionless (denoted by tilde) quantities are listed below

length: $\underset{\sim}{r} = [r_0]\,\tilde{\underset{\sim}{r}}\,, \quad z = [r_0]\,\tilde{z}$

magnetic induction: $\underset{\sim}{B}(\underset{\sim}{r},t) = [B_0]\,\tilde{\underset{\sim}{B}}(\tilde{\underset{\sim}{r}},\tilde{t})$

density: $\rho(\underset{\sim}{r}) = [\rho_0]\,\tilde{\rho}(\tilde{\underset{\sim}{r}})$

velocity: $\underset{\sim}{v}(\underset{\sim}{r},t) = \left[\frac{B_0^2}{\rho_0}\right]^{1/2} \tilde{\underset{\sim}{v}}(\tilde{\underset{\sim}{r}},\tilde{t})$

time: $t = \left[\frac{r_0^2 \rho}{B_0^2}\right]^{1/2} \tilde{t}$

pressure: $p(\underset{\sim}{r},t) = [B_0^2]\,\tilde{p}(\tilde{\underset{\sim}{r}},\tilde{t})$

magnetic flux: $\psi(\underset{\sim}{r}) = [r_0^2 B_0]\,\tilde{\psi}(\tilde{\underset{\sim}{r}})$

current density: $\underset{\sim}{J}(\underset{\sim}{r}) = \left[\frac{B_0}{r_0}\right] \tilde{\underset{\sim}{J}}(\tilde{\underset{\sim}{r}})$

Substituting these into Eq. (36) and all previous expressions gives the desired relations among the dimensionless quantities, for instance

$$\left[\frac{B_0}{r_0}\right]\left\{\frac{\partial}{\partial \tilde{r}}\left(\frac{1}{\tilde{r}}\frac{\partial \tilde{\psi}}{\partial \tilde{r}}\right) + \frac{1}{\tilde{r}}\frac{\partial^2 \tilde{\psi}}{\partial \tilde{z}^2}\right\} = \left[\frac{B_0}{r_0}\right]\left\{-\tilde{r}_0 \tilde{p}(\tilde{\psi})\right\}$$

Hereafter, the tilde is suppressed and only dimensionless quantities are considered.

Attention is now restricted to a particular class of equilibria by assuming that the magnetic flux function has the following form

$$\psi(r,z) = \psi^{(0)}(r) + \delta\,\psi^{(1)}(r)\cos(kz) + O(\delta^2) \tag{37}$$

where the small parameter δ, $0 < \delta \ll 1$, measures the deviation of the magnetic surfaces from right circular cylinders (δ measures the bumpiness of the magnetic field lines). Because of the assumed form of $\psi(r,z)$, the differential equation for a magnetic surface is

$$d\psi = 0 = \left[\psi^{(0)\prime}(r) + \delta\psi^{(1)\prime}(r)\cos(kz)\right]dr - \left[\delta k\,\psi^{(1)}(r)\sin(kz)\right]dz$$

or, equivalently

$$r'(z) = \delta k \frac{\psi^{(1)}(r)}{\psi^{(0)\prime}(r)}\sin(kz) + O(\delta^2)$$

Hence, the equation of a magnetic surface is

$$r(z) = r_0 - \delta \frac{\psi^{(1)}(r_0)}{\psi^{(0)\prime}(r_0)}\cos(kz) + O(\delta^2) \tag{38}$$

The unit normal to a surface of constant ψ is

$$\hat{n} = \frac{\nabla\psi}{|\nabla\psi|} = \hat{r} - \hat{z}\,\delta k \frac{\psi^{(1)}(r)}{\psi^{(0)\prime}(r)}\sin(kz) + O(\delta^2) \tag{39}$$

Assuming the above form for $\psi(r, z)$ also requires that the equilibrium magnetic field, given by Eqs. (16) and (17), have the form

$$B_r(r,z) = \delta k\, b(r)\sin(kz) + O(\delta^2) \tag{40}$$

$$B_\theta(r,z) \equiv 0 \tag{41}$$

$$B_z(r,z) = a(r) + \delta c(r)\cos(kz) + O(\delta^2) \tag{42}$$

where

$$ra(r) = -\psi^{(0)\prime}(r) \tag{43}$$

$$rb(r) = -\psi^{(1)}(r) \tag{44}$$

$$rc(r) = -\psi^{(1)\prime}(r) \tag{45}$$

In terms of these equilibrium quantities, the flux surfaces and their unit normals are then

$$r(z) = r_0 - \delta \frac{b(r_0)}{a(r_0)} \cos(kz) + O(\delta^2) \tag{46}$$

$$\hat{n} = \hat{r} - \hat{z}\,\delta k \frac{b(r)}{a(r)} \sin(kz) + O(\delta^2) \tag{47}$$

Substituting the assumed form of $\psi(r, z)$, Eq. (37), and the Taylor series expansion of $p'(\psi)$

$$p'(\psi) = p'(\psi^{(0)}) + \delta\psi^{(1)}\cos(kz)\, p''(\psi^{(0)}) + O(\delta^2) \tag{48}$$

into Eq. (36) and expanding order by order in δ, one finds

$$O(1): \quad \left(\frac{1}{r}\psi^{(0)\prime}\right)' = -r p'(\psi^{(0)}) \tag{49}$$

$$O(\delta): \quad \left(\frac{1}{r}\psi^{(1)\prime}\right)' - \frac{k^2}{r}\psi^{(1)} = -r\psi^{(1)} p''(\psi^{(0)}) \tag{50}$$

By multiplying Eq. (49) by $(1/r\ \psi^{(0)\prime})$ and using Eqs. (24) and (43), one can rewrite Eq. (49), casting it in the form

$$\left[p + \tfrac{1}{2}a^2\right]' = 0 \tag{51}$$

which is recognized as the pressure balance relation for a theta pinch.

This relation determines the basic magnetic field, a(r), for a given pressure profile, p(r). An isothermal equation of state is assumed so that the plasma denisty is proportional to the plasma pressure in the equilibrium situation. The density profice is specified so that $(\rho(r)-D)\alpha p(r)$ where D is the (small) density of a uniform background of cold plasma: this is the experimental situation.[18]

Two specific pressure profiles will be considered here - a Gaussian profile[6,9]

$$p(r) = \tfrac{1}{2}\beta \exp(-r^2) \tag{52}$$

(the parameter β is the axial plasma beta, $\left[\frac{p(0)}{p(0)+\frac{1}{2}a^2(0)}\right]$) and a relatively sharp profile[8]

$$p(r) = \tfrac{1}{2}\beta \frac{1-\tanh[\alpha(r^2-1)]}{1+\tanh[\alpha]} \tag{53}$$

(α is a shaprness parameter; $\alpha = 3$ is a typical value). The plasma is assumed to extend to a rigid perfectly conducting wall; however, the hot plasma column is well separated from the wall as in the experimental situation.[18] Thus for sufficiently large values of r the plasma is essentially pressureless. Integrating Eq. (51) yields the first equilibrium relation

$$p(r) + \tfrac{1}{2}a^2(r) = \tfrac{1}{2}a^2(r_{large}) = \tfrac{1}{2} \tag{54}$$

The constant $a(r_{large})$ is unity because of the definition of the characteristic magnetic field B_0. Finally, the basic magnetic field

corresponding to the two given pressure profiles is written down for the Gaussian profile[8,11]

$$\alpha^2(r) = 1 - \beta \exp(-r^2) \tag{55}$$

and for the sharp profile[10]

$$\alpha^2(r) = 1 - \beta \frac{1-\tanh[\alpha(r^2-1)]}{1+\tanh[\alpha]} \tag{56}$$

The problem that remains is to determine subsidiary fields, b(r) and c(r).

By dividing Eq. (49) by r and differentiating with respect to r, one can obtain an expression for $p''(\psi^{(0)})$ which is cast in the convenient form.

$$-r p''(\psi^{(0)}) = \frac{1}{\alpha}\left(\frac{\alpha'}{r}\right)' \tag{57}$$

Substituting Eq. (57) into the right hand side of Eq. (50) produces a second order ordinary differential equation which $\psi^{(1)}(r)$ must satisfy:

$$\left(\frac{1}{r}\psi^{(1)\prime}(r)\right)' = \left[k^2 + \frac{r}{\alpha}\left(\frac{\alpha'}{r}\right)'\right]\frac{\psi^{(1)}}{r} \tag{58}$$

Before turning to the solutions of Eq. (58), which must be found numerically, two other relations among the equilibrium quantities in addition to Eq. (54) may be noted. The first one is an immediate consequence of Eqs. (44) and (45), namely

$$(rb(r))' = rc(r) \tag{59}$$

The second one results from Eq. (58) and the definitions mentioned above; it is conveniently written

$$c' - \frac{rb}{\alpha}\left(\frac{\alpha'}{r}\right)' = k^2 b \tag{60}$$

Finally, one must solve the boundary value problem for $\psi^{(1)}(r)$,

$$\psi^{(1)\prime\prime} - \frac{1}{r}\psi^{(1)\prime} = \left[k^2 + \frac{r}{a}\left(\frac{a'}{r}\right)'\right]\psi^{(1)} \tag{61}$$

$$\psi^{(1)}(0) = 0 \ , \quad \psi^{(1)\prime}(r_w) = -r_w \tag{62}$$

by numerical methods. The subsidiary equilibrium magnetic fields b(r) and c(r) may then be computed from the definition (44) and (45). The boundary condition $\psi^{(1)}(0) = 0$ results from the requirement that b(r) be regular at r = 0; the boundary condition $\psi^{(1)'}(r_w) = -r_w$ results from specifying that the applied $\ell = 0$ helical field have unit value at the conducting wall - $c(r_w) = 1$.

This fixes the value of δ for any particular configuration. The flux surface as in Eq. (38) is determined by the experimental situation. Specification of $\psi^{(1)}(r)$, as by the boundary condition $\psi^{(1)}(r_w) = -r_w$ leaves the parameter δ to be adjusted to fit the actual shape of the bumpy surface.

If the pressure profile is a well behaved function of r, the basic magnetic field, a(r), must also be well behaved, and have a valid power series expansion

$$a(r) = a(0) + \frac{1}{2}a''(0)\,r^2 + \frac{1}{6}a'''(0)\,r^3 + \cdots$$

(note that a(r) has a minimum at r = 0). Using this fact, one finds a power series expansion for the function

$$\frac{r}{a}\left(\frac{a'}{r}\right)' = \frac{1}{2}\frac{a'''(0)}{a(0)}\,r + \frac{1}{3}\frac{a^{IV}(0)}{a(0)}\,r^2 + \cdots$$

One sees that the differential equation (61) has a regular singular point at r = 0, thus, Frobenius' series method[19,20] may be used to find a solution. Assuming

$$\psi^{(1)}(r) = \sum_{n=0}^{\infty} g_n r^{n+\alpha}$$

and substituting into Eq. (61), one finds

$$\alpha(\alpha-2) g_0 r^{\alpha-2} + (\alpha+1)(\alpha-1) g_1 r^{\alpha-1} + [\alpha(\alpha+2) g_2 - k^2 g_0] r^{\alpha}$$
$$+ \left[(\alpha+1)(\alpha+3) g_3 - k^2 g_1 - \frac{1}{2}\frac{\alpha''(0)}{\alpha(0)} g_0\right] r^{\alpha+1} + \cdots = 0$$

Thus

$$\alpha(\alpha-2) g_0 = 0$$
$$(\alpha+1)(\alpha-1) g_1 = 0$$
$$(\alpha+2)\alpha g_2 - k^2 g_0 = 0$$

The indicial equation has solutions $\alpha = 2$ and $\alpha = 0$, the first of which yields a valid series solution

$$\psi_1^{(1)}(r) = g_0 r^2 + \frac{k^2}{8} g_0 r^4 + \cdots$$

This solution satisfies the boundary condition $\psi^{(1)}(0) = 0$. To find a second, linearly independent solution, one uses the standard method of variation of constants, finding

$$\psi_2^{(1)}(r) = \psi_1^{(1)}(r) \int^r \frac{r'\,dr'}{[\psi_1^{(1)}(r')]^2}$$

Integration by parts yields

$$\psi_2^{(1)}(r) = \psi_1^{(1)}(r) \ln(r) + \sum_{n=0}^{\infty} h_n r^n$$

This solution is eliminated by the regularity condition. Therefore, one has for $\psi^{(1)}(r)$, b(r), and c(r)

$$\psi^{(1)}(r) = g_0 r^2\left(1 + \frac{k^2}{8} r^2 + \cdots\right) \tag{63}$$

$$b(r) = -g_0 r\left(1 + \frac{k^2}{8} r^2 + \cdots\right) \tag{64}$$

$$c(r) = -g_0\left(1 + \frac{k^2}{2} r^2 + \cdots\right) \tag{65}$$

It is expected that the first few terms are a good approximation when r is small.

When r is large, the differential equation (62) becomes (a(r) = constant for large r)

$$\psi^{(1)\prime\prime} = k^2 \psi^{(1)} \tag{62a}$$

thus, $\psi^{(1)}(r)$ behaves asymptotically as an exponential function - $\psi^{(1)} \approx e^{\pm kr}$. Unfortunately, one cannot say with absolute certainty which is the proper sign, +kr or -kr, and as the following example will show, this is a possible seat of numerical difficulty.

An Example

Consider the initial value problem

$$y''(x) = y(x); \quad y(0) = a, \quad y'(0) = -a; \quad 0 \le x \le \infty \tag{66}$$

with analytic solution $y(x) = ae^{-x}$. A numerical integration, because of round off and truncation errors, always mixes in a small portion of the other solution, e^{x}, which will always dominate the solution for sufficiently large x. Thus, one always finds a diverging solution. The same difficulty

may occur in integrating Eq. (61); one may find $\psi^{(1)} \sim e^{kr}$ when in fact $\psi^{(1)} \sim e^{-kr}$ is the proper solution. However, this difficulty can be overcome.

Consider the change of variables

$$y(x) = A \exp\left[\int^{x} f(x')\, dx'\right] \tag{67}$$

Then $y'(x) = f(x)\, y(x)$ and $y''(x) = f'(x)\, y(x) + f^2(x)\, y(x)$, and Eq. (66) becomes

$$f'(x) = 1 - f^2(x); \quad f(0) = 1$$

The solution is immediately, $f(x) = -1$, and is also the numerical solution since the computer evaluates f' to be zero (there is no roundoff because a number is subtracted from itself). Using Eq. (67), one finds $y(x) = A \exp[\int^{x} -dx] = Ae^{-x}$. Thus, by using the change of variables (67), the second order differential equation is reduced to one of first order. This alleviates the possibility of finding the wrong solution.

The Specific Problem

Substituting (67) into Eq. (61), one finds

$$f'(r) = \frac{f(r)}{r} - f^2(r) + k^2 + \frac{r}{a}\left(\frac{a'}{r}\right)' \tag{68}$$

while the boundary condition $\psi^{(1)}(r_w) = -r_w$ becomes

$$\frac{1}{A} = -\frac{f(r_w)}{r_w} \exp\left[\int^{r_w} f(r')\, dr'\right] \tag{69}$$

An important feature of the equilibria is evident from Eq. (69), namely, that at a given position, r, within the plasma column, $\psi^{(1)}(r)$ depends on the wall position only through the scale factor A, given by Eq. (69);

the functional form of $\psi^{(1)}(r)$ is not dependent on wall position. The asymptotic form for small r, Eq. (63) is recovered provided that for small r

$$f(r) \sim \frac{2}{r}$$

This asymptotic form provides an initial value for small which is used as a starting point in a numerical integration of Eq. (68) to determine f(r). This function reveals the nature of $\psi^{(1)}(r)$. The constant, A, may then be computed from the normalization condition, Eq. (69).

Figure 6 shows the function $\frac{r}{a}(\frac{a'}{r})'$ for the Gaussian profile while Fig. 7 shows the same function for the sharp profile. Explicitly, this function is

$$\frac{r}{a}\left(\frac{a'}{r}\right)' = -\frac{r^2\beta \exp(-r^2)}{1-\beta\exp(-r^2)}\left[2 + \frac{\beta\exp(-r^2)}{1-\beta\exp(-r^2)}\right] \qquad (70)$$

For the Gaussian profile; for the sharp profile, it is

$$\frac{r}{a}\left(\frac{a'}{r}\right)' = -\frac{r^2\beta\,\mathrm{sech}^2[\alpha(r^2-1)]}{1+\tanh[\alpha]-\beta+\beta\tanh[\alpha(r^2-1)]}\left\{4\alpha\tanh[\alpha(r^2-1)] + \frac{\alpha\beta\,\mathrm{sech}^2[\alpha(r^2-1)]}{1+\tanh[\alpha]-\beta+\beta\tanh[\alpha(r^2-1)]}\right\}$$

Both functions are well behaved and rapidly approach zero with increasing r. Equation (68) is integrated numerically using a standard fourth order Runge-Kutta integration subroutine, RKGS, from the IBM Scientific Subroutine Package. The resulting solution is plotted in Fig. 8 for the Gaussian profile and in Fig. 9 for the sharp profile. The most important feature

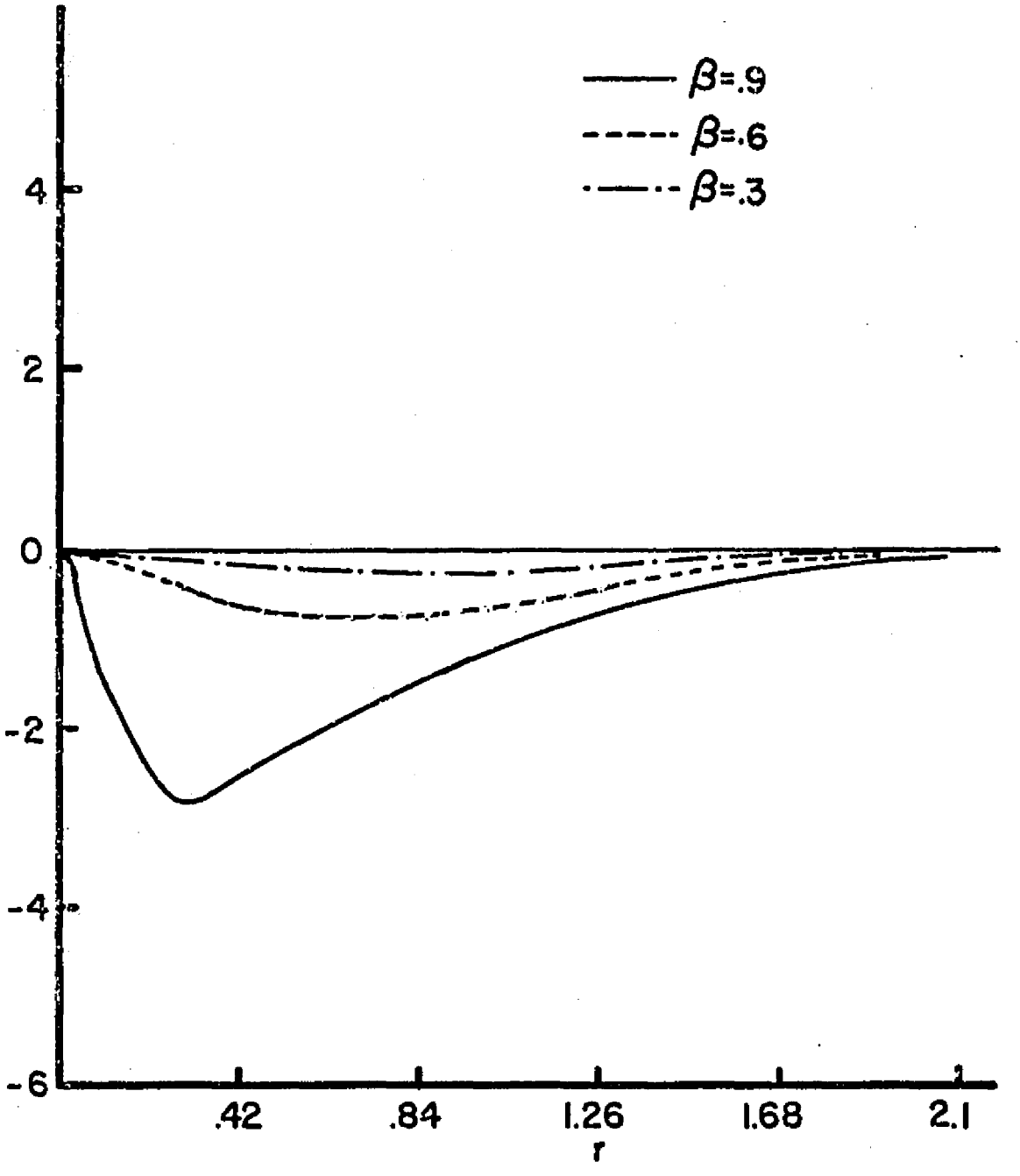

Fig. 6. The equilibrium function $r/a(a'/r)'$ for various values of plasma beta plotted against r, the radius of the plasma column for Gaussian equilibrium profiles. The function is negligibly small for $r > 3.0$.

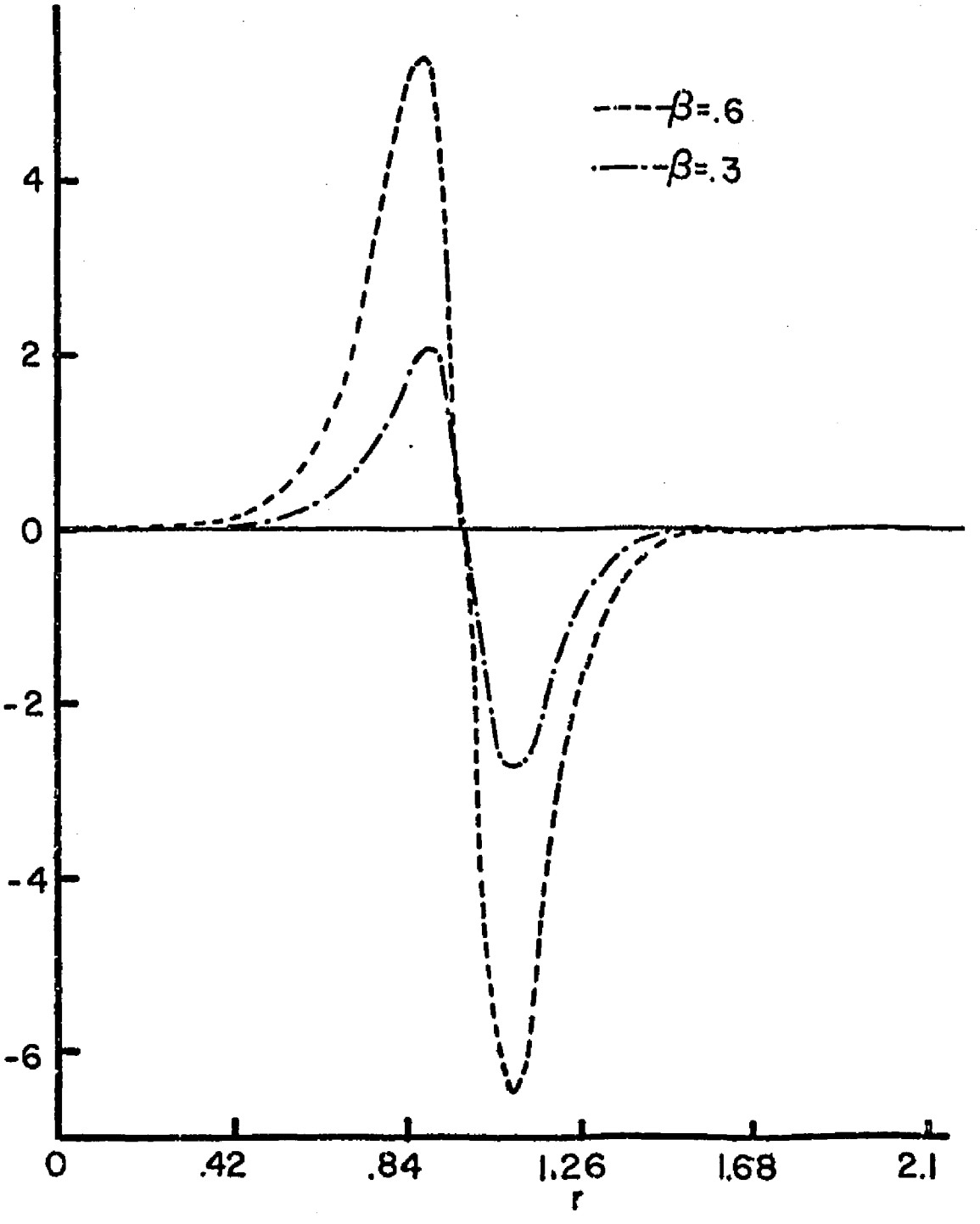

Fig. 7. The equilibrium function $r/a(a'/r)'$ for various values of plasma beta plotted against r, the radius of the plasma column for sharp equilibrium profiles. The function is negligibly small for $r > 1.6$.

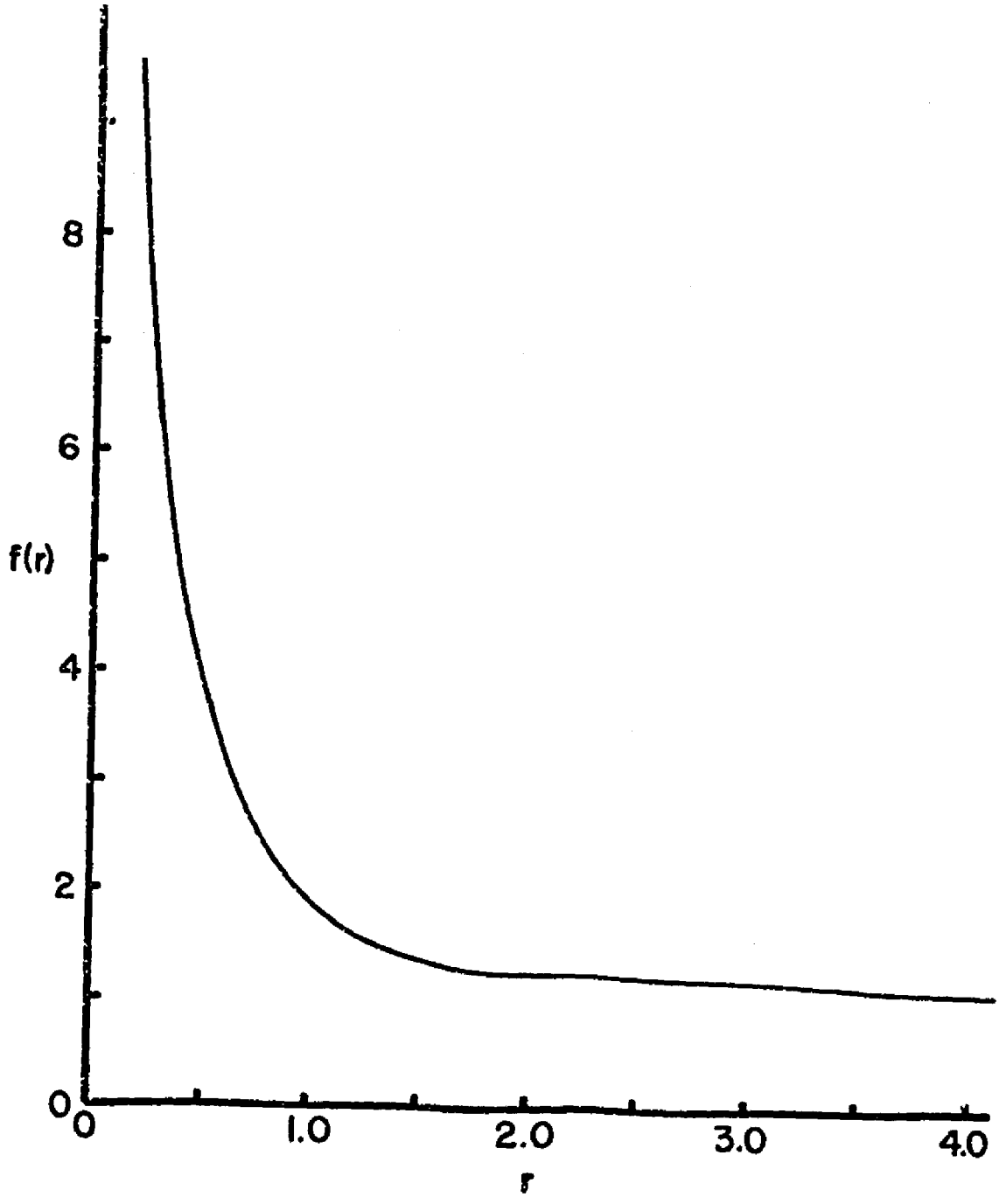

Fig. 8. Numerical solution of the first order differential equation, Eq. (68), for Gaussian equilibrium profiles with $\beta = .8$. The solution approaches the value $f(r) = 1$ for large values of r.

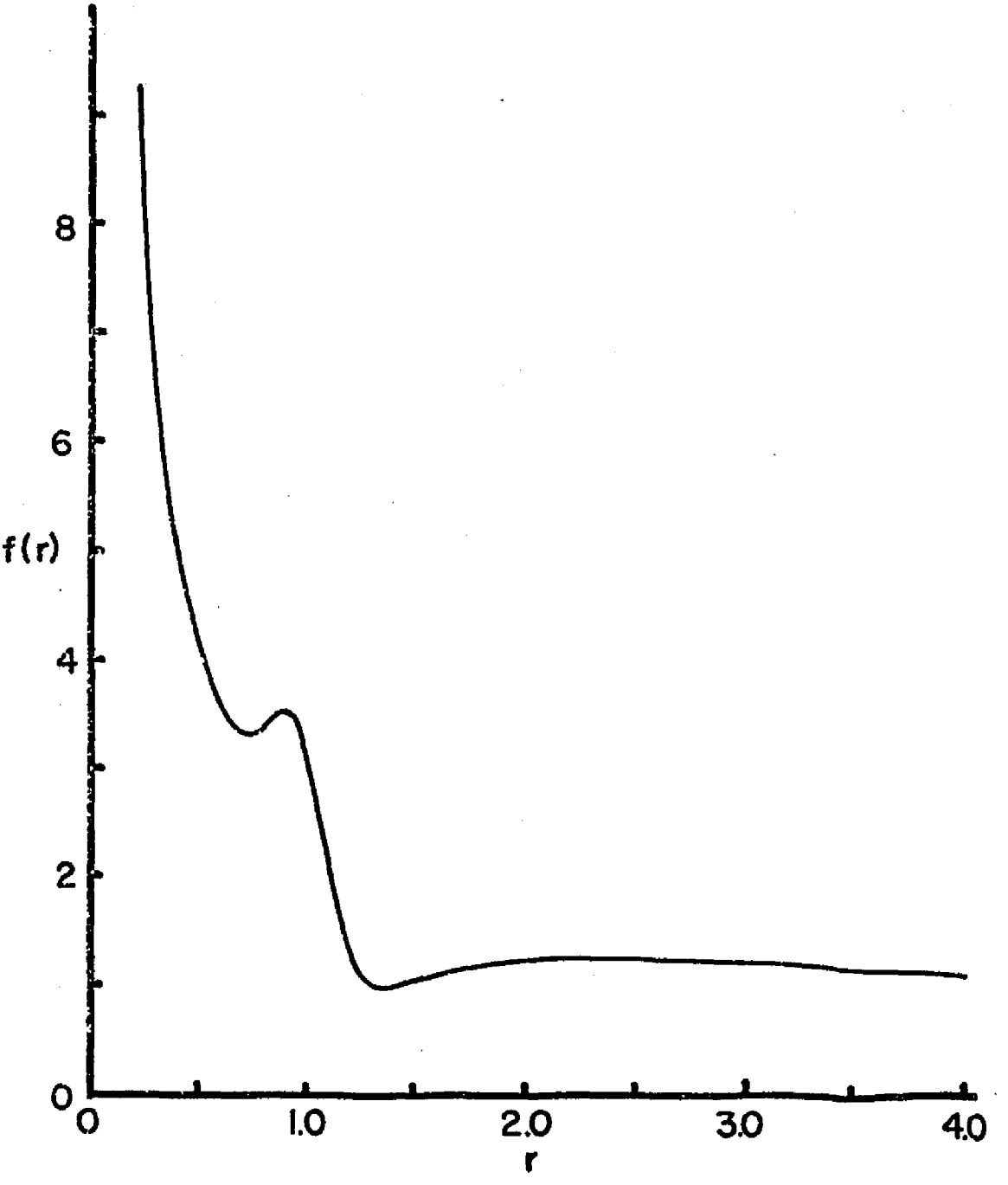

Fig. 9. Numerical solution of the first order differential equation, Eq. (68), for sharp equilibrium profiles with $\beta = .8$. The solution approaches the value $f(r) = 1$ for large values of r.

is that all the solution approach the value +k as r increases. Although an answer can now be obtained by calculating the normalization from Eq. (69), it is convenient to return to the second order equation, Eq. (61), after having established that the proper asymptotic form is $\psi^{(1)}(r) \sim e^{kr}$.

The shooting method[21,22] is employed to numerically solve the boundary value problem

$$\psi^{(1)''}(r) = \frac{1}{r}\psi^{(1)'}(r) + \left[k^2 + \frac{1}{a}\left(\frac{a}{r}\right)'\right]\psi^{(1)}(r) \tag{61}$$

$$\psi^{(1)}(0) = 0 \ , \quad \psi^{(1)'}(r_w) = -r_w \tag{62}$$

The asymptotic form for small r, Eq. (63), provides two initial conditions which are proportional to the unknown constant g_0. This use of Eq. (63) guarantees that the first b.c., $\psi^{(1)}(0) = 0$, is satisfied, while avoiding difficulties because of the singular point at r = 0. Decomposing Eq. (61) into a pair of first order differential equations allows the use of the subroutine RKGS of the IBM Scientific Subroutine Package for integrating the initial value problem. The value of $\psi^{(1)'}(r_w)$ now depends on the initial constant g_0 and one may show this explicitly by defining a function z

$$z(r_w; g_0) \equiv r_w + \psi^{(1)'}(r_w)$$

When $z(g_0)$ vanishes, the solutions of the initial value problem and the boundary problem are identical.

The zeroes of $z(g_0)$ are found by a marching method and the estimates are refined by interval-halving. That is, an initial guess of the position of the zero, G, is given together with an initial increment,

Δ; the integration routine yields $z(r_w, G)$, then $z(r_w; G + \Delta)$, one of which is a better estimate of the position of the zero. If $z(r_w, G + \Delta)$ is better, $z(r_w; G + 2\Delta)$ is computed, etc. If $z(r_w, G)$ is the better estimate, $z(r_w; G - \Delta)$ is computed, then $z(r_w, G - 2\Delta)$, etc. If $z(r_w; G + n\Delta)$ vanishes, then, of course, $G + n\Delta$ is the missing initial value which provides the solution of the boundary value problem. If $z(r_w; G + n\Delta)$ and $z(r_w; G + (n + 1)\Delta)$ have opposite sign, then the zero lies in the interval between these two values. To refine this estimate, $z(r_w; G + (n + 1/2)\Delta)$ is computed. This value is either zero, of the same sign as $z(r_w; G + n\Delta)$, or of opposite sign. If zero, then $G + (n + 1/2)\Delta$ is the desired value; if of different sign from $z(G + n\Delta)$, then the zero lies in the subinterval $(G + n\Delta, G + (n + 1/2)\Delta)$; if of the same sign, the zero lies in the other subinterval. Bisection of the appropriate subinterval is continued until a sufficiently accurate estimate is obtained.

Two classes of bumpy theta pinch equilibria are considered. Finite wave wavelength equilibria are characterized by a finite value of wavevector k, while long wavelength equilibria (see Appendix B) are characterized by a very small value of k. The value $k = 1$ is chosen as representative of the finite wavelength case and $k = 10^{-5}$ as representative of the long wavelength case. Note that wavelength effects are present in the subsidiary fields only; the primary theta pinch field, a(r) is the same for all values of k.

Figures (10) and (11) show the pressure profile and the basic theta pinch field, a(r) for the Gaussian profile and the sharp profile, for typical parameter values. In Figs. (12) and (13) the subsidiary fields, b(r) and c(r), corresponding to the Gaussian pressure profile are

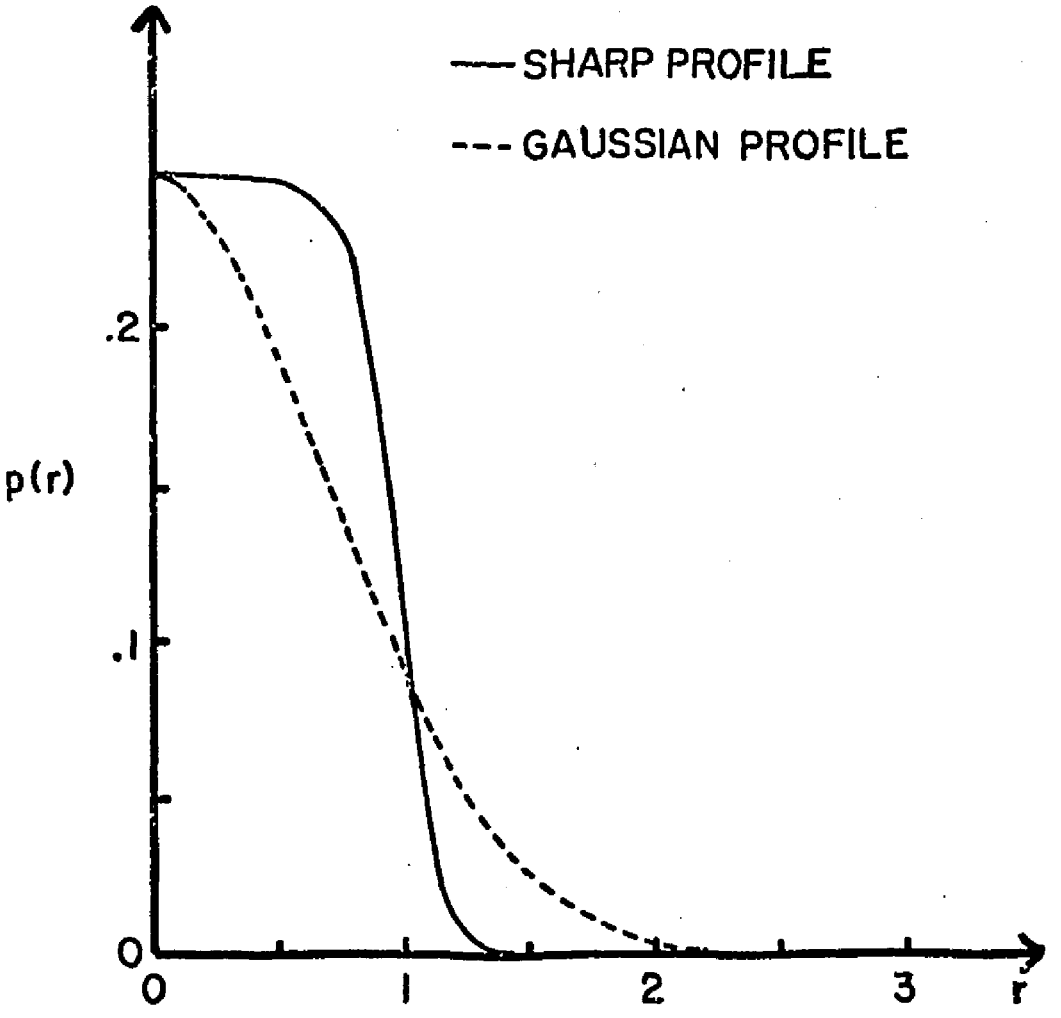

Fig. 10. The equilibrium pressure profiles for $\beta = .5$.

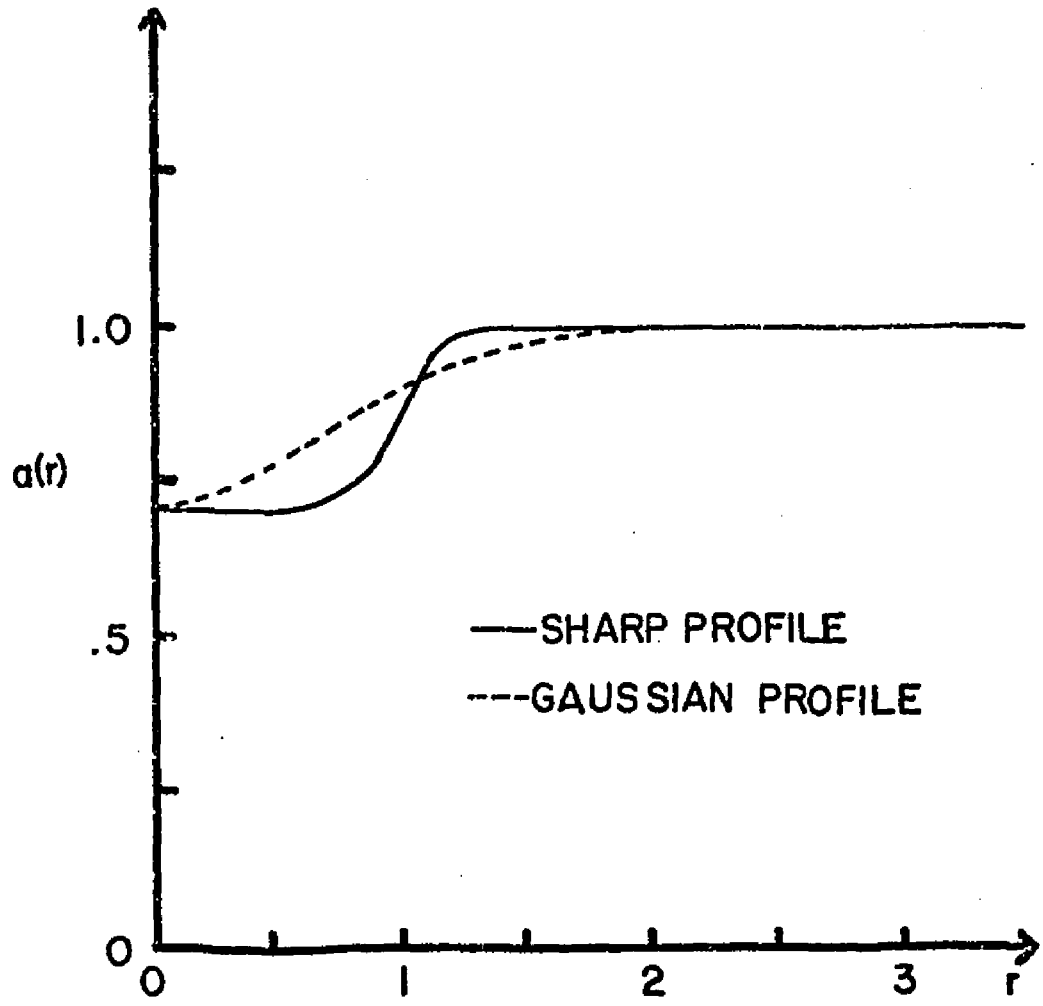

Fig. 11. Profiles of the basic equilibrium magnetic field for $\beta = .5$.

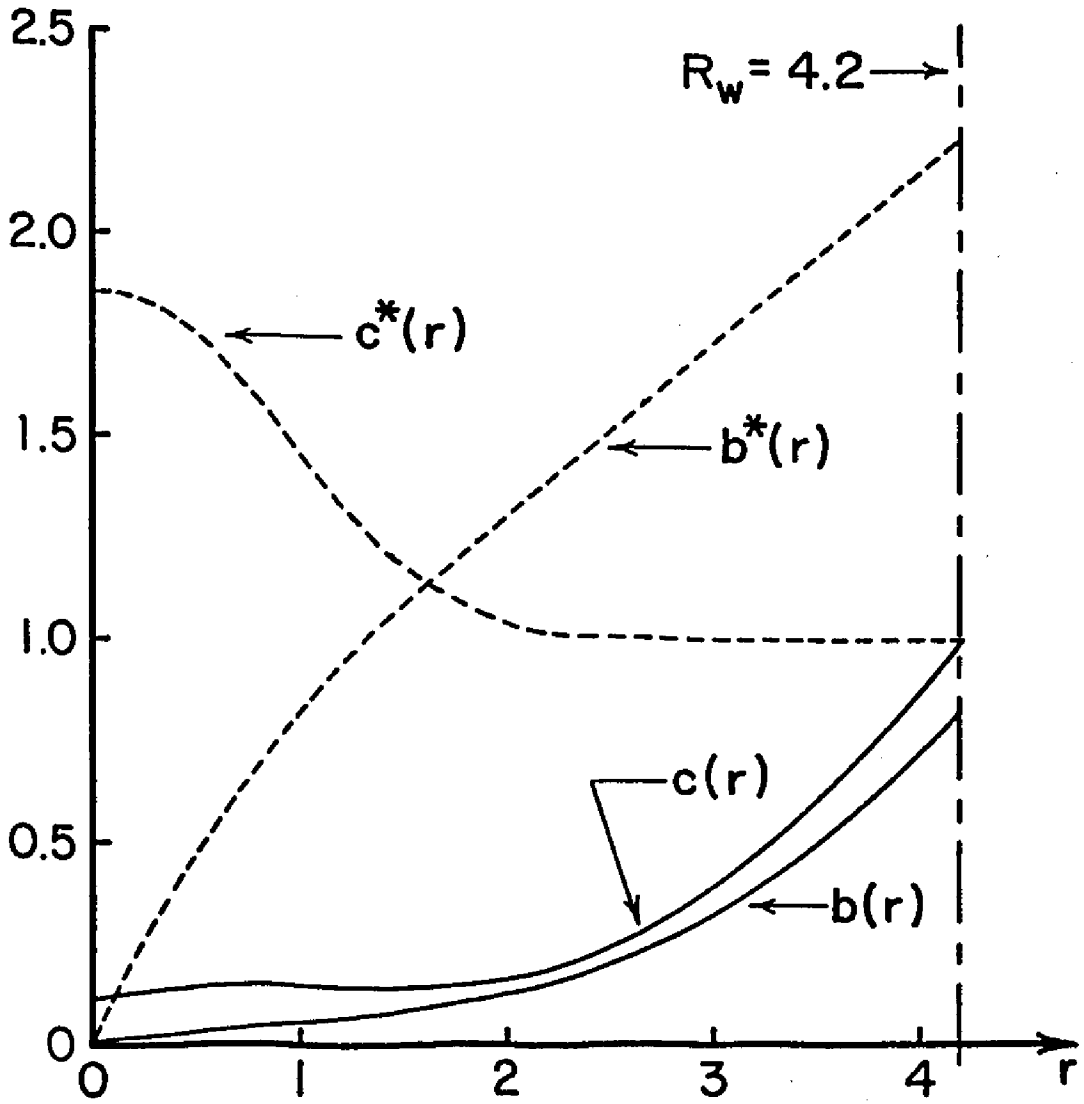

Fig. 12. Typical subsidiary equilibrium magnetic field quantities plotted against r for the finite (k = 1) wavelength (solid curves) and long (k ≈ 0) wavelength case (dashed curves and denoted by asterick) for Gaussian pressure profile with $\beta = .7$ and $r_w = 4.2$.

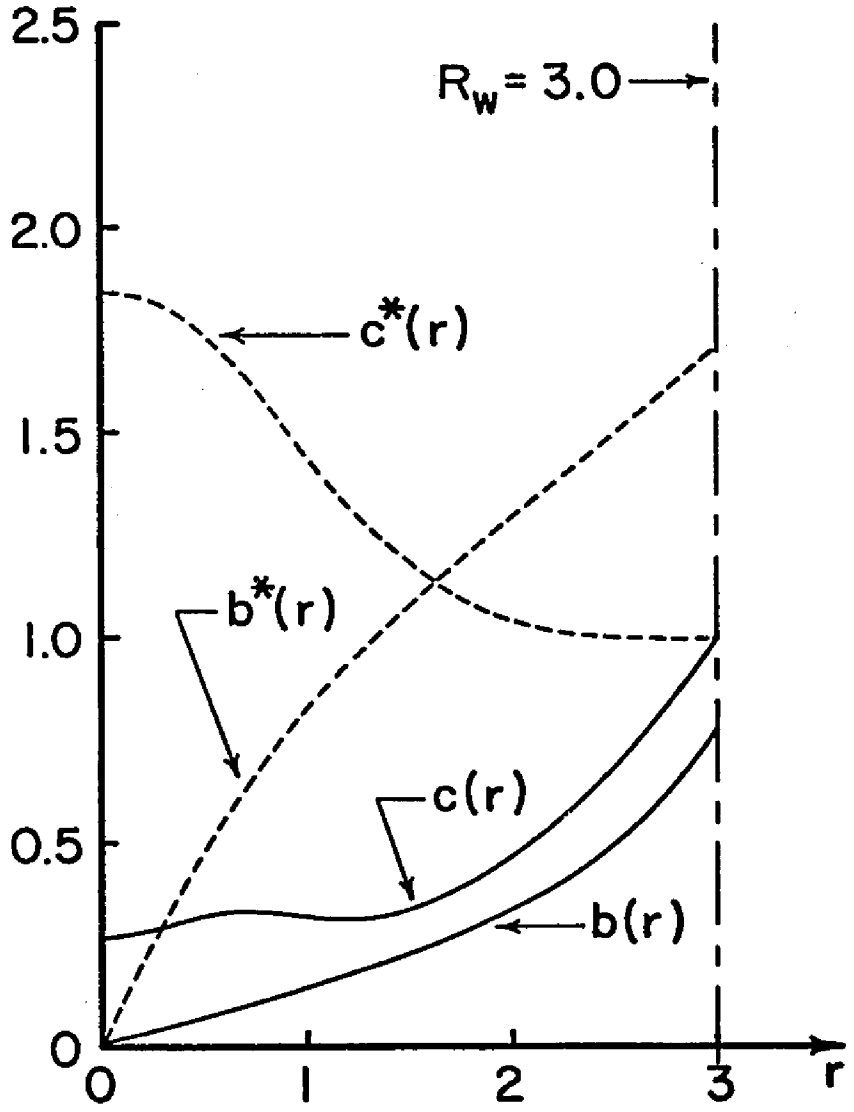

Fig. 13. Typical subsidiary equilibrium magnetic field quantities for finite (k = 1) wavelength (solid curves) and long (k ≈ 0) wavelength case (dashed curves and denoted by asterick) for Gaussian pressure profile with $\beta = .7$ and $r_w = 3.0$. Note that only the finite wavelength field is affected by wall position.

shown for the finite wavelength and long wavelength (denoted by *) cases, for two wall positions, $r_w = 4.2$ and $r_w = 3.0$. In Figs. (14) and (15) the subsidiary fields for the sharp profile are shown for $r_w = 4.2$ and $r_w = 1.6$. One sees that the exponential tail of $\psi^{(1)}(r)$ predicted by Eq. (67a) strongly influences the subsidiary equilibrium magnetic fields in the finite wavelength case (in the long wavelength case, Eq. (62a) becomes $\psi^{(1)''} = \psi^{(1)'}/r$ and predicts quadratic behavior). Because of this exponential tail, the subsidiary fields within the plasma depend on the position of the conducting wall in the finite wavelength case but not in the long wavelength case. That is, the scale factor mentioned in connection with Eq. (69) changes with wall position in the finite wavelength case, but is constant in the long wavelength case. These differences may be expected to affect the stability properties of the equilibria.

D. Summary

For axisymmetric ideal hydromagnetic equilibria the magnetic field, $(B_r(r, z), 0, B_z(r, z))$, is defined in terms of a magnetic flux function, $\psi(r, z)$. Approximate solutions of the second order nonlinear partial differential equation

$$\frac{\partial}{\partial r}\left(\frac{1}{r}\frac{\partial \psi}{\partial r}\right) + \frac{1}{r}\frac{\partial^2 \psi}{\partial z^2} = -r p'(\psi) \qquad (36)$$

are found under the assumption that the flux surfaces deviate slightly from right circular cylinders. This deviation is measured by a small parameter δ in terms of which the flux function is expanded in the form:

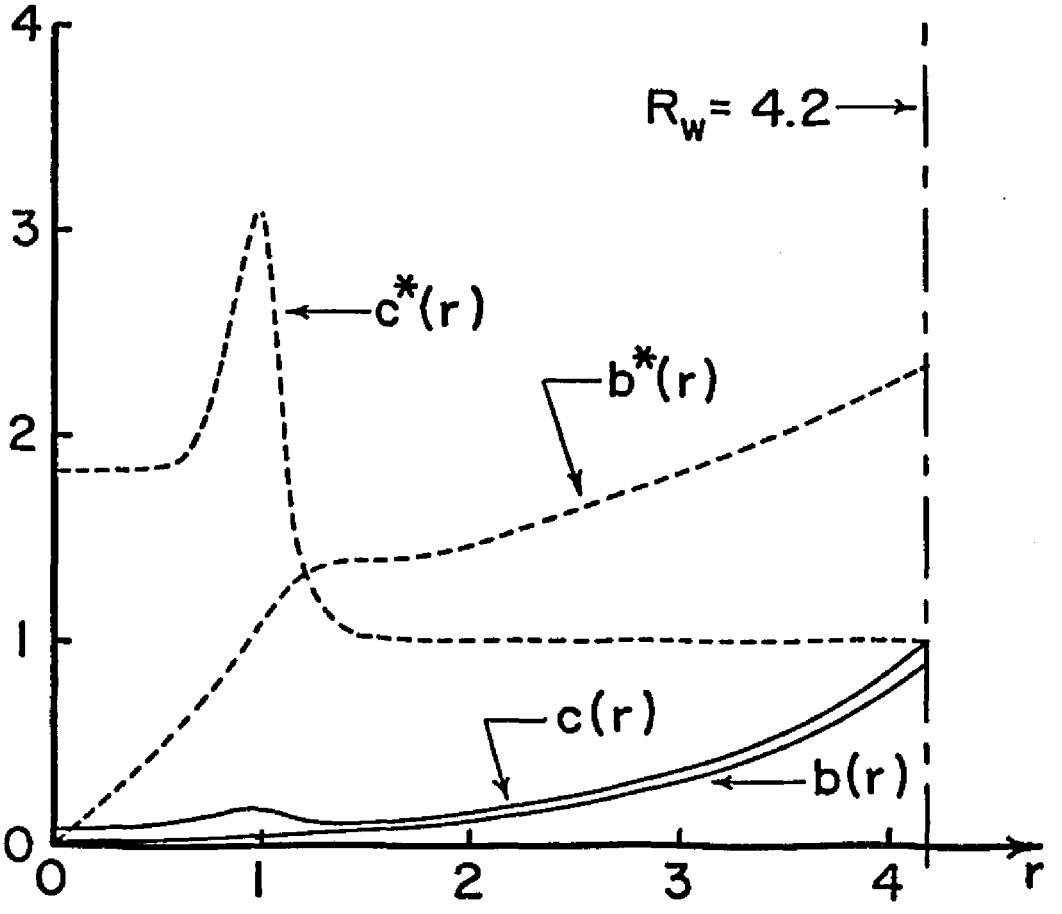

Fig. 14. Typical subsidiary equilibrium magnetic field quantities plotted against r for the finite (k = 1) wavelength (solid curves) and long (k ≈ 0) wavelength case (dashed curves and denoted by asterick) for sharp pressure profile with β= .7 and r_w = 4.2.

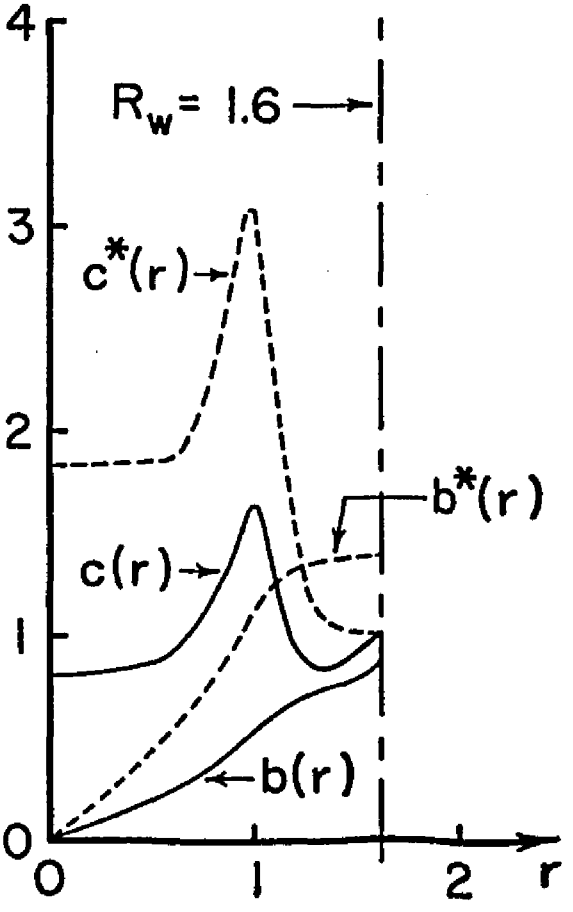

Fig. 15. Typical subsidiary equilibrium magnetic field quantities plotted against r for the finite (k = 1) wavelength (solid curves) and long (k ≈ 0) wavelength case (dashed curves and denoted by asterick) for sharp pressure profile with β = .7 and r_w = 1.6. Note that only the finite wavelength field is affected by wall position.

$$\psi(r,z) = \psi^{(0)}(r) + \delta\psi^{(1)}(r)\cos(kz) + O(\delta^2) \tag{37}$$

A standard perturbation expansion of Eq. (36) yields several relations among the equilibrium quantities

$$p(r) + \frac{1}{2}a^2(r) = \frac{1}{2} \tag{54}$$

$$(rb)' = rc \tag{59}$$

$$c' - \frac{rb}{a}\left(\frac{a'}{r}\right)' = k^2 b \tag{60}$$

and a second order ordinary differential equation for $\psi^{(1)}(r)$

$$\psi^{(0)''}(r) = \frac{1}{r}\psi^{(0)'}(r) + \left[k^2 + \frac{r}{a}\left(\frac{a'}{r}\right)'\right]\psi^{(0)}(r) \tag{67}$$

The numerical solution of this equation, subject to appropriate boundary conditions completes the determination of the equilibrium magnetic field for given pressure profiles. Two classes of equilibria are considered - finite wavelength equilibria with k = 1 and long wavelength equilibria with $k = 10^{-5}$. Important differences in the behavior of the subsidiary field quantities b(r) and c(r) as the wall position varies are noted.

III. STABILITY OF THE BUMPY THETA PINCH EQUILIBRIA

A. Linear Stability Analysis

In this chapter the stability of the equilibrium configurations which were described in the previous chapter is investigated. The velocity formulation of linearized ideal MHD is employed to study the time evolution of small perturbations of the equilibrium quantities. If the small perturbations remain small as they evolve in time, then the equilibrium configuration is said to be stable; if the small perturbation is found to become large as the time evolution proceeds, then eventually the assumptions that permitted linearization of the equations will become invalid, in this case the equilibrium configuration is said to be unstable. The analysis is undertaken in the standard cylindrical polar coordinate system.

For convenience the linearized equations of ideal MHD are reproduced below in terms of the dimensionless variables of the previous chapter.

$$\frac{\partial \rho_1}{\partial t} + (\underset{\sim}{u}_1 \cdot \nabla)\rho_0 + \rho_0(\nabla \cdot \underset{\sim}{u}_1) = 0 \tag{1}$$

$$\rho_0 \frac{\partial \underset{\sim}{u}_1}{\partial t} = -\nabla p_1 + (\nabla \times \underset{\sim}{B}_1) \times \underset{\sim}{B}_0 + (\nabla \times \underset{\sim}{B}_0) \times \underset{\sim}{B}_1 \tag{2}$$

$$\frac{\partial \underset{\sim}{B}_1}{\partial t} = \nabla \times (\underset{\sim}{u}_1 \times \underset{\sim}{B}_0) \tag{3}$$

$$\frac{\partial p_1}{\partial t} - \frac{\gamma p_0}{\rho_0}\frac{\partial \rho_1}{\partial t} + (\underset{\sim}{u}_1 \cdot \nabla)p_0 - \frac{\gamma p_0}{\rho_0}(\underset{\sim}{u}_1 \cdot \nabla)\rho_0 = 0 \tag{4}$$

The velocity formulation results when Eq. (2) is differentiated once with respect to time, yielding

$$\rho_0 \frac{\partial^2 \underset{\sim}{u}_1}{\partial t^2} = -\nabla \frac{\partial p_1}{\partial t} + \left(\nabla \times \frac{\partial \underset{\sim}{B}_1}{\partial t}\right) \times \underset{\sim}{B}_0 + \left(\nabla \times \underset{\sim}{B}_0\right) \times \frac{\partial \underset{\sim}{B}_1}{\partial t} \quad (5)$$

Direct substitution then produces a second order partial differential equation which must be satisfied by the perturbed velocity field, $\underset{\sim}{u}$, $(\underset{\sim}{x},t)$. The differential equation may be interpreted as the result of action of a linear operator operating on the velocity field; this linear operator involves the equilibrium quantities as coefficients. Because of the symmetries of the equilibrium, i.e. the trivial invariance under infinitesimal time translation and infinitesimal azimuthal displacement this linear operator commutes, trivially, with the two linear operator, $\frac{\partial}{\partial t}$ and $\frac{\partial}{\partial \theta}$. Since two linear operators which commute possess simultaneous eigenfunctions, the perturbed velocity field can be expanded in terms of the eigenfunctions of the two operators $\frac{\partial}{\partial t}$ and $\frac{\partial}{\partial \theta}$, namely $e^{-i\omega t}$ and $e^{im\theta}$, where ω is an arbitrary parameter and single-valuedness is assured by restricting m to be an integer. Furthermore, each value of the two parameters, ω and m can be treated independently since Eq. (5) is a linear equation.

Upon substituting and rearranging, Eq. (5) becomes

$$-\rho\omega^2 \underset{\sim}{u}_1(\omega,m;r,z) + \nabla P(\omega,m;r,z) = \underset{\sim}{T}(\omega,m;r,z) \quad (7)$$

where P, the "total pressure", and $\underset{\sim}{T}$, the "tension", are given by

$$P = i\omega\left(p_1 + \underset{\sim}{B}_0 \cdot \underset{\sim}{B}_1\right) \quad (8)$$

$$\underset{\sim}{T} = i\omega\left[\left(\underset{\sim}{B}_1 \cdot \nabla\right)\underset{\sim}{B}_0 + \left(\underset{\sim}{B}_0 \cdot \nabla\right)\underset{\sim}{B}_1\right] \quad (9)$$

The factor $e^{-i\omega t}\, e^{im\theta}$ has been suppressed. Various quantities are now written down using the following notation: $\underset{\sim}{B}_0 = (B_r, 0, B_z)$; $\underset{\sim}{B}_1 = (b_r, b_\theta, b_z)$; $\underset{\sim}{u}_1 = (u, v, w)$. One finds

$$i\omega b_r = \frac{\partial}{\partial z}(uB_z - wB_r) - \frac{im}{r} v B_r \tag{10}$$

$$i\omega b_\theta = \frac{\partial}{\partial r}(vB_r) + \frac{\partial}{\partial z}(vB_z) \tag{11}$$

$$i\omega b_z = \frac{1}{r}\frac{\partial}{\partial r}(rwB_r) - u\frac{\partial B_z}{\partial r} - B_z\left(\frac{1}{r}\frac{\partial}{\partial r}(ru) + \frac{im}{r}v\right) \tag{12}$$

$$P \equiv i\omega(p_1 + \underset{\sim}{B}_0 \cdot \underset{\sim}{B}_1) = -(\gamma p + B_z^2)\left(\frac{1}{r}\frac{\partial}{\partial r}(ru) + \frac{im}{r}v\right) - (\gamma p + B_r^2)\frac{\partial w}{\partial z} \tag{13}$$
$$- wB_r\frac{\partial B_z}{\partial r} + \frac{B_z}{r}\frac{\partial}{\partial r}(rwB_r) - uB_z\frac{\partial B_r}{\partial z} + B_r\frac{\partial}{\partial z}(uB_z) - B_r^2\frac{im}{r}v$$

$$T_r = \left\{B_r\frac{\partial}{\partial r} + \frac{\partial B_r}{\partial r} + B_z\frac{\partial}{\partial z}\right\}\left[\frac{\partial}{\partial z}(uB_z - wB_r) - \frac{im}{r}vB_r\right] \tag{14}$$
$$+\left\{\frac{\partial B_r}{\partial z}\right\}\left[\frac{1}{r}\frac{\partial}{\partial r}(rwB_r) - u\frac{\partial B_z}{\partial r} - B_z\left(\frac{1}{r}\frac{\partial}{\partial r}(ru) + \frac{im}{r}v\right)\right]$$

$$T_\theta = \left\{B_r\frac{\partial}{\partial r} + \frac{B_r}{r} + B_z\frac{\partial}{\partial z}\right\}\left[\frac{\partial}{\partial r}(vB_r) + \frac{\partial}{\partial z}(vB_z)\right] \tag{15}$$

$$T_z = \left\{B_r\frac{\partial}{\partial r} + B_z\frac{\partial}{\partial z} + \frac{\partial B_z}{\partial z}\right\}\left[\frac{1}{r}\frac{\partial}{\partial r}(rwB_r) - u\frac{\partial B_z}{\partial r} - B_z\left(\frac{1}{r}\frac{\partial}{\partial r}(ru) + \frac{im}{r}v\right)\right] \tag{16}$$
$$+\left\{\frac{\partial B_z}{\partial r}\right\}\left[\frac{\partial}{\partial z}(uB_z - wB_r) - \frac{im}{r}vB_r\right]$$

These expressions are used in the analysis that follows.

It is recalled that the equilibrium magnetic field components have the following form

$$B_r = \delta k b(r)\sin(kz) + \mathcal{O}(\delta^2)$$
$$B_z = a(r) + \delta c(r)\cos(kz) + \mathcal{O}(\delta^2) \tag{17}$$

To make the expressions for P and $\underset{\sim}{T}$, Eqs. (13)-(16), explicit, a representation for the form of the perturbed velocity field, $\underset{\sim}{u}_1$, is assumed which resembles that of magnetic flux function.

$$u = e^{-i\omega t} e^{im\theta} e^{il k\delta z}\left[u^{(0)}(r) + \delta u^{(1)}(r)\cos(kz) + O(\delta^2)\right] \quad (18)$$

$$v = e^{-i\omega t} e^{im\theta} e^{il k\delta z}\left[v^{(0)}(r) + \delta v^{(1)}(r)\cos(kz) + O(\delta^2)\right] \quad (19)$$

$$w = e^{-i\omega t} e^{im\theta} e^{il k\delta z}\left[w^{(0)}(r) + \delta w^{(1)}(r)\sin(kz) + O(\delta^2)\right] \quad (20)$$

Here the dependence on θ and t is shown explicitly. If m = 1 this perturbation is, to lowest order in δ, a kink mode of wavenumber $\ell k\delta$ (ℓ is a real number). The wavenumber is small and is scaled to the small quantity $k\delta$; the wavelength of the mode is large. In high beta theta pinch experiments very long wavelength kink modes are the only unstable modes that are observed.[1,12] Equation (7) will now be investigated for modes of this type.

B. Modes with $\omega = O(1)$ in $k\delta$

Substitution of Eqs. (18)-(20) into Eqs. (13)-(16) yields

$$P = -(\gamma p + a^2)\left(\frac{1}{r}\frac{d}{dr}(ru^{(0)}) + \frac{im}{r}v^{(0)}\right) + O(\delta^2)$$

$$\underset{\sim}{T} = 0 + O(\delta)$$

Then to lowest order in δ Eq. (7) becomes

$$\begin{aligned} -\rho\omega^2 u^{(0)} &= \frac{d}{dr}\left[(\gamma p + a^2)\left(\frac{1}{r}\frac{d}{dr}(ru^{(0)}) + \frac{im}{r}v^{(0)}\right)\right] \\ -\rho\omega^2 v^{(0)} &= \frac{im}{r}\left[(\gamma p + a^2)\left(\frac{1}{r}\frac{d}{dr}(ru^{(0)}) + \frac{im}{r}v^{(0)}\right)\right] \\ -\rho\omega^2 w^{(0)} &= 0 \end{aligned} \quad (21)$$

Thus, the perturbed flow must be transverse to the basic magnetic field $a(r)\hat{z}$. In what follows an arrow over a quantity denotes the r - θ component vector, $\vec{v}^{(0)} = u^{(0)}\hat{r} + {}^{(0)}\hat{\theta}$. Equation (21) is rewritten in this notation

$$\rho\omega^2\vec{v}^{(\omega)} + \vec{\nabla}\left[(\gamma p + a^2)\,\vec{\nabla}\cdot\vec{v}^{(\omega)}\right] = 0 \tag{22}$$

Introducing a velocity potential, $\chi(r)$, such that

$$\vec{v}^{(\omega)} = \frac{1}{\rho}\vec{\nabla}\chi$$

one finds that χ satisfies the following differential equation

$$\vec{\nabla}\left\{\left[\frac{\gamma p + a^2}{\rho}\right]\left[\frac{\rho}{r}\left(\frac{r}{\rho}\chi'\right)' + \left(\frac{\rho\omega^2}{\gamma p + a^2} - \frac{m^2}{r^2}\right)\chi\right]\right\} = 0 \tag{23}$$

Thus

$$\left[\frac{\gamma p + a^2}{\rho}\right]\left[\frac{\rho}{r}\left(\frac{r}{\rho}\chi'\right)' + \left(\frac{\rho\omega^2}{\gamma p + a^2} - \frac{m^2}{r^2}\right)\chi\right]e^{im\theta}e^{il k\delta z} = f^n(z) \tag{24}$$

Two separate cases must be included; first the situation with $m \neq 0$ is considered, then $m = 0$ is discussed. Since this work is concerned with kink modes with $m = 1$, little space is devoted to the less interesting $m = 0$ sausage mode.

After dividing by $e^{il k\delta z}$, if $m \neq 0$ the left hand side of Eq. (24) is a function of r and θ while the right hand side is a function of z; this is possible only if the function of z is a constant, A. If one then divides by $e^{im\theta}$ the left hand side of the equation is a function of r alone while the right hand side is a function of θ alone, $Ae^{-im\theta}$; this is possible only if both the left-hand side and the right-hand side

separately equal the same constant, B. The right-hand side of Eq. (24) is thus seen to give

$$(\text{constant})e^{-im\theta} = \text{constant}$$

which is possible only if both constants are identically zero. Therefore, the velocity potential for these modes satisfies the self-adjoint ordinary differential equation

$$\frac{\rho}{r}\left(\frac{r}{\rho}\chi'\right)' + \left(\frac{\rho\omega^2}{\gamma p + a^2} - \frac{m^2}{r^2}\right)\chi = 0 \qquad (25)$$

which is similar to Bessel's equation (if the primary magnetic field and, consequently, the plasma pressure and density, are constants Eq. (25) is Bessel's equation). Appropriate boundary conditions are a) regularity of $\chi(r)$ at $r = 0$, and b) since the plasma is assumed to extend to a rigid, perfectly conducting wall, the vanishing of the normal velocity component there,

$$\hat{n} \cdot \underset{\sim}{u}_1 \Big|_{wall} = 0$$

To lowest order in δ this requirement becomes

$$u(r_w) = \frac{1}{\rho(r_w)}\chi'(r_w) = 0$$

hence

$$\chi'(r_w) = 0 \qquad (26)$$

Here, r_w is the mean position of the (bumpy) conducting wall. Equations (25) and (26) constitute a standard eigenvalue problem of Sturm-Liouville type. The eigenfunctions form a complete set and the real eigenvalues

form a discrete spectrum which exhibits a lower bound. The smallest eigenvalue corresponds to an eigenfunction with no nodes, the next smallest eigenvalue corresponds to an eigenfunction with one node, etc. In the case where the equilibrium profiles are constant, the eigenfunctions are the Bessel functions and the eigenvalues are the zeroes of their derivatives, if the wall radius is normalized to unity. It is well known that these zeroes are non-negative; thus, there are no unstable modes of this type if the profiles are constants. For the diffuse profile case the eigenvalue problem must be solved by numerical methods.

The eigenvalue problem is solved by the shooting method[21,22] using the numerical procedure described in the previous chapter. Initial values are obtained from an asymptotic expansion of Eq. (25) valid for small values of r, then with a value assumed for the eigenvalue parameter, Eq. (25) is integrated to the mean position of the conducting wall, r_w. If Eq. (26) is satisfied, the assumed value of the parameter is an eigenvalue; if Eq. (26) is not satisfied, the assumed value is modified and the procedure repeated. In Fig. (16) a portion of the computed spectrum is shown; the eigenvalues resulting from Eq. (25) with m = 0 are also shown in Fig. (16) although these do not represent modes of the plasma. It is no surprise that there are no unstable modes since this portion of the spectrum of the bumpy theta pinch is identical to that of an ordinary linear theta pinch which is known to be MHD stable. Typical eigenfunctions are sketched in Fig. (17).

The case with m = 0 is slightly more complicated. Unlike the case for $m \neq 0$, upon division by $e^{i\ell k\delta z}$ the left-hand side of Eq. (24) is

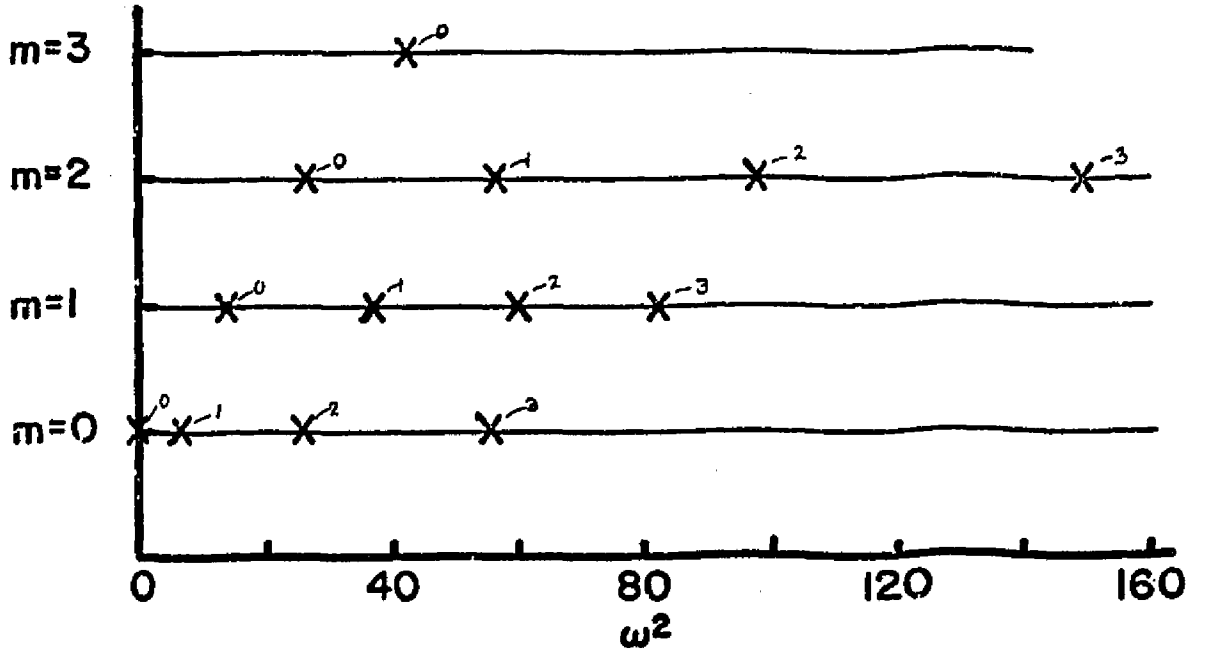

Fig. 16. Numerically computed eigenvalues of modes with $\omega = \mathcal{O}(1)$ in $k\delta$. The modes are stable. The eigenvalues with m = 0 are not normal modes of the plasma but are necessary to compute the solutions of the m = 0 case. These are for a Gaussian pressure and density (D = .001) profile with β = .5, γ = 5/3, and r_w = 4.2. The small numbers refer to the number of nodes of the eigenfunctions.

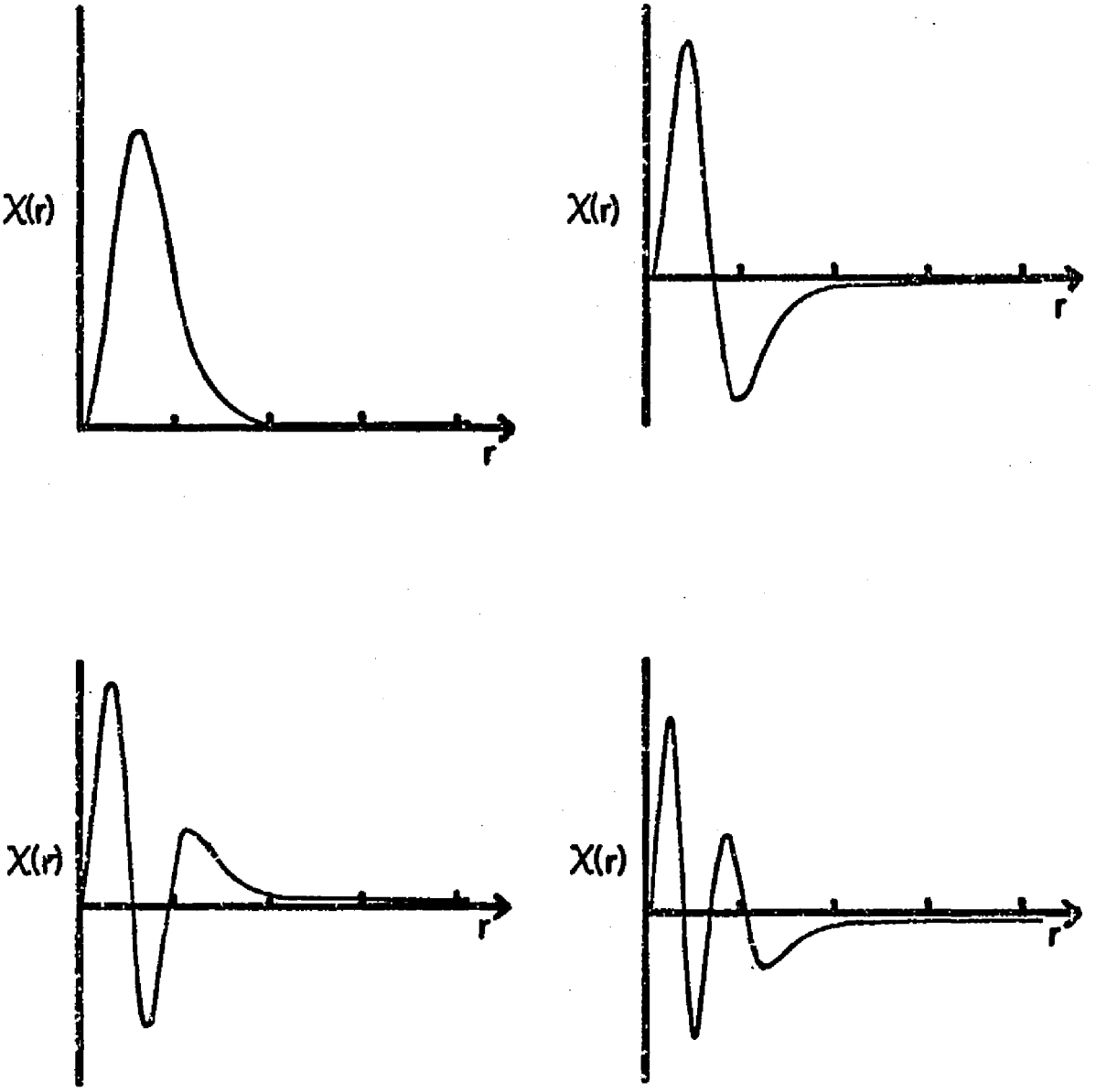

Fig. 17. Typical eigenfunctions for modes with $\omega = O(1)$ in $k\delta$ with $m = 2$ and $n = 0, 1, 2, 3$ (n is the number of radial nodes). These are for a Gaussian pressure and density ($D = .001$) profile with $\beta = .5$, $\gamma = 5/3$, and $r_w = 4.2$.

a function of r alone while the right-hand side is a function of θ alone. This is possible only if each side of the equation separately equals the same constant, A. Then upon division by the non-zero quantity $(\frac{\gamma p + a^2}{\rho})$ one finds that the velocity potential must satisfy the inhomogeneous equation

$$\frac{\rho}{r}\left(\frac{r}{\rho}\chi'\right)' + \frac{\rho\omega^2}{\gamma p + a^2}\chi = \frac{A\rho}{\gamma p + a^2} \tag{27}$$

To solve this equation, the solutions of Eq. (25) with m = 0 are used. It is well known that Eq. (25) produces a complete set of orthogonal eigenfunctions $\chi_0(y_{0n}\frac{r}{r_w})$. Thus, a Green's function can be represented in terms of this complete set as can the Dirac delta function. Then by Green's theorem the solution of Eq. (27) is found to be an integral of the product of the Green's function and the inhomogeneous term. This procedure is not carried out explicitly since the m = 0 modes have not proven to be experimentally important in high beta theta pinches.[1,10]

C. Modes with $\omega = \mathcal{O}(k\delta)$ in $k\delta$

Again, substitution of Eqs. (18)-(20) into Eqs. (13)-(16) yields

$$p = -(\gamma p + a^2)(\vec{\nabla}\cdot\vec{v}^{(\omega)}) + \mathcal{O}(\delta)$$

$$\underset{\sim}{T} = 0 + \mathcal{O}(\delta)$$

Then, since $\omega = \mathcal{O}(k\delta)$ the equation of motion, Eq. (7), becomes

$$\nabla p = \underset{\sim}{T} + \mathcal{O}(\delta^2) \tag{28}$$

This immediately implies

$$\nabla p = 0 + \mathcal{O}(\delta) \tag{29}$$

and

$$\nabla \times \underset{\sim}{T} = 0 + \mathcal{O}(\delta^2) \tag{30}$$

Equation (29) yields, upon expansion in δ

$$\vec{\nabla}\left[-(\gamma p + a^2)\,\vec{\nabla}\cdot\vec{v}^{(0)}\right] = 0$$

hence

$$(\gamma p + a^2)\,\vec{\nabla}\cdot\vec{v}^{(0)} = f^{n}(z)$$

Since only the kink mode is experimentally relevant, it is assumed that $m \neq 0$; then, as in the previous section, the constants must vanish, giving

$$\vec{\nabla}\cdot\vec{v}^{(0)} = 0 \tag{31}$$

Thus the perturbed flow is incompressible to lowest order (the z variation is of higher order in δ). Equation (31) is automatically satisfied upon introduction of a velocity stream function $\chi_0(r)$ such that

$$u^{(0)} = \frac{im}{r}\chi_0$$

$$v^{(0)} = -\chi_0'$$

With the condition given by Eq. (31) imposed, the total pressure, P, is reduced from an $\mathcal{O}(1)$ quantity to an $\mathcal{O}(\delta)$ quantity.

Proceeding with substitution and algebraic manipulation the following expressions are obtained from the components of $\underset{\sim}{T}$.

$$T_r = \delta k^2 a\left[-a u^{(1)} - \left(c - \frac{a'b}{a}\right)\frac{im}{r}\chi_0 + \frac{im}{r}b\chi_0' - 2\frac{a'b}{a}\frac{im}{r}\chi_0\right]\cos(kz) + \delta k^3 a b w^{(0)}\sin(kz) + \mathcal{O}(\delta^2) \tag{32}$$

$$T_\theta = -\delta k^2 a\left[a v^{(\omega)} + (b\chi_o')' - c\chi_o'\right]\cos(kz) + O(\delta^2) \tag{33}$$

$$T_z = \delta k a\left[a\vec{\nabla}\cdot\vec{v}^{(\omega)} + k^2 b\,\frac{im}{r}\chi_o\right]\sin(kz) + \delta k^2 a\left[\frac{1}{r}(rbw^{(\omega)})' - \frac{a'b}{a}w^{(\omega)}\right]\cos(kz) + O(\delta^2) \tag{34}$$

The equilibrium relation Eq. (II-60) and Eq. (31) have been used. At this point it is convenient to introduce the following auxiliary variables and notation:

$$\bar{u}^{(\omega)} \equiv -\frac{ru^{(\omega)}}{im} \tag{35}$$

$$y_1 \equiv a\bar{u}^{(\omega)} + b\chi_o' - \left(c - \frac{a'b}{a}\right)\chi_o \tag{36}$$

$$y_2 \equiv a v^{(\omega)} + (b\chi_o')' - c\chi_o' \tag{37}$$

Direct differentiation of Eq. (35) and the definition of $\vec{\nabla}\cdot\vec{v}^{(1)}$ yield

$$\bar{u}^{(\omega)\prime} = v^{(\omega)} - \frac{r}{im}\vec{\nabla}\cdot\vec{v}^{(\omega)} \tag{38}$$

This together with Eqs. (36) and (37) gives

$$y_1' = \frac{a'}{a}y_1 + y_2 + \left[\frac{a'}{a}\left(c - \frac{a'b}{a}\right) - \left(c - \frac{a'b}{a}\right)'\right]\chi_o - \frac{ar}{im}\vec{\nabla}\cdot\vec{v}^{(\omega)} \tag{39}$$

Equations (32)-(34) may now be rewritten in terms of the new variables

$$T_r = \delta\frac{im}{r}k^2 a\left[y_1 - 2\frac{a'b}{a}\chi_o\right]\cos(kz) + \delta k^3 abw^{(\omega)}\sin(kz) \tag{40}$$

$$T_\theta = -k^2 a\delta y_2\cos(kz) \tag{41}$$

$$T_z = \delta \frac{im}{r} ka \left[\frac{ar}{im}\vec{\nabla}\cdot\vec{v}^{(0)} + k^2 b\chi_0\right]\sin(kz) + \delta k^2 a\left[\frac{1}{r}(rbw^{(0)})' - \frac{a'b}{a}w^{(0)}\right]\cos(kz) \quad (42)$$

Expanding Eq. (30) to (δ) gives:

$$-\frac{m^2}{r^2}ka\left[\frac{ar}{im}\vec{\nabla}\cdot\vec{v}^{(0)} + k^2 b\chi_0\right]\sin(kz) + \frac{im}{r}k^2 a\left[\frac{1}{r}(rbw^{(0)})' - \frac{a'b}{a}w^{(0)}\right]\times \cos(kz) - k^3 a y_2 \sin(kz) = 0 \quad (43)$$

$$-\frac{im}{r}k^3 a\left[y_1 - 2\frac{a'b}{a}\chi_0\right]\sin(kz) + k^4 abw^{(0)}\cos(kz) - \frac{d}{dr}\left\{\frac{im}{r}ka\times \left[\frac{ar}{im}\vec{\nabla}\cdot\vec{v}^{(0)} + k^2 b\chi_0\right]\sin(kz) + k^2 a\left[\frac{1}{r}(rbw^{(0)})' - \frac{a'b}{a}w^{(0)}\right]\cos(kz)\right\} = 0 \quad (44)$$

$$-\frac{1}{r}\left[k^2 ray_2\right]'\cos(kz) + \frac{m^2}{r^2}k^2 a\left[y_1 - 2\frac{a'b}{a}\chi_0\right]\cos(kz) - \frac{im}{r}k^3 abw^{(0)}\sin(kz) = 0 \quad (45)$$

Since these equations are valid for all values of z the coefficients of sin (kz) and cos (kz) must vanish independently, so, Eq. (45) gives

$$y_2' = -\frac{y_2}{r}\left(1 + \frac{ra'}{a}\right) + \frac{m^2}{r^2}\left(y_1 - 2\frac{a'b}{a}\chi_0\right) \quad (46)$$

and

$$w^{(0)} = 0 \quad (47)$$

This expansion procedure therefore leads to modes with flow transverse to the primary magnetic field. Equations (43) and (47) then give

$$-\frac{ar}{im}\vec{\nabla}\cdot\vec{v}^{(0)} = k^2\left(\frac{r^2}{m^2}y_2 + b\chi_0\right) \quad (48)$$

Finally, Eqs. (44) and (48) reproduce Eq. (46).

Equation (30) leads to the two conditions Eqs. (46) and (48), but since there are three components of the original equation of motion, Eq. (38), there may be one additional condition which has not been exposed.[23] To reveal it the explicit forms of P and $\underset{\sim}{T}$ valid to $\mathcal{O}(\delta)$ are written down again and Eqs. (46) and (48) are imposed so that Eq. (30) remains satisfied. One finds:

$$P = -\delta\gamma p(\nabla\cdot\underset{\sim}{u}_1)^{(1)} - \delta\frac{r}{im}k^2 a y_2 \cos(kz) + \mathcal{O}(\delta^2) \tag{49}$$

$$T_r = \delta\frac{im}{r}ka\left(y_1 - 2\frac{\alpha b}{a}\chi_0\right)\cos(kz) + \mathcal{O}(\delta^2) \tag{50}$$

$$T_\theta = -\delta k^2 a y_2 \cos(kz) + \mathcal{O}(\delta^2) \tag{51}$$

$$T_z = \delta\frac{r}{im}k^3 a y_2 \sin(kz) + \mathcal{O}(\delta^2) \tag{52}$$

where $(\nabla\cdot\underset{\sim}{u}_1)^{(1)}$ is the full divergence of the perturbed velocity valid to $\mathcal{O}(\delta)$. When these expressions are substituted into Eq. (28) it is easily seen that

$$\nabla\cdot\underset{\sim}{u}_1 = 0 + \mathcal{O}(\delta^2) \tag{53}$$

Thus, the perturbed flow is incompressible to $\mathcal{O}(\delta)$.[23]

The equation of motion valid to $\mathcal{O}(\delta)$ yields the three conditions, Eqs. (46), (48) and (53). To proceed with the expansion these conditions are imposed and the equation of motion is written down valid

to $\mathcal{O}(\delta^2)$. The three components of the equation of motion are

$$-\rho\omega^2 \frac{im}{r}\chi_o + \frac{\partial}{\partial r}P = T_r + \mathcal{O}(\delta^3) \tag{54}$$

$$-\rho\omega^2 \chi_o' + \frac{im}{r}P = T_\theta + \mathcal{O}(\delta^3) \tag{55}$$

$$\frac{\partial}{\partial z}P = T_z + \mathcal{O}(\delta^3) \tag{56}$$

The explicit expressions for P and the three components of $\underset{\sim}{T}$ involve terms which are independent of z as well as terms proportional to sin(kz) and cos (kz), and sin (2kz) and cos (2kz); again, Eqs. (54)-(56) are valid for all values of z, hence the coefficients of the various Fourier components must vanish independently. It is seen that Eq. (54)-(57) lead to nine separate equations, however, all except those which are relations among the terms of P and $\underset{\sim}{T}$ that are independent of z would involve the higher corrections to the equilibrium magnetic field components and the perturbated velocity components if a more general expansion than Eqs. (17)-(20) were used. Since only the first order (in δ) corrections to the equilibrium magnetic field and perturbed velocity are needed in this analysis, many of the nine equations are of no interest and will thus be ignored. The relevant portions of the expressions of P and $\underset{\sim}{T}$ are explicitly.

$$P = \delta(P)^{(0)} - \delta^2 ac\vec{\nabla}\cdot\vec{v}^{(0)} - \frac{im}{r}k^2 b\left(y_1 - \frac{a'b}{a}\chi_o - \frac{1}{2}b\chi_o'\right) + \frac{1}{2}ka\left(\frac{a'b}{a}w^{(0)} - \frac{1}{r}(rbw^{(0)})'\right] + \mathcal{O}(\delta^2 \sin(2kz)) \tag{57}$$

$$T_r = \delta(T_r)^{(1)} + \delta^2 \frac{im}{r}\left\{-\ell^2 a^2 \chi_0 + \frac{1}{2}\left[b y_1' + 2b' y_1 + \frac{\alpha' b}{a} y_1 - b\left(c + \frac{\alpha' b}{a}\right)' \chi_0 - \frac{\alpha' b}{a}\frac{\alpha' b}{a}\chi_0 - 2\frac{\alpha' b}{a} b \chi_0' + \frac{\alpha' b}{a}\frac{b}{r}\chi_0 - \frac{\alpha' b}{a} b' \chi_0 - b\left(\frac{\alpha r}{im}\vec{\nabla}\cdot\vec{v}^{(1)}\right)\right\}\right\} \quad (58)$$

$$T_\theta = \delta(T_\theta)^{(1)} + \delta^2\left\{\ell^2 a^2 \chi_0' - \frac{1}{2}\left[\left(c - \frac{\alpha' b}{a}\right) y_2 + \frac{m^2}{r^2} b\left[y_1 - 2\frac{\alpha' b}{a}\chi_0\right]\right]\right\} \quad (59)$$

$$T_z = \delta(T_z)^{(1)} + O(\delta^2 \cos(2kz)) \quad (60)$$

One immediately sees that Eq. (56) is satisfied trivially, also, that $w^{(1)}$ occurs only in the expression for P and it may be eliminted by substitution of Eq. (55) into Eq. (54). This yields a second order differential equation (Eq. (61) below) which together with Eqs. (39), (46), and (48) form a closed system of equations involving the variables χ_0, χ_0', y_1, y_2, and $\vec{\nabla}\cdot\vec{v}^{(1)}$. The divergence could be eliminated algebraically, but it is more convenient to retain it for purposes of comparison with the long wavelength theory of Weitzner.[8] Thus, the transverse, incompressible modes with $\omega =$ (kδ) are governed by the fourth order system of differential equations (the modes are three-dimensionally imcompressible, but two dimensionally compressible).

$$\frac{1}{r}\left[(\rho\omega^2 - \ell^2 a^2) r \chi_0'\right]' - \frac{m^2}{r^2}(\rho\omega^2 - \ell^2 a^2)\chi_0 = \frac{1}{2}\left\{-\frac{m^2}{r^2} b \frac{\alpha r}{im}\vec{\nabla}\cdot\vec{v}^{(1)} + \left[\frac{\alpha'}{a}\chi\right.\right. \quad (61)$$
$$\left.\left.\left(c - \frac{\alpha' b}{a}\right) - \left(c - \frac{\alpha' b}{a}\right)'\right] y_2 + \frac{m^2}{r^2}\frac{\alpha' b}{a}\left[2y_1 + \left[3\left(c - \frac{\alpha' b}{a}\right) - 2\frac{b}{r}\right]\chi_0\right] - \frac{m^2}{r^2} b\left(c - \frac{\alpha' b}{a}\right)'\chi_0\right\}$$

$$y_1' = \frac{\alpha'}{a} y_1 + y_2 + \left[\frac{\alpha'}{a}\left(c - \frac{\alpha' b}{a}\right) - \left(c - \frac{\alpha' b}{a}\right)'\right]\chi_0 - \frac{\alpha r}{im}\vec{\nabla}\cdot\vec{v}^{(1)} \quad (39)$$

$$y_2' = -\frac{1}{r}\left(1+\frac{ra'}{a}\right)y_2 + \frac{m^2}{r^2}\left(y_1 - 2\frac{a'b}{a}\chi_0\right) \tag{46}$$

$$-\frac{ar}{im}\vec{\nabla}\cdot\vec{v}^{\omega} = k^2\left(\frac{r^2}{m^2}y_2 + b\chi_0\right) \tag{48}$$

One feature of this system is immediately apparent from Eq. (61), namely that the differential equation in singular at any position r such that $\omega^2 = \ell^2 a^2/\rho$. Since a and ρ are monotone functions of r, there is a continuous set of values for ω for which the differential equation is singular, $\ell^2(1 - \beta) \leq \omega^2 \leq \ell^2/D$. This continuum of real frequencies is the Alfven continuum and arises because the Alfven wave propagates one dimensionally along the magnetic field lines in three dimensional space (see Appendix D for derivation of the eigenvalue problem, like Eqs. (39), (46), (48) and (61), for an ordinary theta pinch).

The equilibrium magnetic field components have valid power series expansions, the first few terms of which are

$$a(r) = a(0) + \frac{1}{2}a''(0)r^2 + \frac{1}{6}a'''(0)r^3 + \cdots$$

$$b(r) = b'(0)r + \frac{1}{6}b'''(0)r^3 + \cdots$$

$$c(r) = 2b'(0) + \frac{2}{3}b'''(0)r^2 + \cdots$$

From these all the coefficients that occur in the system of differential equations may be worked out. It is found that

$$\frac{a'b}{a} = \frac{a''(0)b'(0)}{a(0)}r^2 + \cdots$$

$$\left(c - \frac{a'b}{a}\right) = 2b'(0) + \left(\frac{2}{3}b'''(0) - \frac{a''(0)b'(0)}{a(0)}\right)r^2 + \cdots$$

$$\frac{a'}{a}\left(c - \frac{a'b}{a}\right) - \left(c - \frac{a'b}{a}\right)' = 4\left(\frac{a''(0)b'(0)}{a(0)} - \frac{1}{3}b'''(0)\right)r + \cdots$$

Upon substitution of these forms and an assumed power series solution into the differential equations (39), (46), (48) and (61), exactly four solutions result; two solutions are regular at r = 0 and two solutions are irregular there. The four solutions are

$$\begin{aligned} \chi_0 &= r^{\pm m} + \cdots \\ y_1 &= \left[1 + \frac{2-m^2}{2(1\pm m)}\right] \frac{a''(0)b'(0)}{a(0)} r^{2\pm m} + \cdots \\ y_2 &= \frac{\mp m^3}{2(1\pm m)} \frac{a''(0)b'(0)}{a(0)} r^{1\pm m} + \cdots \end{aligned} \tag{62}$$

and

$$\begin{aligned} \chi_0 &= \frac{(m^2 \pm 2m)\left(\frac{a''(0)b'(0)}{a(0)}\right)}{(\rho(0)\omega^2 - k^2 a^2(0))4(1\pm m)} r^{2\pm m} + \cdots \\ y_1 &= r^{\pm m} + \cdots \\ y_2 &= \pm m\, r^{-1\pm m} + \cdots \end{aligned} \tag{63}$$

The general solution of the system of equations is a linear combination of the four solutions but since regularity is required for a physically meaningful fluid velocity, two of the solutions, the irregular ones, are eliminated. Thus, two regularity conditions are imposed on the general solution. Two additional conditions must be imposed to determine the solution completely, these are the boundary conditions imposed at the plasma-conducting wall interface.

The velocity component normal to the conducting wall must vanish.

$$\hat{n} \cdot \underset{\sim}{u}_1 \Big|_{wall} = 0 \tag{64}$$

The equation of the conducting wall and its unit normal are, from the previous chapter

$$r(z) = r_w - \delta \frac{b(r_w)}{a(r_w)} \cos(kz) + \mathcal{O}(\delta^2) \tag{II-46}$$

$$\hat{n}_w = \hat{r} - \hat{z}\delta k \frac{b(r_w)}{a(r_w)} \sin(kz) + \mathcal{O}(\delta^2) \tag{II-47}$$

Upon expansion in powers of δ, Eq. (64) becomes

$$u\Big|_{r(z)} = 0 + \mathcal{O}(\delta^2) \tag{65}$$

This gives upon expansion

$$u^{(0)}(r_w) + \delta u^{(1)}(r_w)\cos(kz) - \delta \frac{b(r_w)}{a(r_w)} u^{(0)\prime}(r_w)\cos(kz) = 0 \tag{66}$$

To lowest order in δ this condition is

$$u^{(0)}(r_w) = \frac{im}{r_w} \chi_0(r_w) = 0$$

thus,

$$\chi_0(r_w) = 0 \tag{67}$$

The next order in δ gives

$$-\frac{im}{r_w}\left[a(r_w)u^{(1)}(r_w) + b(r_w)\chi_0'(r_w) - \left(c - \frac{a'b}{a}\right)\chi_0(r_w)\right] = 0$$

Thus,

$$y_{11}(r_w) = 0 \tag{68}$$

The eigenvalue problem is now completely specified by the system of differential equations (39), (46), (48) and (61), the two regularity conditions, and the two boundary conditions, Eqs. (67) and (68). The eigenfunctions must be determined numerically. This is accomplished by

the shooting method as described in section IIIB; the problem is only slightly more complicated than the previous one. As mentioned earlier the general solution consists of a linear combination of four solutions. Two of the solutions are eliminated because they are irregular leaving a linear combination of two regular solutions. It is this linear combination which must satisfy the boundary conditions at the plasma-conducting wall interface. The condition is

$$\begin{aligned} \alpha \chi_0^{(1)}(r_w) + \beta \chi_0^{(2)}(r_w) &= 0 \\ \alpha y_1^{(1)}(r_w) + \beta y_1^{(2)}(r_w) &= 0 \end{aligned} \tag{69}$$

where α and β are constants and the superscripts identify the independent solutions of the system of equations. As always, if there are solutions to Eq. (69), then the determinant of the coefficient matrix must vanish. The boundary conditions become

$$\chi_0^{(1)}(r_w) y_1^{(2)}(r_w) - \chi_0^{(2)}(r_w) y_1^{(1)}(r_w) = 0 \tag{70}$$

The actual numerical procedure involves the simultaneous integration of ten differential equations. Two of these give the subsidiary equilibrium magnetic field components, b and c. The fourth order system is integrated twice for the two sets of initial conditions given in Eqs. (62) and (63). The result of the integration is tested against the condition given by Eq. (70). If Eq. (70) is satisfied then the assumed parameter value is an eigenvalue and the linear combination of the two independent solutions is an eigenfunction; if Eq. (70) is not satisfied, then the parameter is adjusted and the process repeated.

In Figs. (18), (19), and (20) the normalized growth rate squared (γ^2) of the most unstable mode is plotted against plasma beta for the Gaussian pressure profile. In Fig. (18), the conducting wall is located at $r_w = 4.2$ and the subsidiary fields are normalized so that $c(4.2) = 1$. In Fig. (19), the wall is located at $r_w = 3.0$ and the equilibrium fields normalized so that $c(3.0) = 1$. In Fig. (20), the wall is located at $r_w = 3.0$ but the fields are normalized so that $c(4.2) = 1$. Thus, in Fig. (20) the equilibrium magnetic field is identical to that of the case represented in Fig. (18), this illustrates the wall stabilization predicted by very general arguments based on analysis of δW, the energy principle of ideal MHD. Notice that the growth rates for the finite wavelength case are substantially smaller than those of the long wavelength case. The major reason for this is the less effective penetration of the equilibrium magnetic field into the plasma. When the conducting wall is located nearer the plasma the subsidiary equilibrium fields have a smaller distance to penetrate and the growth rates increase in the finite wavelength case, but decrease slightly in the long wavelength case.

Figures (21) and (22) show the normalized growth rate squared versus plasma beta for the sharp pressure profile for both long wavelength ($k \simeq 0$) and finite wavelength ($k = 1$) cases. In Fig. (21) the conducting wall is located at $r_w = 4.2$ while in Fig. (22) the wall is at $r_w = 1.6$. Again the finite wavelength affects the penetration of the subsidiary fields and this has a profound effect on the growth rates of the finite wavelength case, but not the long wavelength case.

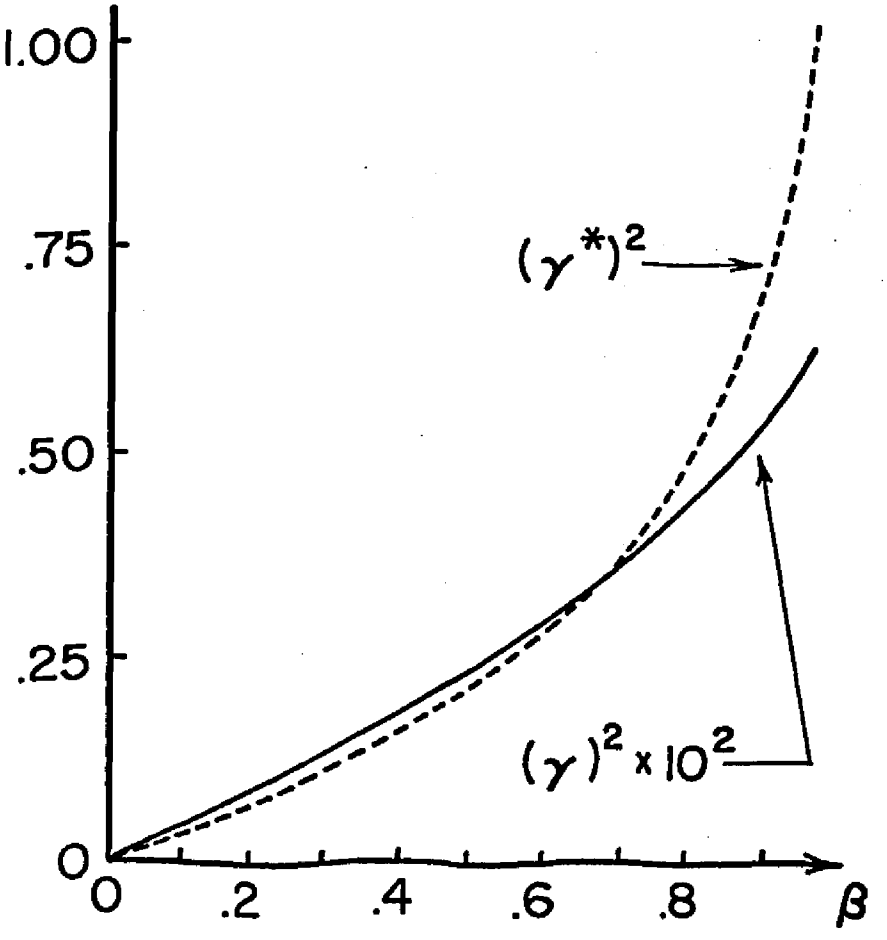

Fig. 18. Normalized growth rate squared versus plasma beta for least stable mode of finite (k = 1) wavelength case (solid curve) and long (k ≈ 0) wavelength case (dashed curve) for Gaussian pressure and density (D = .01) profiles with $r_w = 4.2$. Note that the eigenvalues for the finite wavelength case are two orders of magnitude smaller than those of the long wavelength case. (m = 1, ℓ = 0).

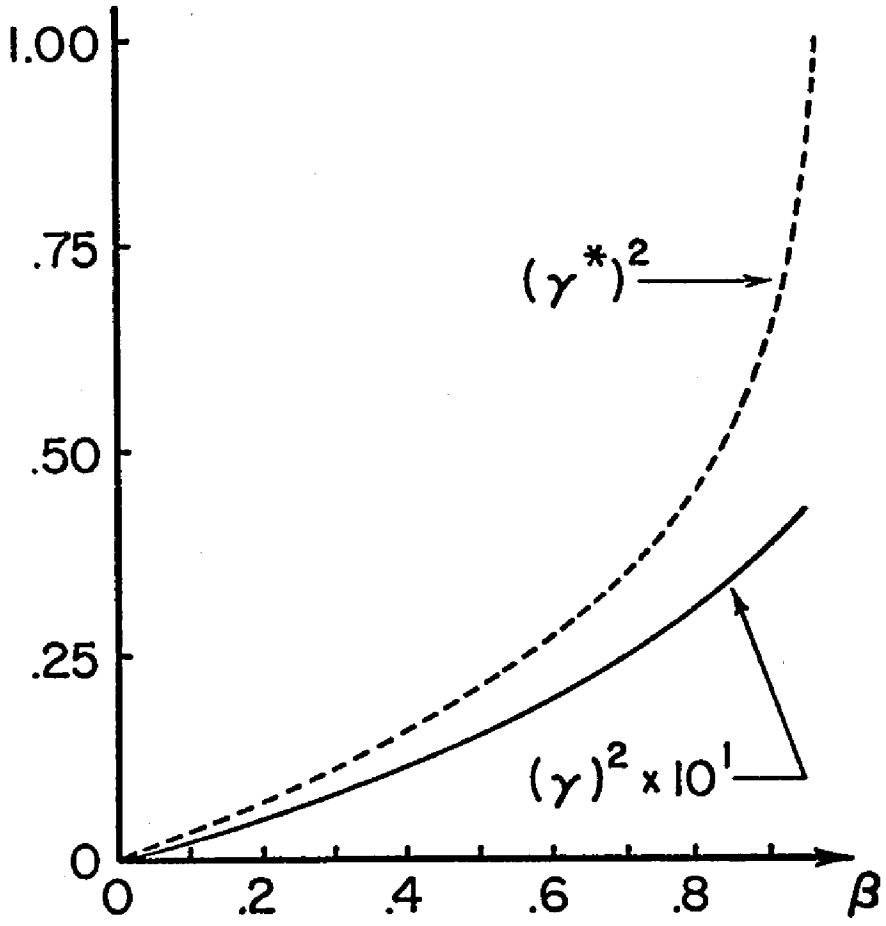

Fig. 19. Normalized growth rate squared versus plasma beta for least stable mode of finite (k = 1) wavelength case (solid curve) and long (k ≈ 0) wavelength case (dashed curve) for Gaussian pressure and density (D = .01) profiles with r_w = 3.0. Growth rates for the long wavelength case are decreased slightly from those of Fig. (18) while those of the finite wavelength case are dramatically increased. This is due to the increased penetration of the subsidiary equilibrium magnetic field. (m = 1, ℓ = 0).

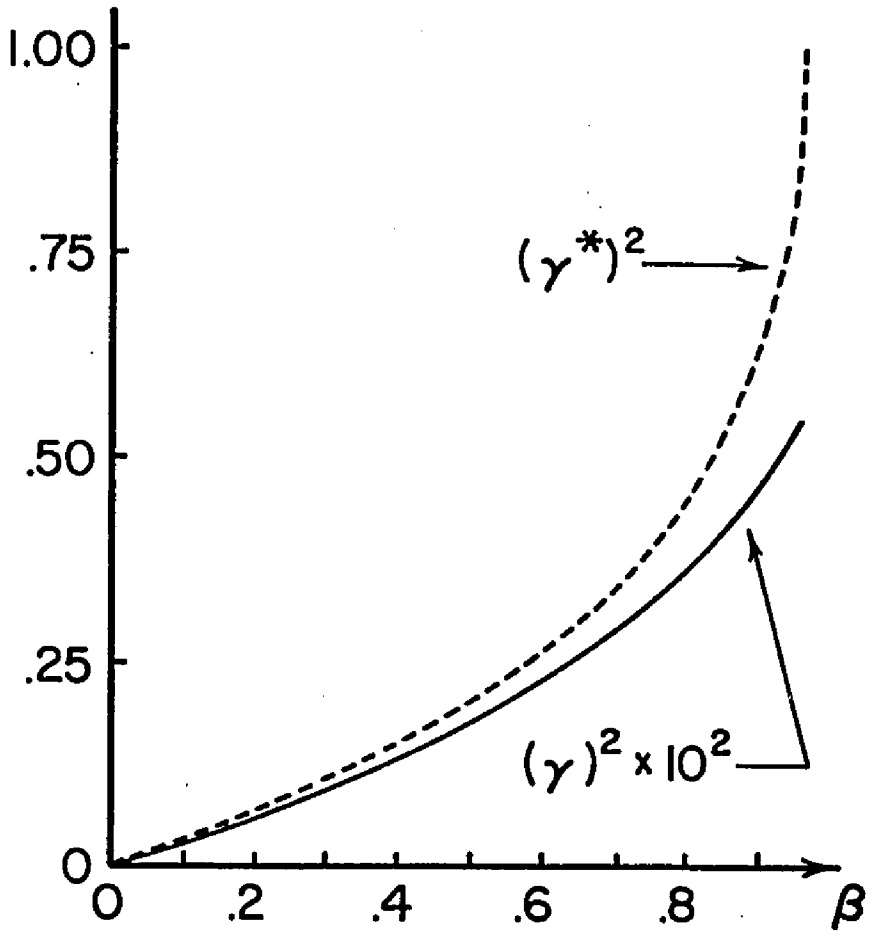

Fig. 20. Same illustration as Fig. (19) but with the subsidiary equilibrium magnetic field of the finite (k = 1) wavelength case renormalized so that the field is the same as that in Fig. (18). The growth rates of both cases are now slightly decreased in agreement with the wall stabilization predicted by δW analysis. (m = 1, ℓ = 0).

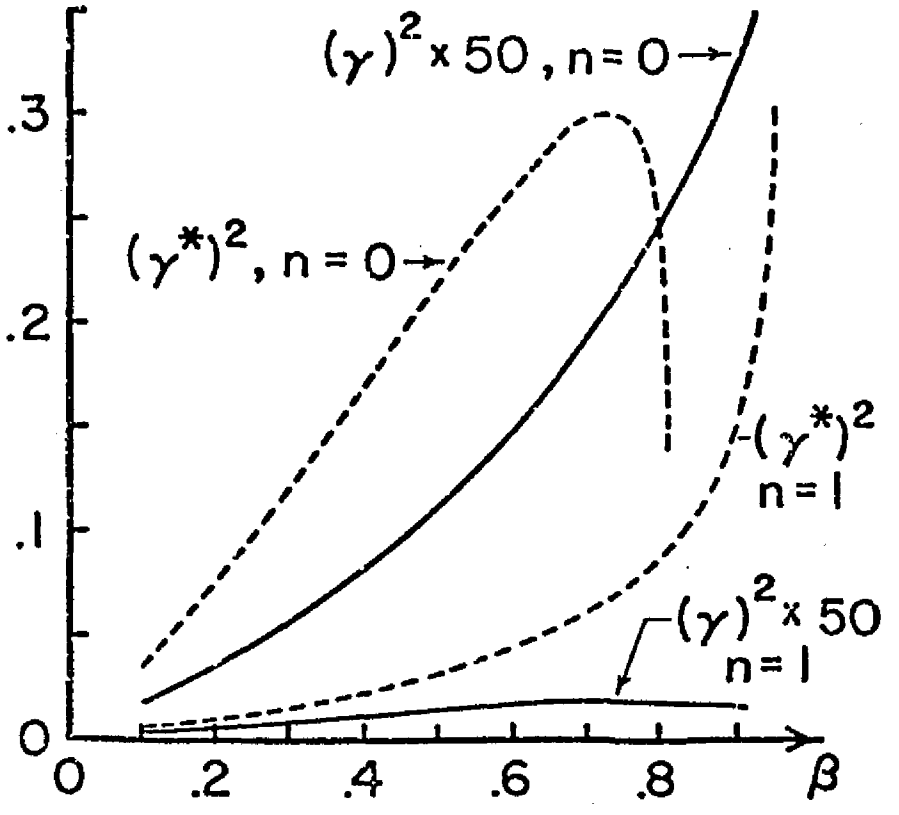

Fig. 21. Normalized growth rate squared versus plasma beta for the finite (k = 1) wavelength case (solid curves) and long (k ≈ 0) wavelength case (dashed curves) for sharp pressure and density (D = .01) profiles with $r_w = 4.2$. n denotes the number of radial nodes of the eigenfunction (m = 1, ℓ = 0).

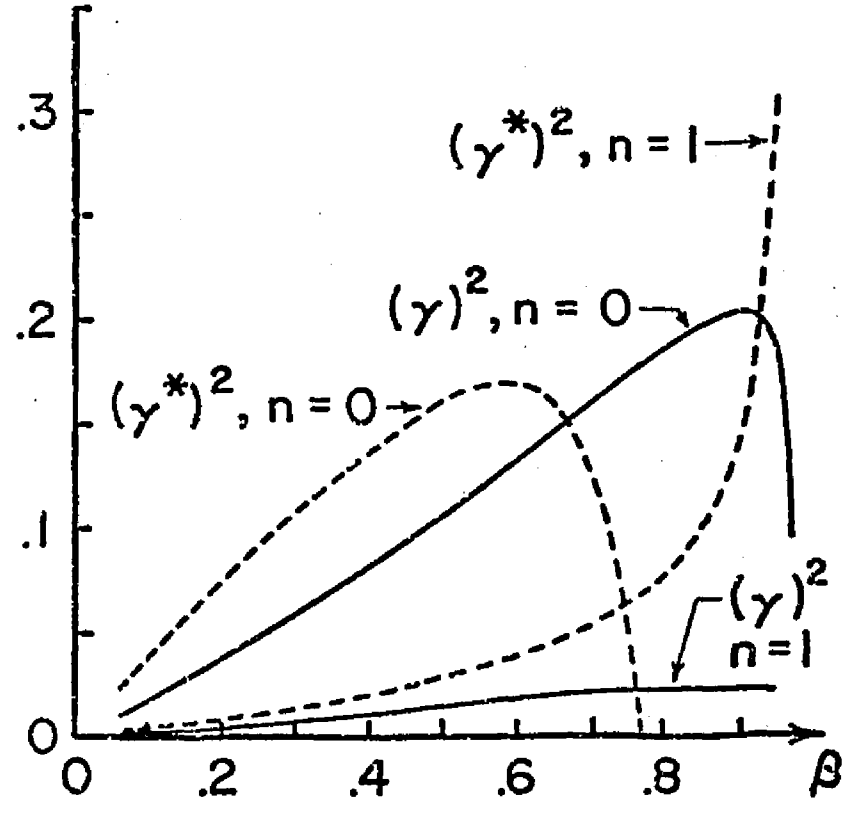

Fig. 22. Normalized growth rate squared versus plasma beta for the finite (k = 1) wavelength case (solid curves) and long (k ≈ 0) wavelength case (dashed curves) for sharp pressure and density (D = .01) profiles with r_w = 1.6. Note the high beta stabilization of the n = 0 mode for both finite and long wavelength cases. (m = 1, ℓ = 0).

Before turning to the spectral properties of the system it should be mentioned that the system of Eqs. (39), (46), (48) and (61) reduces to that derived by Weitzner in his long wavelength theory[8] of the bumpy theta pinch upon making the finite wavenumber vanishingly small. In fact, the two dimensional divergence in Eq. (48) then vanishes and the variable $\bar{u}^{(1)}$ may be interpreted as a velocity stream function. The formulation of the problem is then identical to Weitzner's formulation in every detail. An important difference between the finite wavelength and long wavelength formulations of the problem is that the modes are two dimensionally compressible in the finite wavelength case but are two dimensionally incompressible in the long wavelength case.

IV. SPECTRAL PROPERTIES OF THE BUMPY THETA PINCH

A. General Theory

In this chapter some features of the spectrum of eigenvalues of the system of differential equation derived in the last chapter for the bumpy theta pinch are investigated along lines following the earlier work of Weitzner.[10] The investigation is eased by what is known generally about the linearized equations of ideal MHD. The system of equations of the velocity formulation is self-adjoint so that eigenvalues are real and eigenfunctions are orthogonal. These properties are valid for the bumpy theta pinch configuration in particular. Other properties of the spectrum are peculiarities of the bumpy theta pinch and reflect the expansion procedure which led to the derivation of the differential equations.

For convenience, the system of differential equations is reproduced below.

$$-\frac{ar}{im}\vec{\nabla}\cdot\vec{v}^{(0)} = k^2\left(\frac{r^2}{m^2}y_2 + b\chi_0\right) \tag{1}$$

$$y_1' = \frac{a'}{a}y_1 + y_2 + \left[\frac{a'}{a}\left(c-\frac{a'b}{a}\right) - \left(c-\frac{a'b}{a}\right)'\right]\chi_0 - \frac{ar}{im}\vec{\nabla}\cdot\vec{v}^{(0)} \tag{2}$$

$$y_2' = -\frac{1}{r}\left(1+\frac{ra'}{a}\right)y_2 + \frac{m^2}{r^2}\left(y_1 - 2\frac{a'b}{a}\chi_0\right)$$

$$\frac{1}{r}\left[(\rho\omega^2 - l^2a^2)r\chi_0'\right]' - \frac{m^2}{r^2}(\rho\omega^2 - l^2a^2)\chi_0 = \frac{1}{2}\left\{-\frac{m^2}{r^2}b\frac{ar}{im}\vec{\nabla}\cdot\vec{v}^{(0)}\right. \tag{3}$$

$$\left. + \frac{m^2}{r^2}\frac{a'b}{a}\left[2y_1 - \left[3\left(c-\frac{a'b}{a}\right) - 2\frac{b}{r}\right]\chi_0\right] - \frac{m^2}{r^2}b\left(c-\frac{a'b}{a}\right)'\chi_0\right\} \tag{4}$$

As previously noted, Eq. (4) is singular whenever the quantity $(\rho\omega^2-\ell^2a^2)$ vanishes at any point in the range of r. For the particular equilibrium profiles considered in this work a continuous set of values of the parameter ω^2 lead to singular differential equations, namely

$$\ell^2(1-\beta) \leq \omega^2 \leq \ell^2/D \tag{5}$$

where $(1 - \beta)$ is the minimum value of $a^2(r)$ and D is the minimum value of the density. The singular solutions of Eq. (4) which satisfy the boundary conditions are singular eigenfunctions and the corresponding eigenvalues belong to the continuous spectrum. As was mentioned, this is the Alfven continuum. The continuum consists of a line segment, given in Eq. (5), on the positive half of the real ω^2 axis in the complex ω^2-plane for any nonvanishing wavenumber, ℓ. It is bounded away from the origin, $\omega^2 = 0$, for all values of beta less than unity. As the wavenumber, ℓ, vanishes, the line segment degenerates to a single point $\omega^2 = 0$. Thus, the Alfven continuum does not touch the origin in the ω^2-plane except when the perturbation wavenumber vanishes and in this case the continuum degenerates to a single isolated point.

Equations (1)-(4) also admit discrete eigenvalues; these occur whenever the regular solutions satisfy the boundary conditions. The regular solutions of a system of ordinary differential equations which involve a parameter in the coefficients, such as Eqs. (1)-(4), are interpreted as analytic functions of the parameter.[25] The region of analyticity does not include, of course, the line segments and isolated points that make up the continuous spectrum since the differential equations are

singular there. Hence, the boundary conditions, like Eq. (III-69), for the regular solution of Eqs. (1)-(4) involve analytic functions of ω^2 as coefficients and the condition what ω^2 be an eigenvalue is of the form

$$A(\omega^2) = 0$$

Where $A(\omega^2)$ is analytic except on the points of the previously introduced continuous spectrum. In the regions where $A(\omega^2)$ is analytic, $A(\omega^2)$ can only vanish at isolated points, otherwise it vanishes identically. It is assumed that the system of equations generates a nontrivial eigenvalue problem so that it is not the case that $A(\omega^2)$ vanishes identically; the eigenvalues are the isolated zeroes of $A(\omega^2)$. Furthermore, these isolated zeroes may accumulate only at $\omega^2 = \infty$ or at the tips of the continuous spectrum.

A description of the spectrum of the modes of the bumpy theta pinch is as follows. The eigenvalues are restricted to real values of ω^2; a continuous set of eigenvalues occurs for positive values of ω^2, the corresponding eigenfunction are singular eigenfunctions. This continuum degenerates to a single point, $\omega^2 = 0$, when $\ell = 0$. A point spectrum of isolated eigenvalues also occurs for real values of ω^2; the corresponding eigenfunctions are regular solutions of the ordinary differential equations. This point spectrum may have points of accumulation on the tips of the continuum or at infinity. The direction of accumulation of the discrete eigenvalues is important as it reflects general features of the point spectrum.

B. Localized Modes

The set of Eqs. (1)-(4) may admit highly localized or rapidly oscillating regular eigenfunctions where

$$y_1' \gg y_1$$

$$y_2' \gg y_2$$

$$\chi_0' \gg \chi_0$$

In this case, Eqs. (2) and (3) give

$$y_1 \ll \chi_0$$

and

$$y_2 \ll \chi_0$$

while Eq. (4) yields

$$(\rho\omega^2 - \ell^2 a^2)\chi_0'' \approx 0$$

This is possible only if $(\rho\omega^2 - \ell^2 a^2) \approx 0$. Thus, it is concluded that such highly localized or rapidly oscillating eigenfunctions can only occur for eigenvalues very close to those frequencies associated with the Alfven continuum; in the case where the axial wavenumber, ℓ, vanishes these rapidly varying modes occur for frequencies very close to zero. This situation will be investigated in the rest of this chapter since it is particularly illuminating.

To investigate the behavior of solutions with ω^2 very small when the axial wavenumber, ℓ, is identically zero consideration is given to rapidly varying eigenfunctions localized about a point $r = r_0$. A small parameter, ε, which measures the localization is introduced by writing

$$r - r_0 = \epsilon \xi(r_0, r)$$

where ξ is $\mathcal{O}(1)$ in ϵ. Then

$$\frac{d}{dr} = \frac{1}{\epsilon} \frac{d}{d\xi}$$

and upon algebraic elimination of Eq. (1), Eqs. (2) and (3) require

$$y_1 = \mathcal{O}(\epsilon)$$
$$y_2 = \mathcal{O}(\epsilon)$$

if it is assumed that χ_0 is $\mathcal{O}(1)$ in ϵ. Then with the frequency small

$$\omega = \epsilon \tilde{\omega}$$

Equation (4) gives to leading order in ϵ

$$\rho(r_0)\tilde{\omega}^2 \chi_0''(\xi) + \frac{m^2}{r_0^2} \frac{a(r_0)b(r_0)}{a(r_0)} \lambda(r_0) \chi(\xi) = 0 \qquad (6)$$

where the equilibrium quantity $\lambda(r)$ is defined

$$\lambda(r) = \frac{b(r)}{r} - 2\left(c(r) - \frac{a(r)b(r)}{a(r)}\right) \qquad (7)$$

Thus, $\chi_0(\xi)$ is governed by a differential equation which describes the motion of a harmonic oscillator; in this approximation χ_0 vanishes outside the localized region about r_0, hence, solutions of Eq. (6) must satisfy homogeneous boundary conditions. If $\lambda(r) > 0$, then solutions of Eq. (6) are locally oscillatory if $\tilde{\omega}^2 > 0$; if $\tilde{\omega}^2 < 0$ then the solutions are locally exponentiating. Likewise if $\lambda(r) < 0$, then the solutions of Eq. (6) are locally exponentiating or oscillatory depending on the sign of $\tilde{\omega}^2$. Only if the solutions are oscillatory may the phase be adjusted by slight variations in the value of $\tilde{\omega}^2$ so as to match the required boundary conditions. Thus, the situation is summarized as follows. For

those regions in r where $\lambda(r) > 0$ there are infinitely many stable eigenfunctions which are localized in those regions. For those regions in r where $\lambda(r) < 0$ there are infinitely many unstable eigenfunctions which are localized in those regions. Thus, if $\lambda(r) > 0$, then $\omega^2 = 0$ is an accumulation point of a stable discrete spectrum, while is $\lambda(r) < 0$, then $\omega^2 = 0$ is an accumulation point of an unstable discrete spectrum.

In Fig. (23) λ and λ^* (starred quantities refer to the long wavelength case) are plotted against r for two values of plasma beta, $\beta = .9$ and $\beta = .95$, using the sharp pressure profile, Eq. (II-53). For the long wavelength case one finds for $\beta = .90$ that there should be two classes of unstable modes, one localized inside the plasma, one localized outside the plasma, as well as one class of stable modes localized near the surface of the plasma column. As the plasma beta increases the unstable modes localized outside the plasma disappear. For the finite wavelength case only one class of modes, unstable modes, is found when $\beta \leq .94$ while for $\beta > .95$ there are both externally and internally localized unstable modes as well as one stable class of modes. In the next three figures, Figs. (24)-(26), eigenfunctions are shown for various values of plasma beta, the lowest beta values for the uppermost plot, the highest beta values for the lower most graph. For the lowest beta value, the eigenfunctions have n = 1, n = 2, and n = 3 radial nodes, they are all unstable modes and are localized outside the plasma. As the plasma beta increases, the trajectories, $-\omega^2(\beta)$ (as in Fig. (20)), are followed and one sees:

(i) (Fig. (24)) The n = 1 externally localized mode becomes an n = 1 internally localized mode.

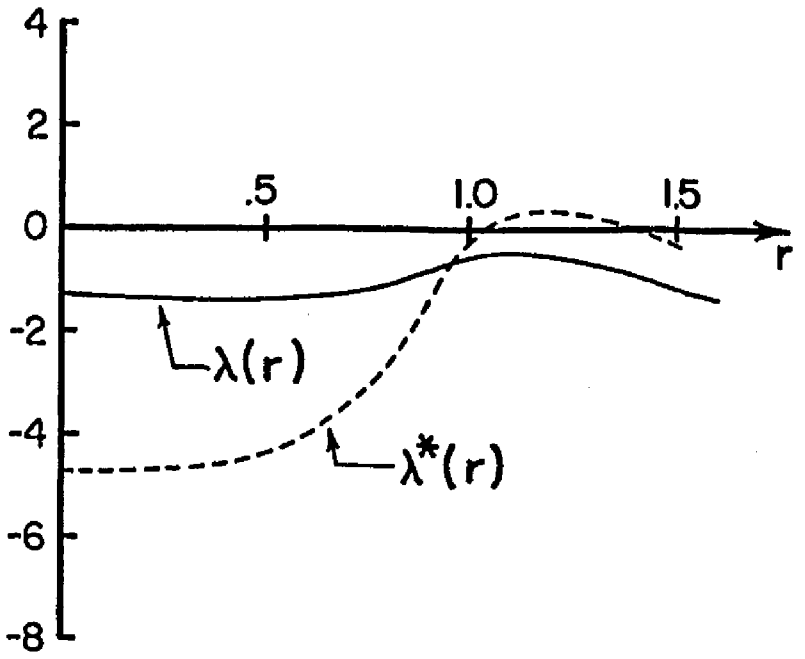

Fig. 23a. Plot of the equilibrium function $\lambda(r)$ for sharp profiles with $\beta = .9$ for finite ($k = 1$) and long ($k \simeq 0$) wavelength cases which indicates three classes of localized modes are possible in the long wavelength case, but only one class for the finite wavelength case.

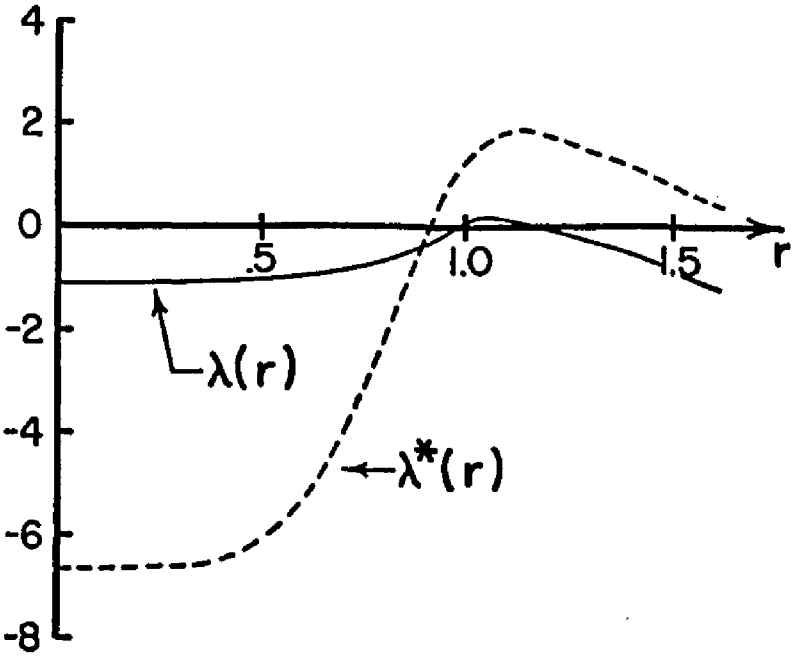

Fig. 23b. Plot of the equilibrium function $\lambda(r)$ for sharp profiles with $\beta = .95$ for finite ($k = 1$) and long ($k \simeq 0$) wavelength cases which indicates that three classes of localized modes are possible for the finite wavelength case and two for the long wavelength case.

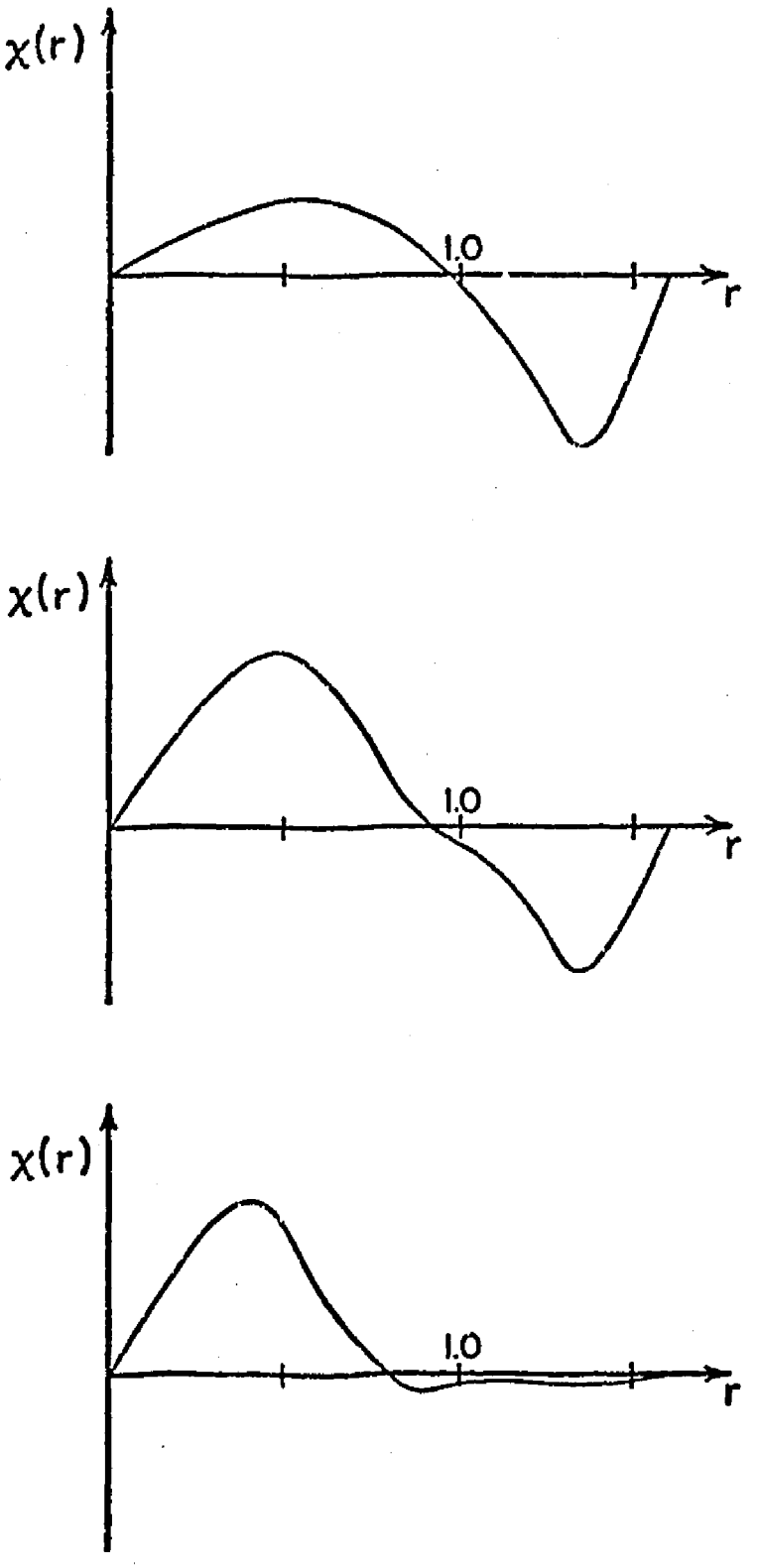

Fig. 24. High beta dependence of the eigenfunction with one radial node (top, $\beta = .90$; middle, $\beta = .93$; bottom, $\beta = .96$) showing a change in localization of the mode from outside to inside the plasma column.

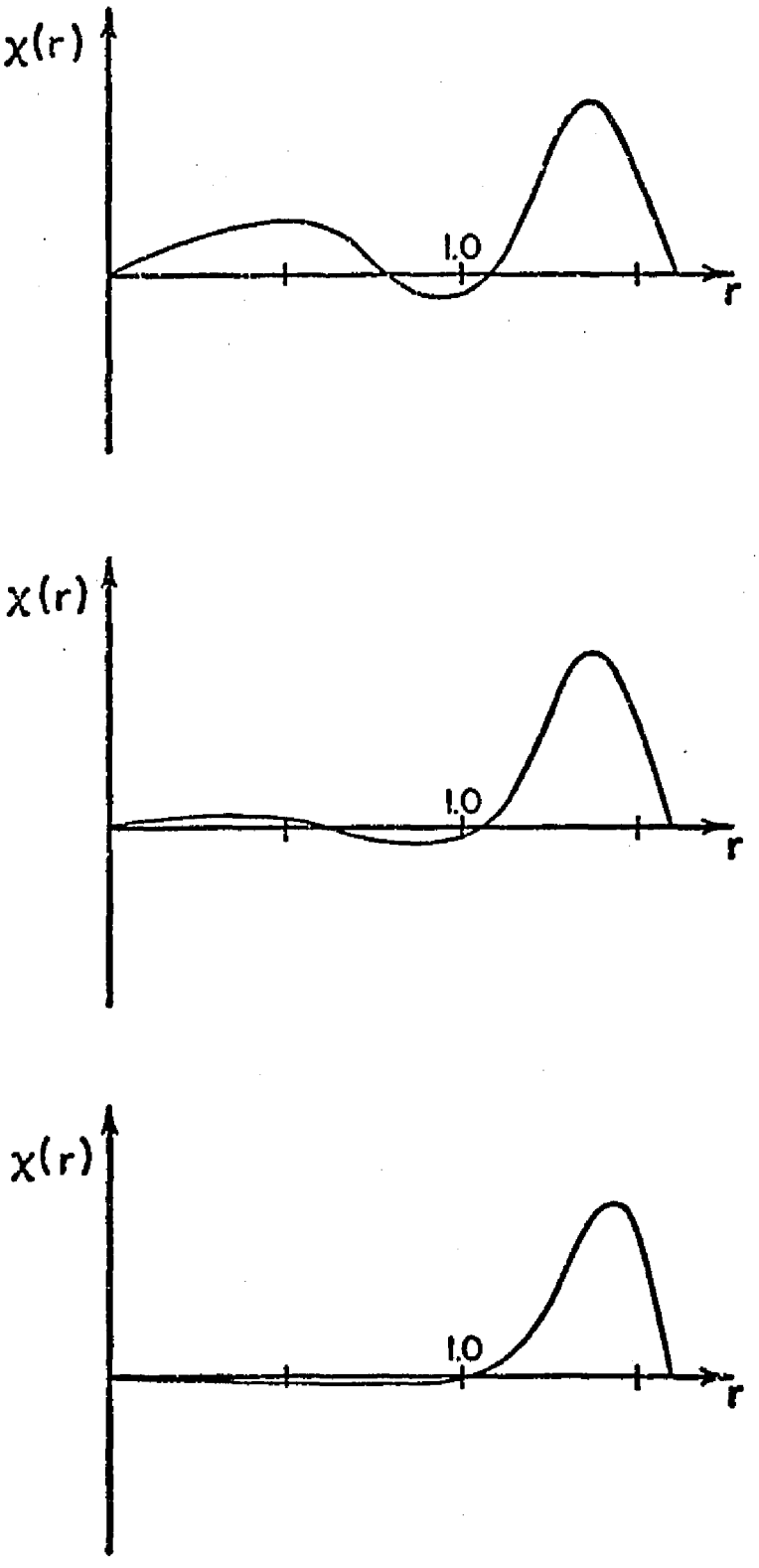

Fig. 25. High beta dependence of the eigenfunction with two radial nodes (top, $\beta = .90$; middle, $\beta = .93$; bottom, $\beta = .96$) showing an inward progression of the first node. This node eventually disappears leaving an eigenfunction with only node and with external localization. Thus, for high beta values there are two eigenvalues which correspond to eigenfunctions with one node. The spectrum of eigenvalues is, therefore, non-Sturmian.

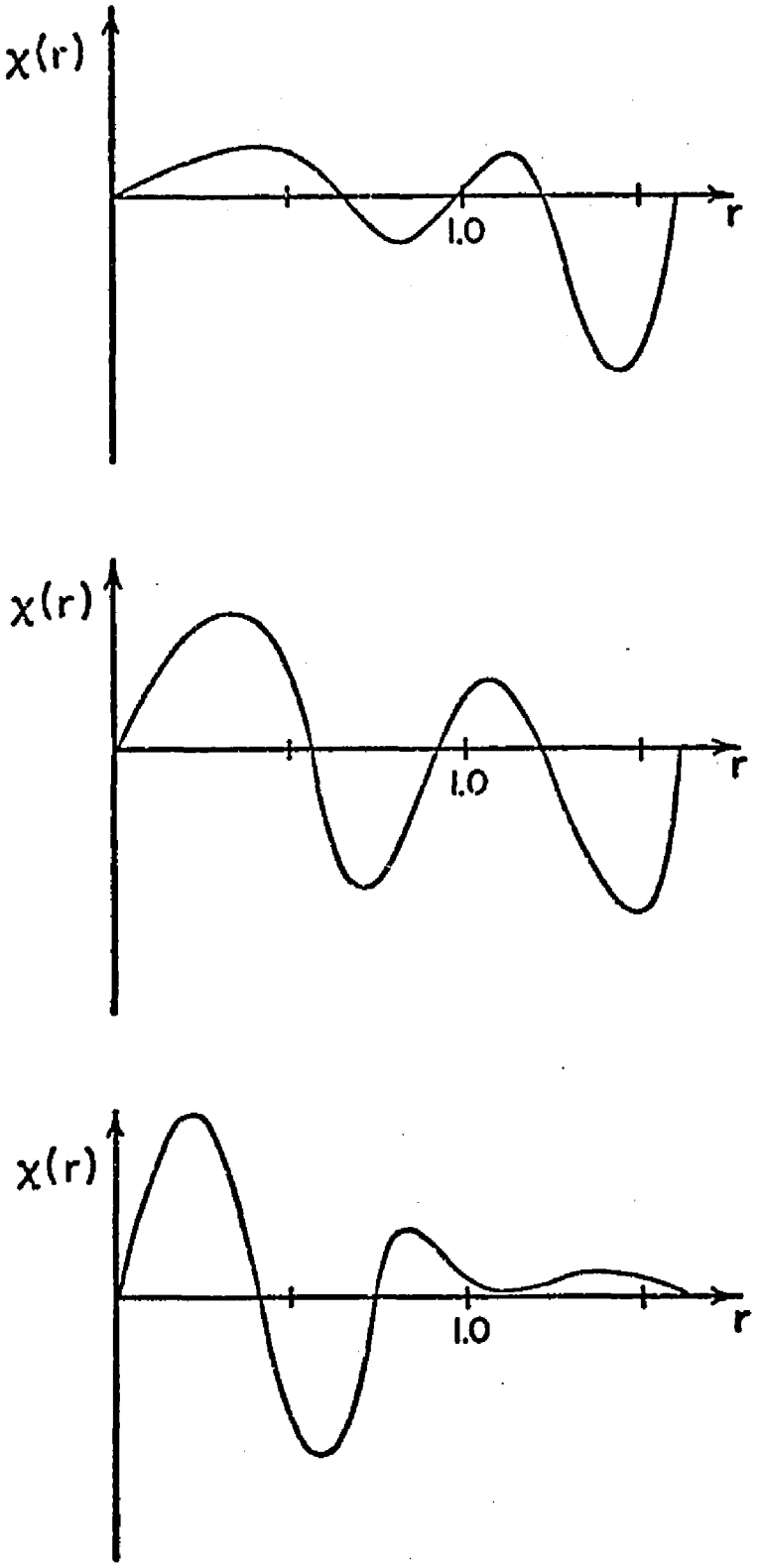

Fig. 26. High beta dependence of the eigenfunction with three radial nodes (top, $\beta = .90$; middle, $\beta = .93$; bottom, $\beta = .96$) showing an inward progression of the first node. This node eventually disappears leaving an eigenfunction with only two nodes and with localization switching from external to internal. Note that the bottom figure has been reflected through the line $\chi = 0$ (the first minimum of the middle figure becomes the first maximum of the bottom figure.

(ii) (Fig. (25)) The n = 2 externally localized mode loses a node and becomes an n = 1 externally localized mode. Thus, there are two classes of unstable modes.

(iii) (Fig. (26)) The n = 3 externally localized mode loses a node and becomes an n = 2 internally localized mode.

Stable eigenfunctions are found for extremely high beta values. The mode with n = 1 nodes appears before the n = 0 mode. This behavior of the stable spectrum has been reported by Freidberg, et al.[8] in connection with the long wavelength calculation.

C. Summary

The eigenvalue spectrum of the bumpy theta pinch consists of point spectra and the Alfven continuum. When the plasma beta is not too large the computed unstable eigenvalues exhibit Sturmian behavior. For higher beta values, however, the discrete spectrum is complicated and not simply Sturmian or anti-Sturmian. An unusual change takes place in the nodal structure of the eigenfunctions giving rise to two classes of unstable modes. Stable eigenfunctions achieve a finite oscillation frequency in the high beta limit. The finite wavelength case thus exhibits the same features as the long wavelength case, but only at much higher beta values. In view of the physical parameters relevant in most high beta theta pinch experiments one would not expect to observe the wall stabilization of the n=0 mode in a finite wavelength bumpy theta pinch, but this would be easily observed for a long wavelength theta pinch.

V. EQUILIBRIUM AND STABILITY OF THE BUMPY SCREW PINCH

In this chapter the influence of a weak magnetic shear (i.e. a weak theta component of the equilibrium magnetic field) on the stability of the bumpy theta pinch will be investigated.

A. Equilibrium

The axisymmetric equilibrium is governed by Eq. (II-29)

$$\frac{\partial}{\partial r}\left(\frac{1}{r}\frac{\partial \psi}{\partial r}\right)+\frac{1}{r}\frac{\partial^2 \psi}{\partial z^2}=-rp'(\psi)-\frac{1}{r}\chi(\psi)\chi'(\psi) \qquad \text{(II-29)}$$

where $B_r=\frac{1}{r}\frac{\partial \psi}{\partial z}$, $B_\theta=\frac{\chi}{r}$, and $B_z=-\frac{1}{r}\frac{\partial \psi}{\partial z}$.

The equilibrium magnetic field is assumed to have the form

$$\underset{\sim}{B}=\left(\delta k b(r)\sin(kz),\ \delta k d(r),\ a(r)+\delta c(r)\cos(kz)\right)$$

That is, a weak magnetic shear (i.e., $B_\theta = \delta k d(r) \neq 0$) is added to the bumpy field lines of the previous problem. It is evident that the quantity d(r) enters Eq. (II-29) at $\mathcal{O}(\delta^2)$ since $\chi(\psi) = \mathcal{O}(\delta)$; thus, the r and z components of the bumpy screw pinch equilibrium magnetic field are identical to those of the bumpy theta pinch which were detailed in Chapter II. The theta component of the equilibrium magnetic field is an arbitrary function of r.

B. Stability

The addition of a theta component to the equilibrium magnetic field (magnetic shear) results in slightly more complicated expressions

for P and the three components of $\underset{\sim}{T}$ which occur in the equation of motion

$$-\rho\omega^2 \underset{\sim}{y}_1 + \nabla P = \underset{\sim}{T} \qquad \text{(III-2)}$$

The four quantities for the screw pinch are

$$T_r = \left\{B_r\frac{\partial}{\partial r} + \frac{\partial B_r}{\partial r} + B_\theta\frac{im}{r} + B_z\frac{\partial}{\partial z}\right\}\left[\frac{im}{r}(uB_\theta - vB_z) - \frac{\partial}{\partial z}(wB_r - uB_z)\right]$$
$$-\left\{2\frac{B_\theta}{r}\right\}\left[\frac{\partial}{\partial z}(vB_z - wB_\theta) - \frac{\partial}{\partial r}(uB_\theta - vB_r)\right] + \left\{\frac{\partial B_r}{\partial r}\right\}\left[\frac{1}{r}\frac{\partial}{\partial r}\left[r\times\right.\right. \qquad (1)$$
$$\left.\left.(wB_r - uB_z)\right] - \frac{im}{r}(vB_z - wB_\theta)\right]$$

$$T_\theta = \left\{B_r\frac{\partial}{\partial r} + \frac{B_r}{r} + B_\theta\frac{im}{r} + B_z\frac{\partial}{\partial z}\right\}\left[\frac{\partial}{\partial z}(vB_z - wB_\theta) - \frac{\partial}{\partial r}(uB_\theta - vB_r)\right]$$
$$+\left\{\frac{\partial B_\theta}{\partial r} + \frac{B_\theta}{r}\right\}\left[\frac{im}{r}(uB_\theta - vB_r) - \frac{\partial}{\partial z}(wB_r - uB_z)\right] + \left\{\frac{\partial B_\theta}{\partial z}\right\}\times \qquad (2)$$
$$\left[\frac{1}{r}\frac{\partial}{\partial r}\left[r(wB_r - uB_z)\right] - \frac{im}{r}(vB_z - wB_\theta)\right]$$

$$T_z = \left\{B_r\frac{\partial}{\partial r} + B_\theta\frac{im}{r} + \frac{\partial B_z}{\partial z} + B_z\frac{\partial}{\partial z}\right\}\left[\frac{1}{r}\frac{\partial}{\partial r}\left[r(wB_r - uB_z)\right] - \frac{im}{r}(vB_z - wB_\theta)\right] \qquad (3)$$
$$+\left\{\frac{\partial B_z}{\partial r}\right\}\left[\frac{im}{r}(uB_z - vB_r) - \frac{\partial}{\partial z}(wB_r - uB_z)\right]$$

$$P = -(\gamma p + B_z^2)\left(\frac{1}{r}(ru)' + \frac{im}{r}v\right) - (\gamma p + B_r^2)\frac{\partial w}{\partial z} - B_r^2\frac{im}{r}v - B_\theta^2\left(\frac{1}{r}(ru)'\right.$$
$$\left.+\frac{\partial w}{\partial z}\right) + uB_\theta\left[\frac{1}{r}(rB_\theta)' - r\left(\frac{B_\theta}{r}\right)'\right] - uB_z\frac{\partial B_r}{\partial z} - wB_r\frac{\partial B_z}{\partial r} + uB_r\frac{\partial B_z}{\partial z} + vB_\theta\frac{\partial B_r}{\partial r}$$
$$+B_r\left\{\frac{im}{r}B_\theta + B_z\frac{\partial}{\partial z}\right\}u + B_\theta\left\{B_r\frac{\partial}{\partial r} + B_z\frac{\partial}{\partial z}\right\}v + B_z\left\{B_r\frac{\partial}{\partial r} + \frac{B_r}{r} + B_\theta\frac{im}{r}\right\}w \qquad (4)$$
$$+wB_z\frac{\partial B_r}{\partial r}$$

Upon explicit evaluation it is found that the differences between the above expressions and the corresponding expressions for the bumpy theta

pinch enter at $\mathcal{O}(\delta^2)$. Thus the modes with $\omega = \mathcal{O}(1)$ in $k\delta$ are identical to those of the unsheared system discussed in Chapter III. For the modes with $\omega = \mathcal{O}(k\delta)$ one again finds, exactly as in Chapter III that

$$y_1' = \frac{a'}{a} y_1 + y_2 + \left[\frac{a'}{a}\left(c - \frac{a'b}{a}\right) - \left(c - \frac{a'b}{a}\right)'\right]\chi_0 - \frac{ar}{im}\vec{\nabla}\cdot\vec{v}^{(1)} \tag{5}$$

$$y_2' = \frac{1}{r}\left(1 + \frac{ra'}{a}\right) y_2 + \frac{m^2}{r^2}\left(y_1 - 2\frac{a'b}{a}\chi_0\right) \tag{6}$$

$$-\frac{ar}{im}\vec{\nabla}\cdot\vec{v}^{(1)} = k^2\left(\frac{r^2}{m^2} y_2 + b\chi_0\right) \tag{7}$$

$$\nabla\cdot\underset{\sim}{u}_1 = 0 + \mathcal{O}(\delta^2) \tag{8}$$

Upon expanding to $\mathcal{O}(\delta^2)$ one finds

$$T_r = \delta(T_r)^{(1)} - \delta^2 k^2 \frac{im}{r}\left\{\left(la + \frac{m}{r}d\right)^2\chi_0 - \frac{1}{2}\left[by_1' + 2b'y_1 + \frac{a'b}{a}y_1 - b\left(c + \frac{a'b}{a}\right)'\chi_0 - \frac{a'b}{a}\frac{a'b}{a}\chi_0 - 2\frac{a'b}{a}b\chi_0' + \frac{a'b}{a}\frac{b}{r}\chi_0 - \frac{a'b}{a}b'\chi_0 - b\frac{ar}{im}\vec{\nabla}\cdot\vec{v}^{(1)}\right] - 2d\left[\frac{la}{m}\chi_0' + d'\frac{\chi_0}{r} + d\left(\frac{\chi_0}{r}\right)'\right]\right\} + \mathcal{O}(\delta^2\sin(2kz)) \tag{9}$$

$$T_\theta = \delta(T_\theta)^{(1)} + \delta^2\left(la + \frac{m}{r}d\right)^2\chi_0' - \frac{1}{2}\left[\left(c - \frac{a'b}{a}\right)y_2 + \frac{m^2}{r^2}b\left(y_1 - 2\frac{a'b}{a}\chi_0\right)\right] - 2\frac{m}{r}\frac{d}{r}\left(la + \frac{m}{r}d\right)\chi_0\Big\} + \mathcal{O}(\delta^2\sin(2kz)) \tag{10}$$

Following the same procedure to eliminate P as described previously, one finds the eigenvalue equation

$$\frac{1}{r}\left[\left[\rho\omega^2 - \left(la + \frac{m}{r}d\right)^2\right] r\chi_0'\right]' - \frac{m^2}{r^2}\left[\rho\omega^2 - \left(la + \frac{m}{r}d\right)^2\right]\chi_0 = \frac{1}{2}\left\{\frac{m^2}{r^2}b\frac{ar}{im}\vec{\nabla}\cdot\vec{v}^{(1)} + \left[\frac{a'}{a}\left(c - \frac{a'b}{a}\right) - \left(c - \frac{a'b}{a}\right)\right]y_2 + \frac{m^2}{r^2}\frac{a'b}{a}\left[2y_1 - \left[3\left(c - \frac{a'b}{a}\right) - 2\frac{b}{r}\right]\chi_0\right] - \frac{m^2}{r^2}b\left(c - \frac{a'b}{a}\right)'\chi_0\right\} - 2\frac{m^2}{r^2}\left[la'\frac{d}{r} + \left(\frac{d}{r}\right)'\left(la + \frac{m}{r}d\right)\right]\chi_0 \tag{11}$$

Thus, the eigenvalue equations of the bumpy theta pinch are changed in the following way: a) The factor (ℓa) becomes $(\ell a + \frac{m}{r} d)$ on the left hand side; b) an additional term appears on the right hand side. This additional term arises because of the shear and is identical to the right hand side of the normal mode equation of an ordinary screw pinch (see Appendix E). The ordinary screw pinch is known to be unstable,[17,26] hence this study examines the relative importance of terms on the right hand side of Eq. (11) which arise solely from bumpiness and others which arise solely from shear.

To make the problem explicit a profile for the theta component of the equilibrium magnetic field must be specified. One profile is considered

$$d(r) = d_0(1 - \exp(-r))/(1+r) \tag{12}$$

Then for small values of r

$$d(r) = d_0 r(1 - \tfrac{3}{2}r + \cdots)$$

The asymptotic form of the solutions for small values of r, are found to differ from those of the bumpy theta pinch, Eqs. (III-49) and (III-50) in only one detail; that being that the factor $(\rho(0)\omega^2 - \ell^2 a^2(0))$ in Eq. (III-50) is replaced by the factor $(\rho(0)\omega^2 - (\ell a(0) + m d_0)^2)$.

The boundary conditions are identical to those derived for the bumpy theta pinch. Thus, the structure of the eigenvalue problem is modified only slightly by the addition of the shear of the magnetic field lines. These changes influence the spectrum of eigenvalues, particularly the continuous spectrum and, consequently, the point eigenvalues which

accumulate at the tips of the continuum. The Alfven continuum for the bumpy theta pinch is bounded away from the origin for any nonzero wavenumber, ℓ, and plasma beta less than unity

$$\ell^2(1-\beta) < \omega^2 < \ell^2/D$$

While for vanishing wavenumber the continuum degenerates to a single point at the origin. The Alfven continuum for the bumpy screw pinch can always extend to the origin because of the cancellation which may occur in the sum

$$\ell a(r) + \frac{m}{r} d(r)$$

Thus, when the perturbations are helical and the pitch of the helix matches the pitch of the field lines at anywhere in the range of r

$$\frac{\ell}{m} = -\frac{d(r)}{r a(r)}$$

the continuum hits the origin. For m = 1, negative wavenumbers are particularly prone to instabilities since the continuum extends to the origin and since point eigenvalue can accumulate only on the tips of the continuum. This is the essence of the Suydam criterion[25] for instability in the diffuse linear pinch (screw pinch). The asymmetry in dependence on axial wavenumber is illustrated in Figs. (27) and (28) which show normalized growth rate squared plotted against axial wavenumber, ℓ, for a particular value of plasma beta. The asymmetry in ℓ is characteristic of a screw pinch (modes increasing unstable the smaller the azimuthal wavenumber, m). As the magnitude of the theta component

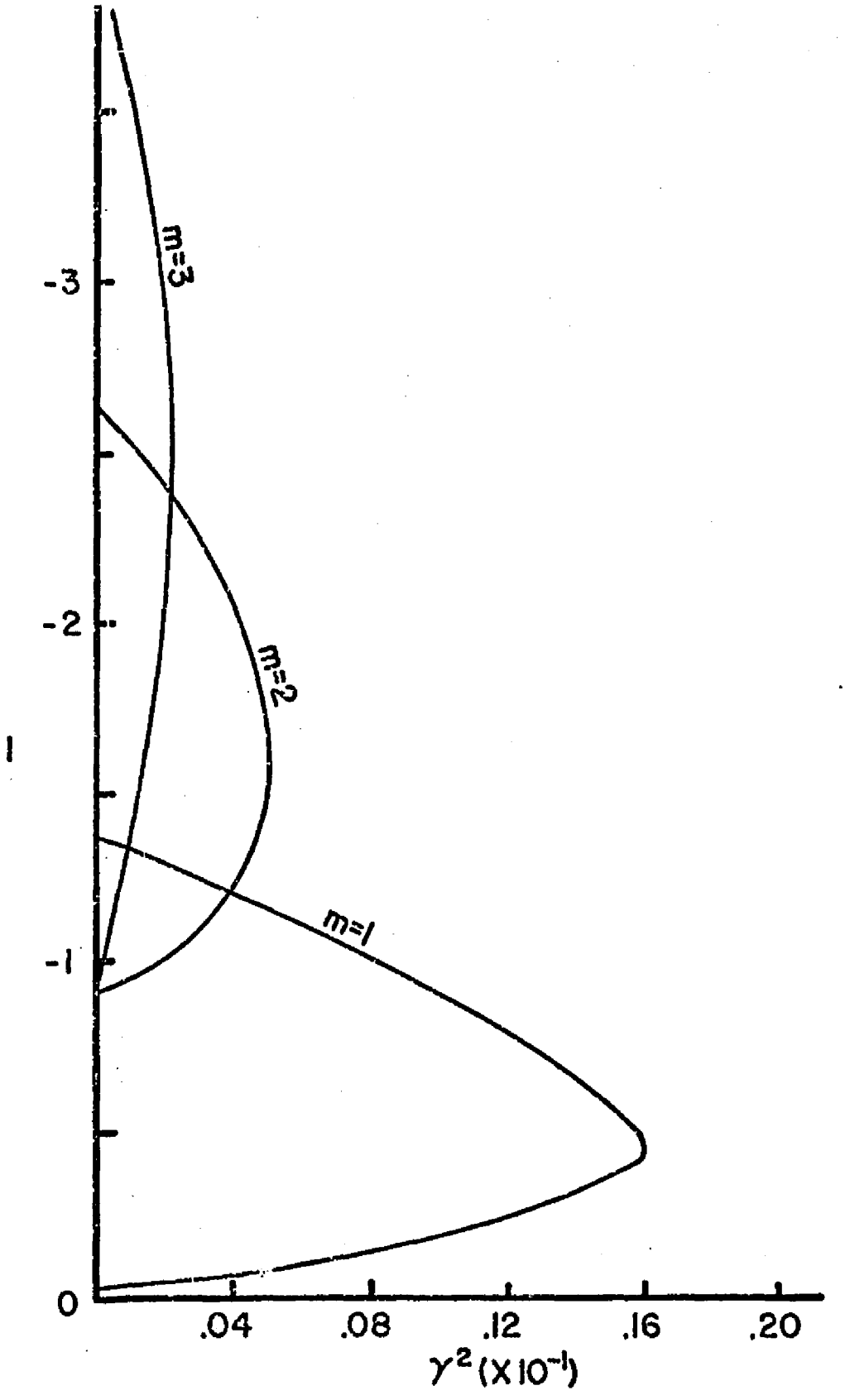

Fig. 27. Normalized growth rate squared versus axial wavenumber for least stable modes of the bumpy screw pinch for Gaussian profiles with $\beta = .5$, $r_w = 4.2$, and $d_0 = 1$.

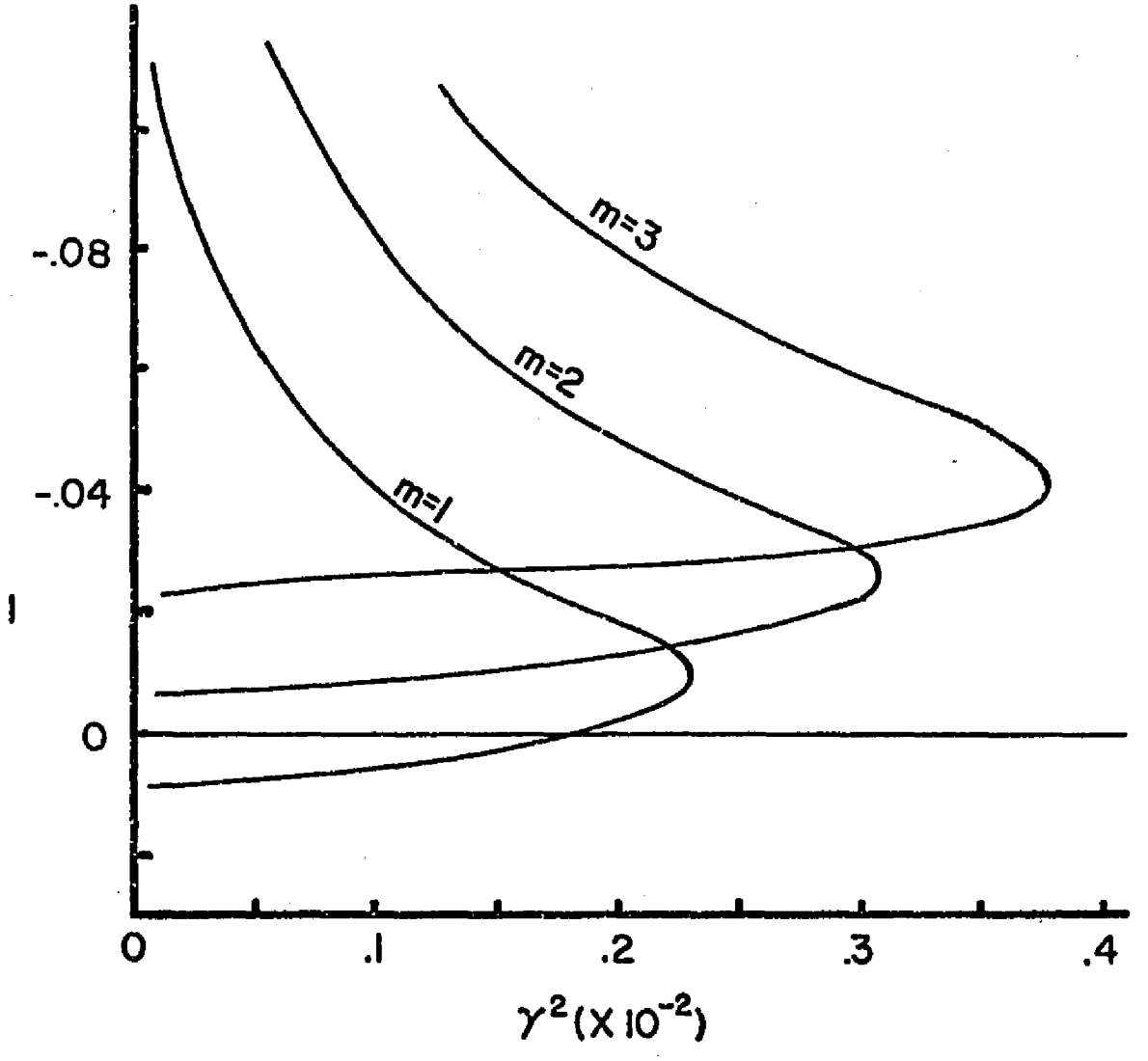

Fig. 28. Normalized growth rate squared versus axial wavenumber for least stable modes of the bumpy screw pinch for Gaussian profiles with $\beta = .5$, $r_w = 4.2$, and $d_0 = .1$.

of the equilibrium magnetic field is reduced, the curves become less asymmetric and approach the symmetric curves characteristic of a theta pinch (modes increasingly unstable the larger the azimuthal wavenumber, m). When the theta component vanishes, the growth rates are identical to those of the bumpy theta pinch.

C. Generalization of Four Stability Problems

One can easily derive all the cases discussed in this work from general expressions like Eqs. (5)-(8) and (11). One considers the equilibrium flux function of the form

$$\psi(r,z) = \psi^{(0)}(r) + \delta\lambda_1\psi^{(1)}(r)\cos(kz) + O(\delta^2)$$

and perturbed velocities of the form

$$\underset{\sim}{u}_1(r,\theta,z,t) = e^{-i\omega t}e^{im\theta}e^{ilk\delta z}\left[\underset{\sim}{u}^{(0)}(r) + \delta\lambda_1\underset{\sim}{u}^{(1)}(r,z) + O(\delta^2)\right]$$

and a current flux function

$$\chi(r) = r\delta k\lambda_2 d(r)$$

Here, λ_1, and λ_2 are artificial parameters used to turn the various perturbations on and off. If λ_2 is unity the shear is fully on but if λ_2 is made to vanish the shear uniformly disappears. Likewise, if λ_1 is unity the field lines are bumpy and the perturbed velocity resembles the flux function. If, however, λ_1 vanishes, then the flux surfaces uniformly

become right circular cylinders and the perturbed velocity field regains its translational invariance in the axial direction. In this formulation all the equations governing both equilibrium and perturbed quantities, remain uniformly valid as the artificial parameters are varied from unity to zero (the boundary condition, Eq. (II-62), becomes $\lambda_1 \psi^{(1)'}(r_w) = -\lambda_1 r_w$).

One finds the eigenvalue problem is given by the following system of equations

$$\lambda_1 y_1' = \lambda_1 \left\{ \frac{a'}{a} y_1 + y_2 + \left[\frac{a'}{a}\left(c - \frac{a'b}{a}\right) - \left(c - \frac{a'b}{a}\right)' \right] \chi_0 - \frac{ar}{im} \vec{\nabla}\cdot\vec{v}^{(1)} \right\}$$

$$\lambda_1 y_2' = \lambda_1 \left\{ -\frac{1}{r}\left(1 + \frac{ra'}{a}\right) y_2 + \frac{m^2}{r^2}\left(y_1 - 2\frac{a'b}{a}\chi_0 \right) \right\}$$

$$-\lambda_1 \frac{ar}{im} \vec{\nabla}\cdot\vec{v}^{(1)} = \lambda_1 k^2 \left(\frac{r^2}{m^2} y_2 + b\chi_0 \right)$$

$$\nabla \cdot \underset{\sim}{u}_1 = 0 + \mathcal{O}(\delta^2)$$

$$\frac{1}{r}\left[\left[\rho\omega^2 - \left(la + \lambda_2 \frac{m}{r} d \right)^2 \right] r\chi_0' \right]' - \frac{m^2}{r^2}\left[\rho\omega^2 - \left(la + \lambda_2 \frac{m}{r} d \right)^2 \right] \chi_0$$

$$= \frac{\lambda_1^2}{2} \left\{ -\frac{m^2}{r^2} b \frac{ar}{im} \vec{\nabla}\cdot\vec{v}^{(1)} + \left[\frac{a'}{a}\left(c - \frac{a'b}{a}\right) - \left(c - \frac{a'b}{a}\right)' \right] y_2 + \frac{m^2}{r^2}\frac{a'b}{a}\left[2y_1 \right.\right.$$

$$\left. - \left[3\left(c - \frac{a'b}{a}\right) - 2\frac{b}{r} \right]\chi_0 - \frac{m^2}{r^2} b \left(c - \frac{a'b}{a}\right)' \chi_0 \right\} - \lambda_2 2 \frac{m^2}{r^2}\left[la' \frac{d}{r} \right.$$

$$\left. + \left(\frac{d}{r}\right)'\left(la + \lambda_2 \frac{m}{r} d \right) \right] \chi_0$$

If both λ_1 and λ_2 are unity this system is identical to that derived in this chapter for the bumpy screw pinch. If λ_1 is unity but λ_2 is made to vanish then the system is identical to that derived in Chapter III for the bumpy theta pinch. If λ_2 is unity but λ_1 is made to vanish then the system is identical to that of an ordinary screw pinch discussed in

Appendix E. Finally, if both λ_1 and λ_2 are made to vanish then the system is identical to that of an ordinary theta pinch discussed in Appendix D.

If both parameters, λ_1 and λ_2 vanish identically the spectrum of eigenvalues is purely continuous, however, if either or both perturbations are nonvanishing, the spectrum consists of a discrete spectrum as well as a continuum. The weak shear or small bumpiness is, thus, an example of an extremely singular perturbation of the original theta pinch equilibrium.

VI. APPENDIX

A. Derivation of the cusp velocity

The normal speed locus for the slow magnetosonic wave is determined by the root

$$c^2 - \frac{1}{2}\left[(c_s^2+c_A^2) - \sqrt{(c_s^2+c_A^2)^2 - 4c_s^2c_A^2\cos^2\theta}\right] = 0$$

For the cusp one is particularly interested in the behavior for angles near $\pi/2$. Assuming that cos (θ) is very small, one may approximate the square root by the first two terms of its series expansion finding

$$c^2 - c_c^2\cos^2\theta = 0$$

where $c_c^2 = \left(\frac{c_s^2c_A^2}{c_s^2+c_A^2}\right)$ defines the cusp speed. This is similar to the equation for the Alfven normal loci.

Thus, the portion of the slow normal speed locus corresponding to nearly perpendicular propagation is approximated by a circle of diameter C_c and all the plane waves propagating in these directions converge at two single points of infinite multiplicity. These points propagate strictly one dimensionally.

B. Long Wavelength Equilibria[8]

For long wavelength equilibria, assume $k = \varepsilon << \delta$. Equations (II-49) and (II-50) become

$$\left(\frac{1}{r}\psi^{(0)\prime}\right)' = -r p'(\psi^{(0)}) \tag{B1}$$

$$\left(\frac{1}{r}\psi^{(0)\prime}\right)' = -r\psi^{(1)} p''(\psi^{(0)}) \tag{B2}$$

By following the same procedure described in the text one finds that the long wavelength equilibrium quantities satisfy

$$p + \tfrac{1}{2}a^2 = \tfrac{1}{2} \tag{B3}$$

$$(rb)' = rc \tag{B4}$$

$$c' - \frac{rb}{a}\left(\frac{a'}{r}\right)' = 0 \tag{B5}$$

Equation (B5) is easily rewritten

$$(ac - a'b)' = 0 \tag{B6}$$

Equation (B6) is immediately integrated and yields

$$c - \frac{a'b}{a} = \frac{1}{a} \tag{B7}$$

Substituting Eq. (B7) into Eq. (B4) gives

$$\left(r\frac{b}{a}\right)' = \frac{r}{a^2} \tag{B8}$$

Integration gives

$$b(r) = \frac{a(r)}{r}\int^{r} \frac{r'dr'}{[a(r')]^2} \tag{B9}$$

Equations (B3), (B9), and (B7) determine the long wavelength equilibrium configuration.

C. Equilibrium MHD Characteristics

To determine the characteristics of the system of partial differential equations

$$\nabla\cdot\underset{\sim}{B}=0 \qquad \text{(II-1)}$$

$$\nabla p=(\nabla\times\underset{\sim}{B})\times\underset{\sim}{B} \qquad \text{(II-3')}$$

one follows Jeffrey and Taniuti,[14] introducing a family of surfaces in three dimensional space and finding conditions such that the normal derivatives across this surface can no longer be computed. If the normal derivatives cannot be computed across the surface, then the surface is defined to be characteristic surface. The characteristic surfaces are not dependent on any particular coordinate system, hence, no generality is lost if one examines Eqs. (1) and (3') in a cartesian system. In a surface $\phi(x, y, z)$ = constant one may define a new coordinate system and rewrite the system of partial, differential equations; that part involving the normal derivative for the fourth order system (1) and (3') is written in matrix form

$$\begin{pmatrix} -\frac{\partial\phi}{\partial x} & (\underset{\sim}{B}\cdot\nabla\phi-B_x\frac{\partial\phi}{\partial x})-B_y\frac{\partial\phi}{\partial x} & -B_z\frac{\partial\phi}{\partial x} \\ -\frac{\partial\phi}{\partial y} & -B_x\frac{\partial\phi}{\partial y} & (\underset{\sim}{B}\cdot\nabla\phi-B_y\frac{\partial\phi}{\partial y})-B_z\frac{\partial\phi}{\partial y} \\ -\frac{\partial\phi}{\partial z} & -B_x\frac{\partial\phi}{\partial z} & -B_y\frac{\partial\phi}{\partial z}\ (\underset{\sim}{B}\cdot\nabla\phi-B_z\frac{\partial\phi}{\partial z}) \\ 0 & \frac{\partial\phi}{\partial x} & \frac{\partial\phi}{\partial y} \quad \frac{\partial\phi}{\partial z} \end{pmatrix} \frac{\partial}{\partial\phi}\begin{pmatrix} p \\ B_x \\ B_y \\ B_z \end{pmatrix} \qquad \text{(C1)}$$

The normal derivatives are indeterminate when the determinant of the coefficient matrix vanishes, thus, the vanishing of this determinant provides the condition necessary for the surface ϕ = constant to be characteristic. The evaluation of this determinant is facilitated by recognizing that the second, third, and fourth column of the matrix may be rewritten

$$\begin{pmatrix} \underset{\sim}{B}\cdot\nabla\phi \\ 0 \\ 0 \\ \frac{\partial\phi}{\partial x} \end{pmatrix} - B_x \begin{pmatrix} \frac{\partial\phi}{\partial x} \\ \frac{\partial\phi}{\partial y} \\ \frac{\partial\phi}{\partial z} \\ 0 \end{pmatrix}, \quad \begin{pmatrix} 0 \\ \underset{\sim}{B}\cdot\nabla\phi \\ 0 \\ \frac{\partial\phi}{\partial y} \end{pmatrix} - B_y \begin{pmatrix} \frac{\partial\phi}{\partial x} \\ \frac{\partial\phi}{\partial y} \\ \frac{\partial\phi}{\partial z} \\ 0 \end{pmatrix}, \quad \begin{pmatrix} 0 \\ 0 \\ \underset{\sim}{B}\cdot\nabla\phi \\ \frac{\partial\phi}{\partial z} \end{pmatrix} - B_z \begin{pmatrix} \frac{\partial\phi}{\partial x} \\ \frac{\partial\phi}{\partial y} \\ \frac{\partial\phi}{\partial z} \\ 0 \end{pmatrix}$$

Then the rules of determinants lead to an immediate reduction to

$$\det \begin{pmatrix} -\frac{\partial\phi}{\partial x} & \underset{\sim}{B}\cdot\nabla\phi & 0 & 0 \\ -\frac{\partial\phi}{\partial y} & 0 & \underset{\sim}{B}\cdot\nabla\phi & 0 \\ -\frac{\partial\phi}{\partial z} & 0 & 0 & \underset{\sim}{B}\cdot\nabla\phi \\ 0 & \frac{\partial\phi}{\partial x} & \frac{\partial\phi}{\partial y} & \frac{\partial\phi}{\partial z} \end{pmatrix} = (\underset{\sim}{B}\cdot\nabla\phi)^2 (\nabla\phi)^2 \qquad C2)$$

The characteristic surfaces are thus those which satisfy

$$\underset{\sim}{B}\cdot\nabla\phi = 0 \qquad \text{(counted twice)}$$

$$\nabla\phi = 0 \qquad \text{(counted twice)}$$

The first condition states that the characteristic surface is covered by magnetic field lines, thus, magnetic surfaces are characteristic. The second states that the characteristic surface has no normal, thus, no real surface exists. The fourth order system possesses a doubly

degenerate real characteristic surface and a double degenerate complex surface. The system of partial differential equations is therefore a mixed type, elliptic-hyperbolic, and has multiple characteristics.

D. Long Wavelength Modes of an Ordinary Theta Pinch

In the case of an ordinary theta pinch the equilibrium magnetic field lines are straight and it may be assumed that all quantities vary as

$$f(r,\theta,z,t) = f(r)e^{im\theta}e^{i\ell\delta z}e^{-i\omega t}$$

The wavenumber is $\ell\delta$ and is scaled to the small quantity δ. It is then found that P and the components of $\underline{\underline{T}}$ are

$$P = -(\gamma p + a^2)\left(\frac{1}{r}(ru)' + \frac{im}{r}v\right) - i\delta^2\ell\gamma p w$$

$$T_r = -\delta^2\ell^2 a^2 u$$

$$T_\theta = -\delta^2\ell^2 a^2 v$$

$$T_z = -i\delta\ell a^2\left(\frac{1}{r}(ru)' + \frac{im}{r}v\right)$$

Modes with $\omega = \mathcal{O}(1)$ in δ. The equation of motion in this case is identical to that derived for modes of the bumpy theta pinch with $\omega = \mathcal{O}(1)$ in δ

$$-\rho\omega^2 u + \left[-(\gamma p + a^2)\vec{\nabla}\cdot\vec{v}\right]' = 0 + \mathcal{O}(\delta^2)$$

$$-\rho\omega^2 v + \frac{im}{r}\left[-(\gamma p + a^2)\vec{\nabla}\cdot\vec{v}\right] = 0 + \mathcal{O}(\delta^2)$$

$$-\rho\omega^2 w = 0 + \mathcal{O}(\delta)$$

The modes are transverse. Upon introducing a velocity potential, $\chi(r)$, such that

$$\vec{v} = \frac{1}{\rho}\vec{\nabla}\chi$$

it is found $\chi(r)$ must satisfy the self-adjoint ordinary differential equation

$$\frac{\rho}{r}\left(\frac{r}{\rho}\chi'\right)' + \left(\frac{\rho\omega^2}{\gamma p + a^2} - \frac{m^2}{r^2}\right)\chi = 0$$

subject to the boundary condition $\chi'(r_w) = 0$ and regularity.

Modes with $\omega = \mathcal{O}(\delta)$. Expansion of the equation of motion gives, to lowest order in δ

$$\vec{\nabla}\left[(\gamma p + a^2)\,\vec{\nabla}\cdot\vec{v}\right] = 0$$

Thus, the flow must be incompressible

$$\nabla \cdot \underset{\sim}{u}_1 = 0 + \mathcal{O}(\delta)$$

Then P and the components of $\underset{\sim}{T}$ are no larger than (δ^2)

$$p = -i\delta^2 \ell \gamma p w$$
$$T_r = -\delta^2 \ell^2 a^2 u$$
$$T_\theta = -\delta^2 \ell^2 a^2 v$$
$$T_z = 0$$

A velocity stream function $\chi(r)$ such that

$$u = \frac{im}{r}\chi$$
$$v = -\chi'$$

may be introduced and the equation of motion is found to give

$$-\rho\omega^2 \frac{im}{r}\chi - [i\ell\gamma p w]' = -\ell^2 a^2 \frac{im}{r}\chi$$
$$-\rho\omega^2 \chi' - \frac{im}{r}[i\ell\gamma p w] = \ell^2 a^2 \chi'$$
$$0 = 0$$

Upon elimination of w these two equations give

$$\frac{1}{r}\left[(\rho\omega^2-\ell^2a^2)r\chi'\right]'-\frac{m^2}{r^2}(\rho\omega^2-\ell^2a^2)\chi=0$$

Solutions must satisfy regularity at r = 0 and the boundary condition $\chi(r_w) = 0$ to be physically acceptable.

This equation was studied by Barston[24] who found that the spectrum of eigenvalues consists solely of a continuum of real values. This stable continuum is the Alfven continuum.

E. Ordinary Screw Pinch

Consider the equilibrium magnetic field

$$\underset{\sim}{B} = (0, \delta d(r), a(r))$$

The equation of motion of the perturbed velocity involves the following quantities

$$P=-(\gamma p+a^2)\left(\frac{1}{r}(ru)'+\frac{im}{r}v\right)-i\delta^2\ell\gamma pw+\delta^2\frac{im}{r}adw+\delta^2 ilad v$$
$$-\delta^2 d(du)'-i\delta^4\ell d^2w$$
$$T_r=-\delta^2\left(la+\frac{m}{r}d\right)^2u-\delta^2 2ilad\frac{v}{r}+\delta^2 2\frac{d}{r}(du)'$$
$$T_\theta=-\delta^2\left(la+\frac{m}{r}d\right)^2v-\delta^2 i\left(la+\frac{m}{r}d\right)dr\left(\frac{u}{r}\right)'+\delta^2 la\left(la+\frac{m}{r}d\right)w$$
$$T_z=-i\delta a\left(la+\frac{m}{r}d\right)\left(\frac{1}{r}(ru)'+\frac{im}{r}v\right)-\delta^3\frac{m}{r}d\left(la+\frac{m}{r}d\right)w$$

Following the expansion procedure for modes with $\omega = \Theta(1)$ in δ exactly

the same eigenvalue equation is found for the velocity potential, χ, as was found in the previous cases

$$\frac{\rho}{r}\left(\frac{r}{\rho}\chi'\right)' + \left(\frac{\rho\omega^2}{\gamma p + a^2} - \frac{m^2}{r^2}\right)\chi = 0$$

where

$$\vec{v} = \frac{1}{\rho}\vec{\nabla}\chi$$

For modes with $\omega = \mathcal{O}(\delta)$ one expands the equation of motion order by order in δ and finds to lowest order that the flow is incompressible,

$$\nabla \cdot \underset{\sim}{u}_1 = 0 + \mathcal{O}(\delta^2)$$

Introducing the velocity stream function, $\chi(r)$, one finds

$$P = -\delta^2 i\ell a d\chi' - \delta^2 \frac{im}{r} dr\left(\frac{d\chi}{r}\right)' - \delta^2 i\ell\gamma p w + \delta^2 \frac{im}{r} a d w$$

$$T_r = -\delta^2 \frac{im}{r}\left(\ell a + \frac{m}{r}d\right)^2 \chi + \delta^2 2i\ell a \frac{d}{r}\chi' + \delta^2 2\frac{im}{r} d\left(\frac{d\chi}{r}\right)'$$

$$T_\theta = \delta^2\left(\ell a + \frac{m}{r}d\right)^2 \chi' - \delta^2 \frac{im}{r}\left(\ell a + \frac{m}{r}d\right) r^2\left(\frac{\chi}{r^2}\right)'$$

$$T_z = 0 + \mathcal{O}(\delta^3)$$

The equation of motion then gives the three relations

$$-\rho\omega^2 \frac{im}{r}\chi + P' = -\frac{im}{r}\left(\ell a + \frac{m}{r}d\right)^2 \chi + 2i\ell a \frac{d}{r}\chi' + 2\frac{im}{r} d\left(\frac{d\chi}{r}\right)'$$

$$\rho\omega^2 \chi' + \frac{im}{r} P = \left(\ell a + \frac{m}{r}d\right)^2 \chi' - \frac{im}{r}\left(\ell a + \frac{m}{r}d\right)\chi' - 2\frac{im}{r}\left(\ell a + \frac{m}{r}d\right)\frac{\chi}{r}$$

$$0 = 0$$

Upon elimination of P one finds that $\chi(r)$ must satisfy the eigenvalue equation

$$\frac{1}{r}\left[\left[\rho\omega^2 - \left(\ell a + \frac{m}{r}d\right)^2\right] r\chi'\right]' - \frac{m^2}{r^2}\left[\rho\omega^2 - \left(\ell a + \frac{m}{r}d\right)^2\right]\chi =$$

$$-2\frac{m}{r}\left[\ell a' \frac{d}{r} + \left(\frac{d}{r}\right)'\left(\ell a + \frac{m}{r}d\right)\right]\chi$$

The addition of a theta component to the axial magnetic field of a theta pinch changes the equation of motion in two ways. First, the factor (ℓa) on the left hand side becomes $(\ell a + \frac{m}{r} d)$. Second, a nonzero term appears on the right hand side of the equation. Because of this term on the right hand side, the differential equation may admit well behaved eigenfunctions and a discrete spectrum as well as the singular eigenfunctions and the continuous spectrum described for the ordinary theta pinch.

VII. REFERENCES

1. W. R. Ellis, F. C. Jahoda, R. Kristal, W. E. Quinn, F. L. Ribe, G. A. Sawyer, and R. E. Siemon, Nucl. Fusion 14, 841 (1974).
2. W. R. Ellis, Nucl. Fusion 15, 255 (1975).
3. K. S. Thomas, H. W. Harris, F. C. Jahoda, G. A. Sawyer, and R. E. Siemon, Phys. Fluids 17, 1314 (1974).
4. G. Schmidt, Physics of High Temperature Plasmas: An Introduction (Academic Press, New York, 1966), Chapts. 3 and 4.
5. N. A. Krall and A. W. Trivelpiece, Principles of Plasma Physics (McGraw-Hill, New York, 1973), Chapt. 3.
6. H. Grad and C. K. Chu, Research Frontiers in Fluid Dynamics, ed. R. J. Seeger and G. Temple (Wiley-Interscience, New York, 1965), pp. 308-333.
7. F. A. Haas and J. A. Wesson, Phys. Fluids 10, 2245 (1967).
8. H. Weitzner, Phys. Fluids 16, 237 (1973).
9. J. P. Freidberg and B. M. Marder, Phys. Fluids 16, 247 (1973).
10. J. P. Freidberg, B. M. Marder, and H. Weitzner, Nucl. Fusion 14, 809 (1974).
11. G. Vahala, Phys. Fluids 17, 1449 (1974).
12. K. S. Thomas, C. R. Harder, W. E. Quinn, and R. E. Siemon, Phys. Fluids 15, 1658 (1972).
13. R. A. Dandl, H. O. Eason, A. C. England, G. E. Guest, C. L. Hendricks, and J. C. Sprott, ORNL-TM-3694 (Oak Ridge National Laboratory, November 1971).

14. R. Courant and D. Hilbert, Methods of Mathematical Physics, Vol. II (Wiley-Interscience, New York, 1961), §§ 6.9 and 6.10.

15. A. Jeffrey and T. Taniuti, Nonlinear Wave Propagation with Applications to Physics and Magnetohydrodynamics (Academic Press, New York, 1964), §§ 1.5 and 1.6.

16. R. Kulsrud, Advanced Plasma Theory, ed. N. M. Rosenbluth (Academic Press, New York, 1964), pp. 54-72.

17. W. A. Newcomb, Annals of Physics 10, 232 (1960).

18. J. P. Freidberg, private communication.

19. G. Arfkin, Mathematical Methods for Physicists (Academic Press, New York, 1970), §§ 8.4 and 8.5.

20. E. L. Ince, Ordinary Differential Equations (Dover, New York, 1956), Chapt. 16.

21. H. B. Keller, Numerical Methods for Two-Point Boundary-Value Problems (Blaisdell, Waltham, Mass., 1968).

22. B. Carnahan, H. A. Luther, and J. O. Wilkes, Applied Numerical Methods (Wiley, New York, 1969), pp. 405-406.

23. J. P. Freidberg, private communication.

24. E. M. Barston, Annals of Physics 29, 282 (1964).

25. Ince, op. cit., § 9.5.

26. B. R. Suydam, Magnetohydrodynamic Stability and Thermonuclear Confinement, ed. A. Jeffrey and T. Taniuti (Academic Press, New York, 1966), pp. 166-168.